ज्ञान-विज्ञान विमुक्तये
University Grants Commission

UNIVERSITY GRANTS COMMISSION
SOUTH EASTERN REGIONAL OFFICE, HYDERABAD
MINOR RESEARCH PROJECT

No. F. MRP – 6848/16 (SERO/UGC) Dated 30th JUNE 2017

"MOLECULAR STRUCTURE AND VIBRATIONAL SPECTROSCOPIC ANALYSIS OF SOME ANTIMICROBIAL ACTIVITY COMPOUNDS – A COMBINED EXPERIMENTAL AND QUANTUM CHEMICAL APPROACH"

Dr. F. LIAKATH ALI KHAN
(PRINCIPAL INVESTIGATOR)
ASSOCIATE PROFESSOR &
CONTROLLER OF EXAMINATIONS
PG & RESEARCH DEPARTMENT OF PHYSICS
ISLAMIAH COLLEGE (AUTONOMOUS)
VANIYAMBADI

FEBRUARY - 2020

DECLARATION

I Dr. F. Liakath Ali Khan, Associate Professor of Physics, P.G & Research Department of Physics, Islamiah College (Autonomous), Vaniyambadi, hereby declare that the Minor Research Project No. F. MRP-6848/16(SERO/UGC) dated 30th June 2017 entitled ***"Molecular Structure and Vibrational Spectroscopic Analysis of some Antimicrobial Activity Compounds – A Combined Experimental and Quantum Chemical Approach"*** is a Bonafide Record of Research Work carried out by me during 2017-2019. Further, it is declared that the work presented in the report is original and carried out as per the plan in the proposal and guidelines of the University Grant Commission.

(Dr. F. LIAKATH ALI KHAN)
Principal Investigator

ACKNOWLEDGEMENT

I am ever grateful to the Almighty for the blessings bestowed upon me at all stages of the execution of my UGC Minor Research Project.

I express my profound and sincere gratitude and wish to thank the University Grants Commission, New Delhi and the UGC- South Eastern Region Office, Hyderabad for having approved and provided Financial Assistance to our Minor Research Project on "Molecular Structure and Vibrational Spectroscopic Analysis of Some Antimicrobial Activity Compounds – A Combined Experimental and Quantum Chemical Approach".

I express my heartfelt thanks to the Management of Islamiah College (Autonomous), Vaniyambadi, for extending their good support and timely help during the period of UGC Minor Research Project.

I express my heartfelt and sincere thanks to the Former General Secretary, Vaniyambadi Muslim Educational Society, Janab C. Khaiser Ahmed Sahib and the present General Secretary Janab Gani Azhar Sahib for their constant encouragement and continuous support in carrying out this UGC Minor Research Project successfully.

I express my sincere thanks to former Secretary & Correspondent Dr. Anwarullah Hajee Sahib and the present Secretary & Correspondent Janab. L.M. Muneer Ahmed Sahib for their fullest cooperation and continuous support in carrying out this UGC Minor Research Project successfully

I express my sincere gratitude and heartfelt thanks to our beloved Principal Dr. T Mohamed Ilyas, for his advice, timely suggestions, motivation and kind help in carrying out this UGC Minor Research Project work successfully.

I take this opportunity to thank Mr. Fasiuddin, Assistant professor, Department of Physics for his timely help during period of this UGC Minor Research Project.

Finally, I express my sincere thanks to all our colleagues in the PG & Research Department of Physics, Islamiah College (Autonomous), Vaniyambadi for having supported us in our endeavors.

Dr. F. Liakath Ali Khan
Principal Investigator

CONTENTS

LIST OF TABLES

LIST OF FIGURES

PREFACE

The entire study of the project has been divided into eight Chapters. A short introduction to the theoretical and experimental background of vibrational (FT-IR, FT-Raman), nuclear magnetic resonance (NMR), ultraviolet (UV) spectroscopy is given in the **First chapter**. The basic principle of *ab initio* and Density Functional Theories (DFT) are explained using quantum theory of vibration of the molecular systems. Various approximation methods, through which satisfactory force field of the molecules are computed and discussed. Selection rules for Infrared (IR) and Raman transitions and Fourier Transformation (FT) basics are outlined. The *ab initio* calculations Hartree-Fock (HF) and Density Functional Theory (DFT) vibrational analysis is also briefly given. The Fourier Transform Infrared (FT-IR), Fourier Transform Raman (FT-Raman), NMR, UV-visible spectrophotometers, sources, detectors, sampling techniques and are also elaborated. The concept of Molecular docking, Antimicrobial activity of compounds and importance of Ramachandra Plot also discussed.

The **Chapter Two** deals with the aim and plan of the project work to be undertaken for investigation of molecular structure and vibrational spectroscopic analysis of some antimicrobial activity compounds. The antibacterial and antifungal activity and medicinal application of target compounds (some novel halogenoderivatives of benzimidazole compound) have been discussed. The significance of introduction of halogenations group substitution in 6-position of benzimidazole compound exhibit important biological properties such as anti bacterial, anti fungal, anti-helminthic, anti-allergic, anti-neoplastic, local analgesic, antihistaminic, anti-leishmanial, vasodilator, anti-hypertensive, spasmolytic, and anti-ulcer activities have been discussed. In plan of work title, four types of halogenoderivatives of benzimidazole compounds and various types of parameters to be studied also discussed.

The Third Chapter makes a comprehensive review of the literature regarding the theoretical studies such as molecular structure parameter, vibrational frequencies, electronic absorption spectra, HOMO-LUMO, molecular electrostatic potential (MEP), natural bond orbital (NBO), HF and DFT (B3LYP, B3PW91) methods, ^{1}H –NMR Gauge Including Atomic Orbital (GIAO), Antimicrobial activity and molecular docking studies of the systems selected for the present investigation

Chapter Four discusses the**,** theoretical investigations on the molecular structure, vibrational spectra, FT-IR, Raman, UV and NMR spectral analysis of 6-nitro-2-(4-nitrophenyl)-1H-benzimidazole. A complete vibrational and molecular structure analysis has been performed based on the quantum mechanical approach by *ab initio* HF/6-311++G (d,p) and DFT (B3LYP) 6-311G(d,p)/6-311++G(d,p) calculations. The energy and oscillator strength calculated by Time Dependent Density Functional Theory (TD-DFT) results almost compliments with experimental findings. The ^{1}H NMR chemical shifts of the molecules were calculated using the Gauge-Invariant Atomic Orbital (GIAO) method confirms with the experimental values. The theoretical FT-IR, spectra of title molecule has also been constructed. Vibrational spectral analysis is further supported by the total energy distribution (TED). The minimum energy conformational analysis was carried out with the help of potential energy surface (PES) scan. The redistribution of electron density (ED) in various bonding and antibonding orbitals and E2 energies have been calculated by natural bond orbital (NBO) analysis using DFT method to give clear evidence of stabilization originating from the hyper conjugation of various intra-molecular interactions. The Highest Occupied Molecular Orbital (HOMO) and Lowest Unoccupied Molecular Orbital (LUMO) analysis have been used to elucidate information regarding charge transfer within the molecule. In addition to this the antimicrobial evaluation of 6-nitro-2-(4-nitrophenyl)-1H-benzimidazole

was also performed against some bacteria and fungi using Disc – diffusion method .The inhibition zone of growth was also determined for bacterial and fungal strain.

The Fifth chapter reports the molecular structure, vibrational spectroscopic FT-IR, FT-Raman, UV and NBO analysis of 6 amino-2-(4 nitrophenyl)-1H-benzimidazole by ab initio HF and DFT methods. The FT-IR solid phase (4000-400 cm-1), and UV spectrum in ethanol solution of 6A4NPB was recorded. The optimized geometrical parameters obtained by HF/6-311++G (d,p) and B3LYP/6-311G(d,p)/6-311++G(d,p) calculations are in good agreement with available data. The difference between the observed and scaled wave number values of most of the fundamentals is very small. Vibrational spectral analysis has been done on the basis of TED. The minimum energy conformational analysis was carried out with the help of PES scan. NBO result reflects the charge transfer within the molecule. The theoretically constructed FT-IR and FT-Raman spectra show good correlation with experimentally observed FT-IR spectra. Besides HOMO LUMO analysis and antimicrobial activity, molecular docking was also performed.

In Chapter Six, the experimental FT-IR, UV and NMR spectral analysis by ab initio HF and DFT calculations of 6-chloro-2-(4-aminophenyl)-1H-benzimidazole Quantum mechanical calculations of energies, geometries and vibrational wave numbers of MPTS were carried out by HF/6-311++G(d,p) and B3LYP/6-311G(d,p)/6-311++G(d,p) methods. Comparison of the wave numbers calculated with the DFT method using 6-311++G(d,p) basis set with experimental values reveals that the B3LYP method shows very good

agreement with experimental observation due to inclusion of electron correlation for this method. TD-DFT calculation of the electronic spectra shows good agreement with the experimental UV-visible spectrum. Correlations between the proton and carbon-13 experimental chemical shifts and the GIAO NMR calculations are found to be in good agreement. NBO reflects the charge transfer within the molecule during the intra-molecular interaction. The Lewis and non-Lewis structure of NBOs shows occupancy in s and p orbitals. HOMO, HOMO-1, LUMO and LUMO+1energies have been calculated, the lowering of band gap supports the bioactive property of the molecule. Antimicrobial activity and molecular docking results the synthesized compound is more active against the gram positive bacteria than gram negative, anti fungal activity is remarkable, this is due to presence of bromo and chlorophenyl in the benzimidazole moiety.

A combined experimental and theoretical study on FT-IR, spectra and molecular structure of 6 bromo-2-(4-chlorophenyl)-1H-benzimidazole were carried out in the Seventh Chapter. The present work deals with FT-IR, FT-Raman, spectroscopic analysis of 6B4CPB utilizing ab initio HF/6-311++G(d,p) and B3LYP/6-311G(d,p)/6-311++G(d,p) method. Vibrational spectral analysis has been done on the basis of calculated TED. The NBO analysis confirms the hyperconjugative interaction of the electron occurs from π (C3-C5) to π* (C8-C12), π* (C7-C9) with the stabilization energy of 18.69 and 19.86 kcal/mol. The HOMO and LUMO analysis have been used to elucidate information

regarding charge transfer within the molecule. HOMO–LUMO energy gap has been observed which allows the molecular orbitals to overlap to have a proper electronic communication conjugation. The antimicrobial activity of the compound shows the title compound 6 bromo-2-(4-chlorophenyl)-1H-benzimidazole is one of the most promising compounds for pharmacophore industry; hence toxicology of the compound has to be studied.

Final chapter discuss the summary and conclusion of the project. In this present study halogenoderivatives of benzimidazole compounds were known to possess anti-microbial some novel halogenoderivatives of benzimidazole compounds have been synthesized and characterized by spectral studies such as FT-IR in the region of 4000-400 cm-1, UV-Visible and 1H NMR experimental techniques and computational theoretical studies such as molecular structure parameter, vibrational frequencies, electronic absorption spectra has been investigated using gas and solvent phase. HOMO-LUMO, molecular electrostatic potential (MEP) and natural bond orbital (NBO), of all halogenoderivatives of benzimidazole compound has been computed using the HF and DFT (B3LYP, B3PW91) methods with 6-31+G (d, p) and 6-31++G (d, p) basis sets. All the synthesized compounds were screened for their anti-bacterial and anti-fungal activity using Disc – diffusion method.

LIST OF PUBLICATIONS AND PAPER PRESENTED IN THE INTERNATIONAL SEMINAR

1. **Synthesis, Spectroscopic Studies, Antimicrobial Activity and Theoretical Studies of 6-nitro-2-(4-nitrophenyl)-1H-benzimidazole,** ***Journal of Emerging Technologies and innovative research,*** Volume 6, Issue 5, May 2019, Pages 249-261. By [1]F. Liakath Ali Khan, [1]Fasiuddin G S. [1]Department of Physics, Islamiah College, Vaniyambadi-635 752, Tamil Nadu, India.

2. A research paper related to Minor Research Project entitled " **Synthesis, Spectroscopic (FT-IR, NMR, UV-visible), NLO, HOMO-LUMO, Molecular docking and Antimicrobial activity of 6 bromo-2-(4Chlorophenyl)-1H benzimidazole** presented by the principal investigator in **UGC –Autonomous Funded, One-Day International Seminar on "Recent Advances in Biotechnology (ISRAB-2020)"** held on 9th January, 2020, Organized by the Department of Biotechnology, Islamiah College (Autonomous), Vaniyambadi.

ABBREVIATIONS

B3LYP	:	Becke 3Lee Yang Parr
BLYP	:	Becke Lee Yang Parr
DFT	:	Density Functional Theory
DMSO	:	Dimethyl sulfoxide
ED/EDs	:	Electron Density / Electron Densities
FT	:	Fourier Transform
FT-IR	:	Fourier Transform Infra-Red
FT-Raman	:	Fourier Transform Raman
GIAO	:	Gauge-Invariant Atomic Orbital
HF	:	Hartree-Fock
HOMO	:	Highest Occupied Molecular Orbital
ICT	:	Intra-molecular Charge Transfer
IR	:	Infrared
KS	:	Kohn-Sham
LDA	:	Local Density Approximation
LSDA	:	Local Spin Density Approximation
LUMO	:	Lowest Unoccupied Molecular Orbital
LYP	:	Lee Yang and Parr
m	:	Medium
MEP	:	Molecular Electrostatic Potential
MO/MOs	:	Molecular Orbital / Molecular Orbitals
MP	:	Moller-Plesset
ms	:	Medium strong
NBO/NBOs	:	Natural Bond Orbital / Natural Bond Orbitals
NIR	:	Near Infra-Red

Continued…

NMR	:	Nuclear Magnetic Resonance
PES/PESs	:	Potential Energy Surface / Potential Energy Surfaces
QCISD	:	Quadratic Configuration Integral Spin Density
s	:	Strong
SCF	:	Self-consistent field
SQM	:	Scaled Quantum Mechanics
TD-DFT	:	Time Dependent-Density Functional Theory
TED	:	Total Energy Distribution
UV	:	Ultraviolet
vs	:	Very strong
w	:	Weak
δ	:	in-plane bending
ν	:	Stretching
Γ	:	out-of plane bending
CCDs	:	Charge-Couple Devices
6N4NPB	;	6-nitro-2-(4-nitrophenyl)-1H-benzimidazole
6A4NPH	;	6-amino-2-(4-nitrophenyl)-1H-benzimidazole
6C4APH	;	6-chloro-2-(4-aminophenyl)-1H-benzimidazole
6B4APH	;	6-bromo-2-(4-chlorophenyl)-1H-benzimidazole
MD	;	Molecular Docking
RP	;	Ramachandra Plot

Chapter -I

Introduction to Vibrational Spectroscopic (FT-IR, FT-Raman, UV, NMR) and Quantum Chemical Analysis

Abstract

The working of FT-IR spectrometer, its principle and limitations of IR spectroscopy are outlined. Principle of Raman spectroscopy, working of FT-Raman spectrometer and the uses of Raman spectroscopy are explained. Working of NMR spectrometer and applications of NMR spectroscopy are also reported. Computational details are elaborated. The theoretical aspects of *ab initio* HF method and its limitations are outlined. The DFT theory is also explained using quantum theory of vibration of the molecular systems. The Capability of Gaussian 16W program package and Gauss view 6.0 are discussed. Medicinal chemistry involves the discovery, development, identification and interpretation of the mode of action of biologically active compounds at the molecular level. The widespread use of antibacterial and antifungal infection has lead to serious health hazards. The resistance of wide spectrum antibacterial agents has prompted discovery and modification of new antifungal and antibacterial drugs.

1.1. Introduction to Spectroscopy

Spectroscopy is the study of the interaction between matter and radiated energy. Spectroscopic data is often represented by a spectrum, a plot of the response of interest as a function of wavelength or frequency. Spectroscopy is used in physical and analytical chemistry because atoms and molecules have unique spectra. These spectra can be interpreted to derive information about the atoms and molecules, and they can also be used to detect, identify and quantify chemicals. Spectroscopy is also used in astronomy and remote sensing. Different spectroscopic techniques give different kinds of information [1-4].

Molecular spectroscopy aims to understand the interaction of molecular energy with electromagnetic radiation. A molecule possesses various forms of energy due its different kinds of motion and inter-molecular interactions. Vibrational spectroscopy has been used to make significant contribution in many areas of physics and chemistry as well as in other areas of science. Its important applications are in the study of intra-molecular and inter-molecular forces, molecular structure determinations, computation of degree of association in condensed phases, elucidation of molecular symmetries, identification and characterization of molecules, deducing thermodynamical properties of molecular systems, etc., [5].

In order to “view” a molecule, we must use light having a wavelength smaller than the molecule itself (roughly 1 to 15Å). Such radiation is found in the X-ray crystallography yields remarkably detailed picture of the molecular structures amenable to examination. The chief limiting factor here is the need for high quality crystals of the compound being studied. The spectroscopic techniques described below do not provide a three-dimensional picture of a molecule, but instead yield information about certain characteristic features.

Laser Spectroscopy: Absorption spectroscopy, fluorescence spectroscopy, Raman and surface-enhanced Raman spectroscopy commonly use laser light as an energy source. Laser spectroscopy generally has high resolution and sensitivity.

Ultraviolet-Visible Spectroscopy: Absorption of this relatively high-energy light causes electronic excitation. The easily accessible absorption in this region (wavelengths of 200 to 800 nm) is useful in structural studies only if conjugated π-electron systems are present in the molecule.

Nuclear Magnetic Resonance Spectroscopy: Absorption in the low-energy radio frequency part of the spectrum causes excitation of nuclear spin states. NMR spectrometers are tuned to certain nuclei (like ^{1}H, ^{13}C, ^{19}F and ^{31}P). For a given type of nucleus, high-resolution spectroscopy distinguishes and count atoms in different locations in the molecule.

Infrared Spectroscopy: Absorption of this lower energy radiation causes vibrational and rotational excitation of groups of atoms within the molecule. Because of their characteristic absorptions, identification of functional groups is easily accomplished. The infrared absorption spectrum of a substance is sometimes called its molecular fingerprint.

Raman Spectroscopy: Raman scattering of light by molecules may be used to provide information on a sample's chemical composition and molecular structure.

The IR and Raman spectroscopy's generally yield similar types of information [6-8]. The IR and Raman techniques can be used to gases, liquids and solids. Both the methods have been applied to a wide variety of problems and would yield desirable knowledge such as inter-nuclear distances and vibrational frequencies. The most valuable application of the data of IR and Raman studies are the calculation of the thermodynamic quantities such as the heat capacity, entropy, enthalpy and free energy of gaseous molecules. The fundamental frequencies of vibrations obtained from IR

and Raman spectra have provided considerable information about the inter-atomic forces in various molecules [9, 10].

1.2. Background for FT-IR

Fourier transform infrared (FT-IR) spectroscopy is an interference technique through which recent advances in digital computer technology has demonstrated in superiority to dispersive IR techniques. Fourier transform spectroscopy uses the Michelson interferometer as the multiplex optical device [11]. The block diagram of FT-IR Spectrometer is shown in Fig.1.1.

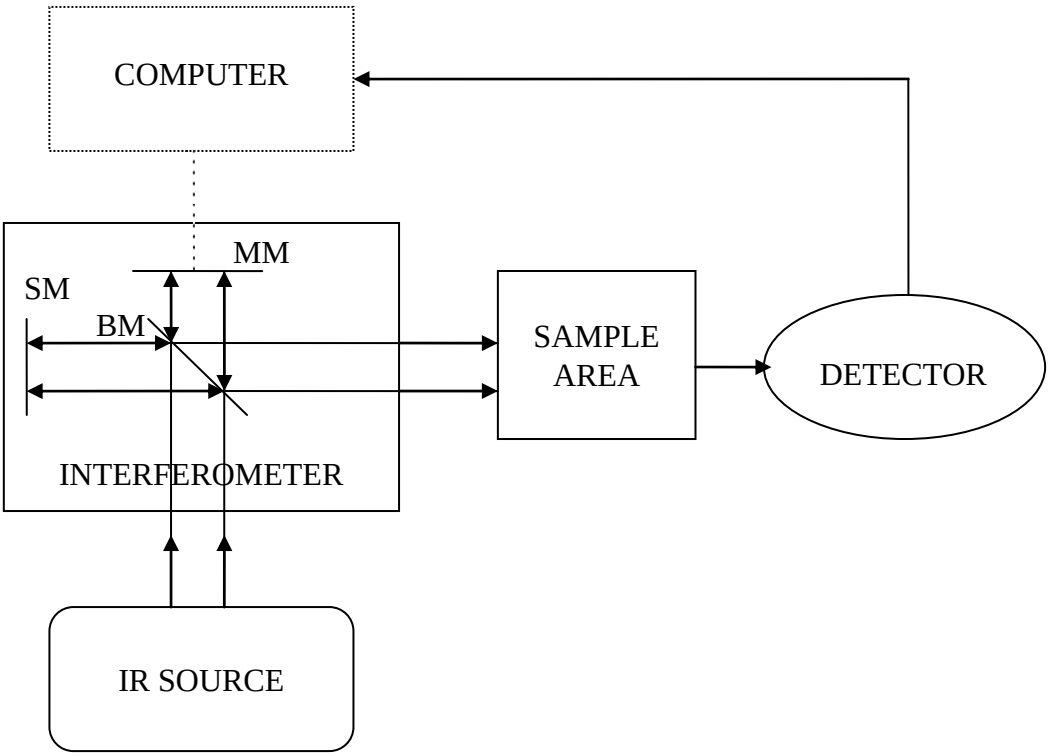

Fig.1.1. Block diagram of FT-IR spectrometer

1.2.1. Source

The most commonly used radiation source is globar operating on the basis of the block body radiation. It consists of a SiC (silicon carbide) dimensions 2 cm in length and 0.5 cm in diameter heated to about 1450 K. The globar is generally used in

the spectral range up to 100μm. The globar is operated in vacuum only. Nernst glower (sintered mixtures of the oxides of Zr, Tm, Ce, Y, and Er) is also used as source in some spectrometers depending upon the spectral range. For more sophisticated applications, gas plasma must be used as radiation source. Besides thermic Microwave generators like klystrons or magnetrons are also used for wide frequency range.

1.2.2. Interferometer

The interferometer is the heart of the FT-IR instrument. The interferometer is the bit that analyses the IR or near IR and hence enable us to generate the spectrum. The classic Michelson interferometer is shown in Fig.1.2 contains a source, detector, stationary and moving mirrors and a beam splitter.

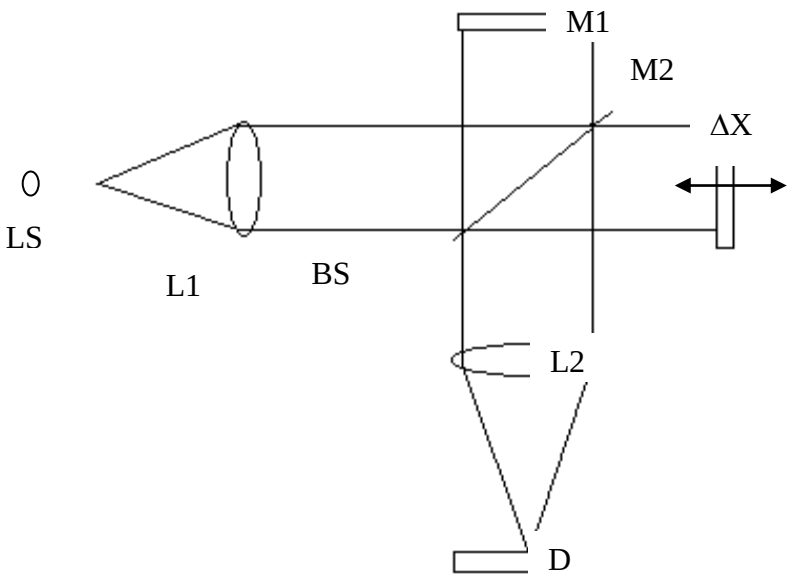

Fig.1.2. Optical path in Michelson Interferometer

(LS-Light Source, L-Lenses, M-Mirrors, BS-Beam Splitter)

The beam splitter is the crystal of potassium bromide coated with germanium [12], splits the incident light equally reflecting half to the stationary mirror while transmitting the other half to the moving mirror. The white light from the source located at the focus of lens L_1 is separated into two parts by the beam splitter. The

reflected part is focused into the detector D after reflection from the stationary mirror M_1 and after a second split by the beam splitter. The transmitted part of the light is also focused onto the detector after it was reflected from the moving mirror M_2 is movable, which produce the path difference between the two beams thereby develop interference pattern at the detector. Their intensity I(x) depends on the position x of the mirror M_2. I(x) is termed interferogram function.

If the incident beams is monochromatic of the form $E(x, t) = E_0 \cos(kx-\omega t)$,

the field E_0 at the detector is

$$E_D = \frac{1}{2}\left\{E_0 \cos(\varpi_0 t - k_0 x) + E_0 \cos\left[k_0(x + 2\Delta x) - \varpi_0 t\right]\right\} \qquad (1.1)$$

where $2\Delta x$ is the optical path difference between the two beams. The intensity at the detector is given by the following expression

$$I(x) = c_0 \varepsilon_0 < E^2 >= \frac{c_0 \varepsilon_0}{4} E_0^2 \left[1 + \cos(4\pi \nu_0 x)\right] \qquad (1.2)$$

In terms of the spectral intensity $I(\nu) = c_0\varepsilon_0 E_0^2 \delta(\nu - \nu_0)/2$, the above equation can be written as

$$I(x) = \frac{1}{2}\int_0^\infty I(\nu)\left[1 + \cos(4\pi\nu x\right] d\nu \qquad (1.3)$$

Generalizing this equation to an arbitrary intensity spectrum $I(\nu)$ yields the basic relationship for Fourier spectroscopy.

$$I'(x) = I(x) - \frac{1}{2}\int_0^\infty I(\nu) d\nu = \frac{1}{2}\int_0^\infty I(\nu)\cos(4\pi\nu x) d\nu \qquad (1.4)$$

The interferogram function I(x) or I'(x) contains the whole information about the spectrum $I(\nu)$. In fact, I'(x) is the Fourier transform of $I(\nu)$ performed with a cosine function. The observed intensity I(x) oscillates around an average intensity $\int I(\nu)\, d\nu/2 = I_0/2$ which is exactly half of the original total intensity of the beam.

For x=0 it reaches its maximum value of I_0 as immediately seen from equation (1.4). This position corresponds to zero optical path differences. It is called the white light position. For $x \rightarrow \infty$, the coherence of the radiation is lost, and therefore the intensity at the detector becomes $I_0 / 2$.

A Fourier transformation of I'(x) yields for x = y/2,

$$\int I'(y/2)\cos(2\pi\nu' y)dy = \frac{1}{2}\int_0^{\infty} I(\nu)d\nu \int \cos(2\lambda\nu y)\cos(2\pi\nu' y)dy = I(\nu')/2 \qquad (1.5)$$

Since the integration over y gives $\delta(\nu - \nu')$. This equation shows that the spectral components of the light are obtained directly from the inteferogram by Fourier transformation, without any spectral dispersion [13]. This Fourier spectroscopy has many basic advantages when compared to dispersive spectroscopy.

The 'energy advantage' originates from the fact that during the whole period of measurement nearly always the total beam intensity is captured by the detector. This means the detection operates on a high signal level which improves the signal-to-noise ratio, particularly for weak radiation sources.

The 'Fellgett' or the 'multiplex advantage' originate from the simultaneous measurement of full spectrum. To obtain spectra from radiation of very low intensity such as from astronomical sources, all the frequencies are recorded simultaneously during spectroscopy as in dispersive spectroscopy, they are said to be 'multiplexed'. In dispersive spectroscopy N parts of the widths $\Delta\nu$ of the spectrum will be measured successively so that for each part only the time T' =T/N is available. The signal-to-noise ratio would be smaller by $\frac{1}{\sqrt{4N}}$.

Interferometer also has greater 'throughput' than dispersive IR methods. 'Throughput', a measure of the optical efficiency of the system, is defined as the product of the area and solid angle of the beam passing from the source to the

detector. Since there is no slit in FT-IR spectrometer, the cross section of the beam of radiation in an interferometer can be much larger than that of a dispersive spectrometer, which leads to considerable improvements in signal-to-noise ratio. But in much chemical and analytical application the sample size limits the energy advantage. The optimum resolution is obtained by using the theoretical relationship r = $F\sqrt{\frac{2}{R_0}}$ where r is the radius of the entrance pinhole and R_0 is the resolution. This yields for the brightness of the interferometer.

$$E = (r^2 \pi A^2) / F^2 = (2 \pi A^2) / R_0 = (2 \pi A^2) / \nu) \delta \nu \qquad (1.6)$$

Where A is the beam diameter in the spectrometer. For dispersive spectrometer the brightness is given by

$$E = (AR_0H\delta\lambda) / F \qquad (1.7)$$

Where H and F are the height of the slit and the focal length of the grating spectrometer respectively. By comparing these two equation 1.6 and 1.7 it is found that for Fourier spectrometer the enhancement of the brightness is of the order of 500 times greater than the grating and prism spectrometer known as the 'Jacquinot advantage'.

The dispersive spectrometer suffer from greater wavenumber errors, of a less predictable form owing to their general mechanical and thermal instability and can also be affected by non-uniform illumination across the monochromator entrance slit [14]. FT spectrometer typically uses the He-Ne lasers as a reference beam to monitor the displacement of the moving optical element, so providing an active internal absolute wavelength calibration [15]. This feature of FT spectrometers is known as the 'Cannes advantage'.

1.2.3. Detector

There are two detector commonly used depending upon the energy reaching the detector. A normal detector for routine work function is based on pyroelectric effect. Crystals such as deuterium triglycine sulphate in temperature resistant alkali halide window, with a permanent electric dipole moment respond to a sudden change in the dipolar order with the generation of compensating surface charges. IR or heat pulses can be origin if such induced disorder. The voltage accompanying the compensation charges can be used to detect the IR to the heat pulse.

The commonly used system is the Golay detector which works under a pneumatic principle. A thin film absorbs the incident IR light. The generated heat increases the pressure in the gas chamber which drives a mirror. The mirror is a part of an optical system that images a grating onto itself. Any small motion of the mirror leads to change in the overlap between grating and the image and thus gives a signal to the detector

1.2.4. Sampling Methods in IR Spectroscopy

A wide range of sampling technique is available for mounting of the sample. The technique depends on whether the sample is a gas, liquid, solid or polymer. Sampling techniques play an important role in recording IR spectrum. A choice of sampling technique is available for all states of matter depending on the applications.

Solids are usually examined as a mull, a pressed disc or as deposited glassy films. Mulls are prepared by grinding the solid and then suspending with 1-2 drops of mulling agent followed by grinding until the suspended particles are less than 2 μm. The mull is then examined as a thin film between flat salt plates. This technique has the advantage of speed but suffers many disadvantages. If the sample concentration is too low, the spectrum is due to mulling agent. On the other hand, if too much sample

is used the mull will not transmit radiation. The commonly used mulling agents are nujol, hexachlorobutadiene and a volt of 3s oil (halogenated hydrocarbon) depending upon the spectral region.

1.2.5. Alkali Halide Disc

The solid is mixed with suitable dry alkali halide (100-200mg) grounded in a mortar or ball mill and subjected to a pressure of about 10 ton/sq.inch in an evacuated dye. This sinters the mixture and produces a clear transparent disc of diameter 10-15 mm. The advantage of this method over mull technique is that it eliminates the problem of bands, which appear due to mulling agent. The most commonly used alkali halide is KBr, which is transparent in the commonly scanning region. The commonly used other alkali halides are NaCl, Csl and CsBr.

1.2.6. Solutions

The sample can be dissolved in a solvent and the spectrum of this solution can be recorded. The solution (usually 5%) is placed in a solution cell, which has length of usually 0.1-1.0 mm. The solvent chosen must satisfy certain criteria: (i) it has to dissolve the compound (ii) it should be non-polar as possible, to minimize solute solvent interactions (iii) it should not react with the sample (iv) it should not absorb IR radiation (v) it should be volatile and not viscous and (vi) it should be pure and dry CS_2, CCl4, $CHCl_3$ and $C_2H_2Cl_4$ are some of the solvents commonly used.

1.2.7. Reflectance Method

Reflectance technique is used for samples with low transmission which cannot be analyzed by the normal transmittance method [16]. This method depends on the total internal reflectance of light. The refractive index of the prism used for this

purpose should be greater than refractive index of the sample and the angle of incidence of IR radiation is greater than the critical angle.

1.2.8. Limitations of Infrared Spectroscopy

Materials such as KBr, NaCl, LiF and the like do not yield characteristic IR absorption spectra. Hence it is fortunate that they are useful as prisms, window materials and other optical components [17]. Molecules such as H_2, O_2, N_2 etc. will not yield any useful IR spectra because no change in dipole moment occurs during their lone stretching vibrations. The detectability limits of the usual IR quantitative procedure are not very great except for analytical methods relaying on absorption arising from vibration involving very highly polar bonds between atoms. The inability to transfer quantitative analytical methods from one instrument to another, even of the same make and model is another limitation. Optical isomers yield identical absorption spectra and therefore IR studies cannot distinguish between them.

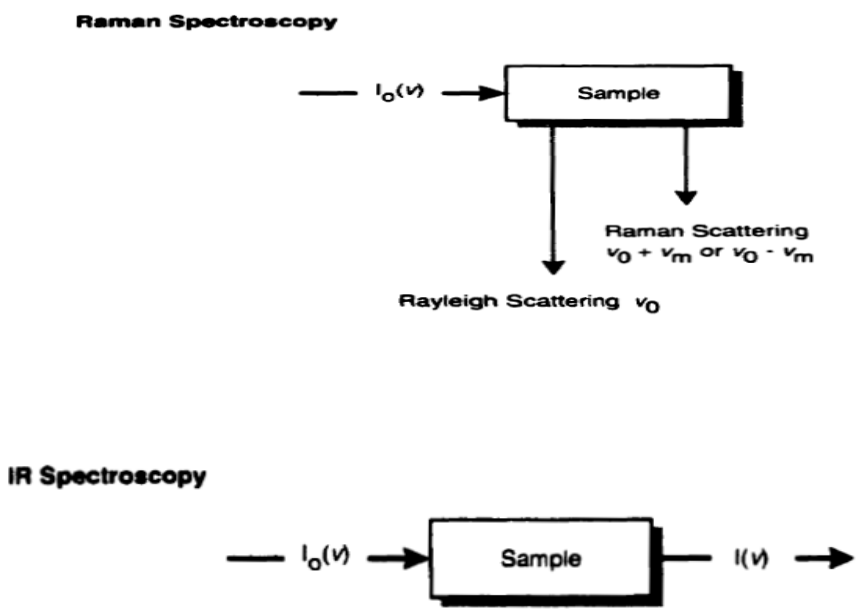

Fig.1.3. Comparison of IR (absorption) and Raman (scattering) spectroscopy

1.3. Fourier Transform Raman Spectroscopy (FT-Raman)

1.3.1. Introduction to Raman Spectroscopy

As stated in the previous section, vibrational transitions can be observed in either IR or Raman spectroscopy. Although Raman is complementary to FT-IR, it is based on different principle. Where IR absorption is based on changes in the dipole moment, Raman spectroscopy involves inelastically scattered light and is based on changes in the polarizability of the molecules. Fig. 1.3 illustrates the differences between the two methods.

1.3.2. The Principles of Raman Spectroscopy

Raman spectroscopy differs from the rotational and vibrational spectroscopy considered above in that it is concerned with the scattering of radiation by the sample, rather than an absorption process. It is named after the Indian physicist who first observed it in 1928, C.V. Raman. Both rotational and vibrational Raman spectroscopy is possible. The energy of the exciting radiation will determine which type of transition occurs - rotational transitions are lower in energy than vibrational transitions. In addition to this, rotational transitions are around 3 orders of magnitude slower than vibrational transitions. Therefore, collisions with other molecules may occur in the time in which the transition is occurring. A collision is likely to change the rotational state of the molecule, and so the definition of the spectrum obtained will be destroyed. Rotational spectroscopy is therefore carried out on gases at low pressure to ensure that the time between collisions is greater than the time for a transition.

In Raman spectroscopy, a sample is irradiated by an intense source (usually a laser) in the UV-visible or IR region and the scattered light is generally observed in a direction perpendicular to the incident beam. The scattered light consists of two types. The elastic Rayleigh scattering is strong and has the same frequency as the incident beam (ν_0). The inelastic Raman scattering is weak, approximately 10^5 times weaker

than the incident beam, and has frequencies of ($\nu_0 \pm \nu_m$) where ν_m, is a vibrational frequency of a given molecule. In Raman spectroscopy, the ν_m is measured as a shift from the incident frequency (ν_0) [18]. Stokes lines are those represented by the (ν_0 - ν_m) shift, while the Anti-Stokes lines are those represented by the ($\nu_0 + \nu_m$) shift, the process of Raman scattering can be explained using electromagnetic theory.

The electric field strength ($\vec{E}$) of the laser beam fluctuates with time (t):

$$\vec{E} = \vec{E}_0 \cos 2\pi\nu_0 t \qquad (1.8)$$

Where $\vec{E}_0$ the vibrational amplitude and ν_0 is the incident beam frequency. The simplest case is that of a diatomic molecule irradiated by this laser where an electric dipole moment (*P)* is induced with the proportionality constant α and is given by

$$P = \alpha\vec{E} = \alpha\vec{E}_0 \cos 2\pi\nu_0 t \qquad (1.9)$$

α is known as the *polarizability*. If a given molecule vibrates with a frequency of ν_m then the nuclear displacement *q* is given by the following equation:

$$q = q_0 \cos 2\pi\nu_m t \qquad (1.10)$$

where q_o is the vibrational amplitude. If the vibration has a small amplitude, then α: is a linear function of q.. Therefore:

$$\alpha = \alpha_0 + \left(\frac{\delta\alpha}{\delta q}\right) \qquad (1.11)$$

The polarizability at the equilibrium point is given as α_0 where $\left(\frac{\delta\alpha}{\delta q}\right)$ is the rate of change of α with respect to the change in q, which is evaluated at the equilibrium position.

Combining al1 the above equations, the following relationships are obtained:

$$P = \alpha\vec{E}_0 \cos 2\pi\nu_0 t \qquad (1.12)$$

$$P = \alpha_0 \vec{E}_0 \cos 2\pi\nu_0 t + \left(\frac{\delta\alpha}{\delta q}\right) q\vec{E}_0 \cos 2\pi\nu_0 t \qquad (1.13)$$

$$P = \alpha_0 \vec{E}_0 \cos 2\pi\nu_0 t + \left(\frac{\delta\alpha}{\delta q}\right) q_0 \cos 2\pi\nu_m t\vec{E}_0 \cos 2\pi\nu_0 t \qquad (1.14)$$

$$P = \alpha_0 \vec{E}_0 \cos 2\pi\nu_0 t + \left(\frac{\delta\alpha}{\delta q}\right) q_0 \vec{E}_0 \left(\cos(2\pi(\nu_0 + \nu_m)t) + \cos(2\pi(\nu_0 - \nu_m)t)\right) \qquad (1.15)$$

Therefore according to classical theory, the first term represents an oscillating dipole that radiates light of frequency ν_0 (Rayleigh scattering), while the second term corresponds to Anti-Stokes Raman scattering ($\nu_0 + \nu_m$) and the third term corresponds to Stokes Raman scattering ($\nu_0 - \nu_m$).

If $\left(\frac{\delta\alpha}{\delta q}\right) = 0$, then the vibration is not Raman active, i.e. the rate of change of polarizability with respect to the vibration must be non-zero for the vibration to be Raman active [15].

1.3.3. Background for Raman Spectroscopy

FT-Raman spectrophotometer is designed to eliminate the fluorescence problem encountered in conventional Raman spectroscopy [19]. The FT-Raman instrument has the following components: i) A near IR (NIR) laser excitation source, generally an Nd:YAG laser working at 1.06μm, ii) an interferometer equipped with an appropriate beam splitter, made of glass, and a detector for the NIR region. The detector is usually In GaAs or Ge semiconductor detector, iii) a sample chamber with scattering optical that match the input port of the Fourier Transform instrument, iv) an optical filter rejection of the Rayleigh-scattering light. Block diagram of such an instrument is shown in Fig.1.4.

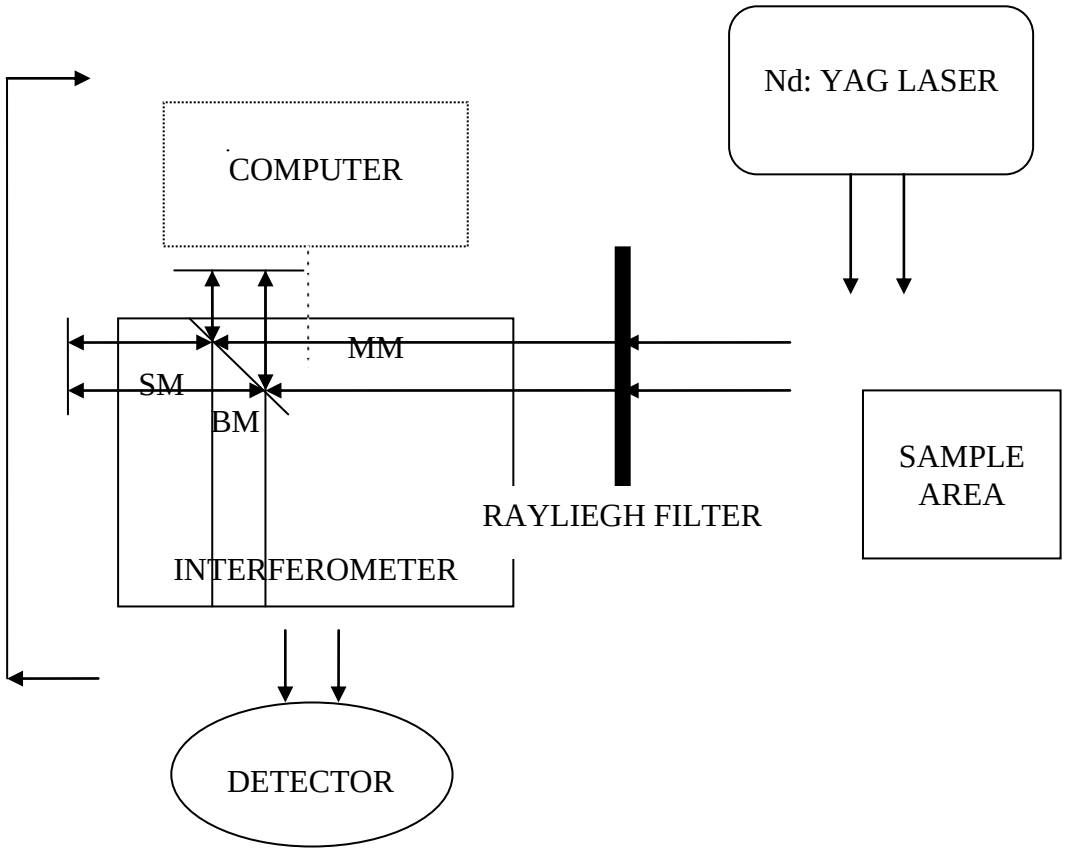

Fig.1.4. Block diagram of FT-RAMAN spectrometer

Fluorescence is eliminated by utilizing an excitation frequency well below the threshold for any fluorescence process. To focus and align the invisible Nd: YAG laser beam a visible He: Ne laser beam is co-aligned with the Nd: YAG beam. Another method of optical alignment can be realized by using fiber optics [20]. With fiber optic components, optical alignment is virtually eliminated which allows rapid switching from one sample to another. One of the advantages of FT instrument is that it can collect all the scattered radiation over the entire range of frequencies simultaneously during the whole period of the detection and it is called multiplexing.

This becomes a disadvantage as the intense Rayleigh line is the primary source of noise. Multiplexing redistributes the noise associated with Rayleigh line across the entire spectrum by the FT process and this is called as multiplexing disadvantage [21]. Interferometer can be combined with Rayleigh line filters (notch filters) in order to prevent the consequences of the multiplex disadvantage. The Rayleigh line filter minimizes the amount of Rayleigh scattered light entering the interferometer [22] and is essential for FT-Raman spectroscopy.

1.3.4. Dual Instruments

Due to the rapid development in the instrumentation techniques, nowadays both IR and Raman spectrophotometer are incorporated into a single instrument assembly and available commercially as a single package. The main advantages of such instruments are: i) Switching over from one technique to other is simple; ii) They are compact and iii) Comparatively cheaper. Bruker's FT-IR spectrophotometer IFS 66/S filter with FRA 106/S. ThermoNicolet's Nexus/Magna FT-IR and FT-Raman systems, ABB Bomen MB157 series these are some of the commercially available dual instrument package. Fig, 1.5 shows the schematic diagram of Brucker's FT-IR spectrophotometer IFS 66/S filter with Raman module FRA 106/S, which was used in the present work.

1.3.5. Sampling Methods in Raman Spectroscopy

Gases, liquids and solids can be studied by Raman spectrometer but the important thing to be taken care of while preparing sample is that they should be dust free. Glass is almost transparent in the Raman frequency region and thus samples in different phases can be measured in glass or silica containers or capillaries [7].

1.3.6. Solids

Solids as poly crystalline material or as a single crystal can be studied with the help of Raman technique. Solvents or alkyl halides or mull are not required for recording the spectra. Solids in the form of fine powder enclosed in a glass or silica fiber can be used. When the measurement is made as a single crystal, depending on the orientation of the crystal axis and polarization of the incident radiation the spectra may vary. Raman spectra can also be recorded for adsorbed species. Samples can also be studied using the Raman technique under various pressures and temperatures [7].

1.3.7. Liquids

Liquids may be examined neat or in solution and normally liquids of about 0.3 ml enclosed in glass or silica containers of capillaries may be required for obtaining good spectrum. Even though water cannot be used as solvent in IR studies, in the Raman studies water is one of a good solvent. Thus spectra of aqueous solutions can be easily studied and also spectra of water soluble biological material can be easily recorded [5].

1.3.8. Uses of Raman Spectroscopy

Raman spectroscopy is useful for analyzing molecules without a permanent dipole moment which would not show up on an IR spectrum. A useful 'exclusion rule' states that for molecules with an inversion centre, no modes can be both IR and Raman active. It can be used to determine bond lengths in non-polar molecules. It is useful for determining the identity of organic and inorganic species in solution, as the Raman transitions for these species are more characteristic than for IR, where the transitions are much more affected by the other species present in the solution.

1.4. Nuclear Magnetic Resonance (NMR) Spectroscopy

NMR spectroscopy is the most powerful tool available for determining the structure of organic compounds. This technique relies on the ability of atomic nuclei to behave like a small magnet and align them with an external magnetic field. When irradiated with a radio frequency signal the nuclei in a molecule can change from being aligned with the magnetic field to being opposed to it. Therefore, it is called "nuclear" for the instrument works on stimulating the "nuclei" of the atoms to absorb radio waves. The energy frequency at which this occurs can be measured and is displayed as an NMR spectrum. The most common nuclei observed using this technique are 1H and 13C, but also 31P, 19F, 29Si and 77Se NMR are available [23]. When the frequency of the rotating magnetic field and that of the processing nucleus (Larmor frequency) become equal, they are said to be in resonance and absorption or emission of energy by the nucleus can occur. A plot of the peak intensities versus the frequencies of absorption constitutes an NMR spectrum. A simple block diagram of an NMR spectrometer is shown in Fig.1.5.

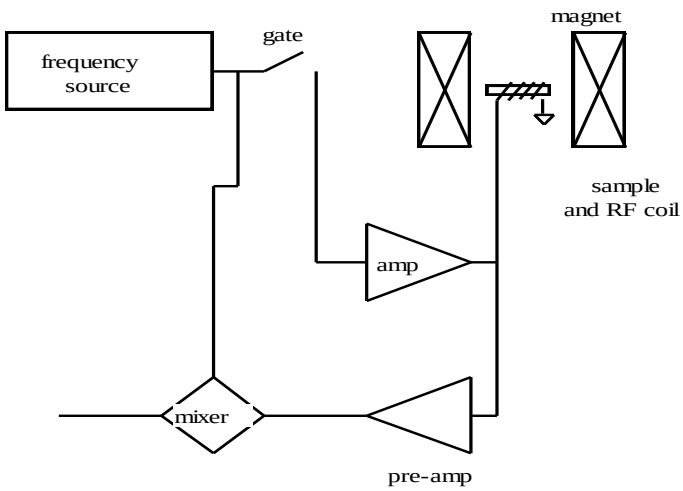

Fig.1.5. Block diagram of NMR spectrometer

The frequency source generates a sin wave at a frequency close to the resonance frequency. This is gated, amplified and applied to the probe to generate an excitation field. Following the excitation and sample consists of a rotating bar magnet that couples into the coil to produce an oscillating voltage across the coil which is detected and amplified. The mixer is used to remove the excitation frequency so that only the offset frequency is recorded.

The ^{1}H nucleus is the most commonly studied by NMR spectroscopy because of its high natural abundance (99.98%) and the fact that it is invariably present in the majority of organic compounds. NMR spectrum provides information about the number of different types of protons and also regarding the nature of the immediate environment of each of them. Despite its low natural abundance (1:1%), ^{13}C is also an important nucleus because carbon forms the back bone of all organic compounds and valuable structural information can be derived by ^{13}C NMR spectroscopy.

1.4.1. Applications of NMR

- To identify and/or elucidate detailed structural information about chemical compounds.

  For example:

- Determining the purity of medicines before they leave the factory
- Identifying contaminants in food, cosmetics, or medications.
- Helping research chemists discover whether a chemical reaction has occurred at the correct site on a molecule.
- Identifying drugs seized by police and customs agents
- Checking the structure of plastics, to ensure they will have the desired properties

1.5. Ultraviolet–visible (UV) spectroscopy

Ultraviolet-visible spectroscopy or ultraviolet-visible spectrophotometry (UV-Vis or UV/Vis) refers to absorption spectroscopy or reflectance spectroscopy in the ultraviolet-visible spectral region. This means it uses light in the visible and adjacent (near-UV and near-infrared (NIR)) ranges. The absorption or reflectance in the visible range directly affects the perceived color of the chemicals involved. In this region of the electromagnetic spectrum, molecules undergo electronic transitions. This technique is complementary to fluorescence spectroscopy, in that fluorescence deals with transitions from the excited state to the ground state, while absorption measures transitions from the ground state to the excited state [24].

The principles of UV centre on the fact that molecules have the ability to absorb ultraviolet or visible light. The absorption corresponds to the excitation of outer electrons in the molecules concerned. When a molecule absorbs energy an electron is promoted from the Highest Occupied Molecular Orbital (HOMO) to the Lowest Unoccupied Molecular Orbital (LUMO).

It must be noted that occupied molecular orbitals with the lowest energy are the σ orbitals, and then at a slightly higher energy are the π orbitals and non-bonding orbitals (those with unshared pairs of electrons) at still a higher energy. The highest energy orbitals belong to π* and σ*, i.e. the unoccupied or as otherwise known as, the antibonding orbitals [4]. The electronic energy levels and transitions are shown in Fig.1.6.

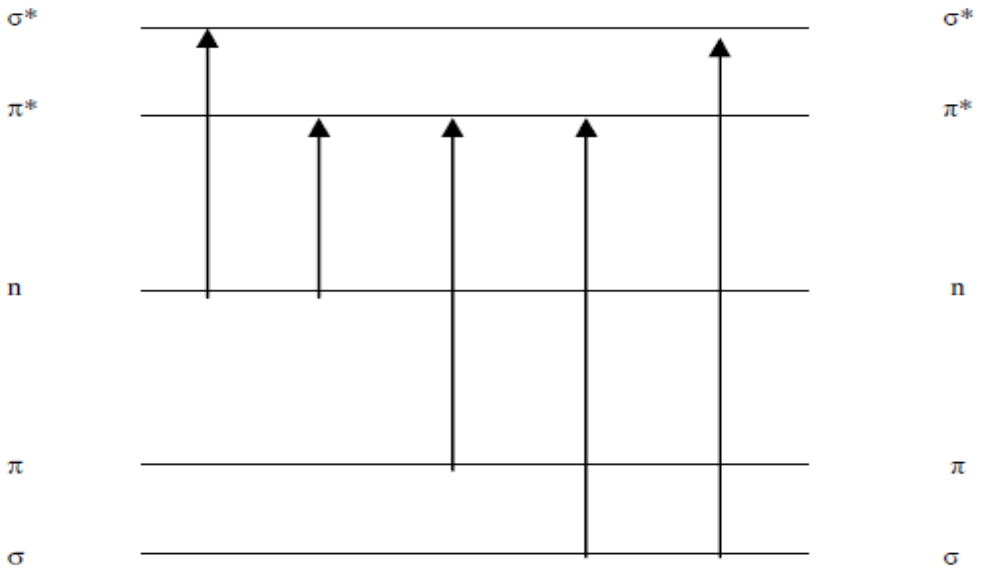

Fig.1.6. Electronic energy levels and transitions

The schematic diagram of a double-beam UV-Visible spectrophotometer is shown in Fig.1.7.

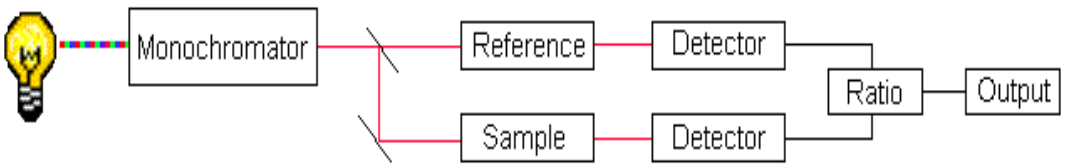

Fig.1.7. Schematic diagram of a double-beam UV-Visible spectrophotometer

1.5.1. Instrumental Components

1.5.1.1. Sources of Visible Radiation

The tungsten filament lamp is commonly employed as a source of visible light. This type of lamp is used in the wavelength range of 350 - 2500 nm. The energy emitted by a tungsten filament lamp is proportional to the fourth power of the

operating voltage. This means that for the energy output to be stable, the voltage to the lamp must be very stable indeed. Electronic voltage regulators or constant-voltage transformers are used to ensure this stability.

1.5.1.2. Wavelength Selector (Monochromator)

All monochromators contain the following component parts;

- An entrance slit
- A collimating lens
- A dispersing device (usually a prism or a grating)
- A focusing lens
- An exit slit

Polychromatic radiation (radiation of more than one wavelength) enters the monochromator through the entrance slit. The beam is collimated, and then strikes the dispersing element at an angle. The beam is split into its component wavelengths by the grating or prism. By moving the dispersing element or the exit slit, radiation of only a particular wavelength leaves the monochromator through the exit slit.

1.5.1.3. Cuvettes

The containers for the sample and reference solution must be transparent to the radiation which will pass through them. Quartz or fused silica cuvettes are required for spectroscopy in the UV region. These cells are also transparent in the visible region. Silicate glasses can be used for the manufacture of cuvettes for use between 350 and 2000 nm.

1.5.1.4. Detectors

The photomultiplier tube is a commonly used detector in UV-Vis spectroscopy. It consists of a *photoemissive cathode* (a cathode which emits electrons when struck by photons of radiation), several *dynodes* (which emit several electrons

for each electron striking them) and an *anode*. A photon of radiation entering the tube strikes the cathode, causing the emission of several electrons. These electrons are accelerated towards the first dynode (which is 90V more positive than the cathode). The electrons strike the first dynode, causing the emission of several electrons for each incident electron. These electrons are then accelerated towards the second dynode, to produce more electrons which are accelerated towards dynode three and so on. Eventually, the electrons are collected at the anode. By this time, each original photon has produced 10^6 - 10^7 electrons. The resulting current is amplified and measured. Photomultipliers are very sensitive to UV and visible radiation. They have fast response times. Intense light damages photomultipliers; they are limited to measuring low power radiation

The linear photodiode array is an example of a *multichannel photon detector*. These detectors are capable of measuring all elements of a beam of dispersed radiation simultaneously. A linear photodiode array comprises many small silicon photodiodes formed on a single silicon chip. There can be between 64 to 4096 sensor elements on a chip, the most common being 1024 photodiodes. For each diode, there is also a storage capacitor and a switch. The individual diode-capacitor circuits can be sequentially scanned. In use, the photodiode array is positioned at the focal plane of the monochromator (after the dispersing element) such that the spectrum falls on the diode array. They are useful for recording UV-Visible absorption spectra of samples that are rapidly passing through a sample flow cell, such as in an HPLC detector.

Charge-Coupled Devices (CCDs) are similar to diode array detectors, but instead of diodes, they consist of an array of photo capacitors. UV/Vis spectroscopy is routinely used in the quantitative determination of solutions of transition metal ions highly conjugated organic compounds, and biological macromolecules.

1.6. Computational details

Development of the performance of computers and the theory has made computational simulations an important tool today; increasingly accurate results can be obtained in a reasonable time for even large and complicated molecular systems. Modeling molecular properties is an important aspect of the quantum mechanical based electronic structure theory calculations [25-27]. The electronic structure methods broadly fall into two methods: semi-empirical methods, *ab initio* and Density Functional Theory (DFT) methods. Semi-empirical methods use parameters derived from experimental data to simplify the computation. They solve an approximate form of the Schrödinger equation that depends on having appropriate parameters available for the type of chemical system under investigation.

Ab initio methods use no experimental parameters in their computations and are based solely on the laws of quantum mechanics and use only physical constants like speed of light(c), masses (m), charges of the electrons and nuclei (e) and Plank's constant (h). They compute solutions to the Schrodinger equation using a series of rigorous mathematical approximations. *Ab initio* computations provide high quality and quantitative predictions for a broad range of system and are not limited to a class of molecules. The simplest type of *ab initio* electronic structure calculation in the Hartree-Fock (HF) scheme, in which the Columbic electron-electron repulsion is not specifically taken into account; only its average effect is included in the calculation.

DFT is a quantum mechanical method used in physics and chemistry to investigate the electronic structure theory, in particular HF theory and its descendants, are based on the complicated many electron wave functions. The main objective of DFT is to replace the many-body electronic wavefunction with the electronic density as the basic quantity [28], whereas the many-body wavefunction is dependent on 3N

variables, three spatial variables for each of the N electrons, the electronic density is only a function of three variables and is a simpler quantity to deal with body conceptually and practically [25-31].

The most common implementation of DFT is through the Kohn-Sham [31] method. Within the framework of Kohn-Sham DFT, the intractable many-body problem of interacting electrons in a static external potential is reduced to a tractable problem of non-interacting electrons moving in an effective potential. The effective potential includes the external potential is reduced to a tractable problem of non-interacting electrons moving in an effective potential. The effective potential includes the external potential and the effects of the Columb interactions between the electronic, e.g. the exchange and correlation interactions. Since from the electronic density is not known explicitly, many functions have been defined to calculate electronic density of the system.

They are broadly classified into Local Density Approximations (LDA) methods (eg.: SVWN which takes into account a local spin density exchange by Slater, combined with the correlations function of Vosko, Wilk and Nusair); Generalized Gradient Approximation (GGA) methods (e.g. BLYP Slater exchange along with corrections involving the gradient of the density combined with the correction function of Lee-Yang and Parr); PW91 (with the non-local correlation provided by Perdew/Wang 91 correction functional); PW86 (the Perdew 86 correction functional) etc ; Hybrid methods (e.g. B3LYP: Becke's three parameter hybrid functional combined with Lee-Yang-Parr correlation functional); BP86 (Becke's 1988 exchange functional combined with the gradient-corrected correction function of Perdew); B3P86 (Becke's three parameter hybrid method with the non-local correlation provided by Perdew/Wang 91 expression) etc [25-31]. The acronyms like GGA, VWN (Vosko, Wilk and Nusair) etc are generic names in practice. The most popular

method to calculate electronic density is the hybrid method and B3LYP is one of the most popular hybrid methods. In B3LYP method, three parameters have been used to give satisfied theoretical results compared to the experimental results in many cases. In all of these approaches, in addition to the choice of method, it is necessary to choose a basis set.

1.6.1. The Hartree-Fock (HF) Theory

The HF method is the most fundamental *ab initio* technique. One electron orbital expanded in basis functions are used in a single Slater determinant to calculate the total energy. The underlying physical laws necessary for the mathematical theory of a large part of physics and the whole of chemistry are thus completely known, and the difficulty is only that the exact application of these laws leads to equations much too complicated to be soluble. An exact solution to the Schrödinger equation is not possible for any but the most trivial molecular systems. However, a number of simplifying assumptions and procedures do make an approximate solution possible for a large range of molecules.

1.6.2. Molecular Orbitals and Electron Spin

The electronic Hamiltonian depends only on the spatial coordinates of the electrons, but to completely describe an electron it is necessary to specify its spin. This is done by introducing two spin functions $\alpha(\omega)$ and $\beta(\omega)$ corresponding to spin up and spin down respectively. The spin orbitals, $\chi(x)$ are made up of a spatial component, $\psi(r)$, and a spin component.

The wave function,ψ, can be represented by a combination of normalized molecular orbitals (MOs) (χ_i,χ_j.....) [28]. The simplest way of defining ψ as a combination of these MOs is by forming their *Hartree product*:

$$\Psi^{HP}(x_1,x_2.....x_N) = \chi_I(x_1)\chi_j(x_2) \ldots.\chi_k(x_N) \qquad (1.16)$$

There are problems with the Hartree product since it does not satisfy the *antisymmetry principle*. This principle is based on the fact that electrons are indistinguishable and demands that the electronic wavefunction (ψ) changes sign with respect to the interchange of the space and spin coordinates of any two electrons [32]. The exchange of any two electrons within the Hartree product (ψ^{HP}) clearly distinguishes between two electrons. Therefore an antisymmetric function must be formed and this is done by taking the determinant of the MOs. Each electron is associated with each orbital if the determinant is expanded.

$$\Psi(x_1, x_2, ..., x_N) = (N!)^{-1/2} \begin{vmatrix} \chi_i(x_1) & \chi_j(x_1) & \cdots & \chi_k(x_1) \\ \chi_i(x_2) & \chi_j(x_2) & \cdots & \chi_k(x_2) \\ \vdots & \vdots & \vdots & \vdots \\ \chi_i(x_N) & \chi_j(x_N) & \cdots & \chi_k(x_N) \end{vmatrix} \qquad (1.17)$$

The simplest trial function is this single Slater determinant function (Equation 1.16) in which N spin-orbitals are occupied by N electrons. HF theory can be equated to single determinant theory. Therefore the goal is to find a set of one - electron functions (χ_a) such that there is a single determinant formed from these orbitals that yields the best possible approximation to the ground state of the N electron system described by an electronic Hamiltonian:

$$|\Psi_0\rangle = |\chi_1 \chi_2 .... \chi_a \chi_b .... \chi_N\rangle \qquad (1.18)$$

1.6.3. The Fock Operator

The HF equation is given by the following expression involving the one-electron Fock operator:

$$f(1)\chi_a(1) = \varepsilon_a \chi_a(1) \qquad (1.19)$$

and the Fock operator is defined as:

$$f(1) = h(1) + v^{HF}(1) = h(1) + \sum_b \left[J_b(1) - K_b(1)\right] \quad (1.20)$$

where $h(1)$ denotes the core Hamiltonian operator which involves the electronic kinetic energy operator and electronic-nuclear attraction operator. It should be noted for clarity that $\chi_a(l)$ is equivalent notation to $\chi_a(x_l)$. The coulomb operator ($J_b(l)$) represents the average local potential at x_i arising from χ_b:

$$J_b(1)\chi_a(1) = \left\lfloor \int dx_2 |\chi_b(2)| r_{12}^{-1} \right\rfloor \chi_a(l) \quad (1.21)$$

The exchange operator ($K_b(1)$) represents the exchange of two electrons and is dependent on the value of χ_a over al1 space and not just at x_i. This operator is defined by the following relation:

$$K_b(1)\chi_a(l) = \left\lfloor \int dx_2 \chi_b^*(2) r_{12}^{-1} \chi_a(2) \right\rfloor \chi_b(l) \quad (1.22)$$

1.6.4. The Hartree-Fock Hamiltonian

An extension of the Fock operator is the HF Hamiltonian which is given by the following relationship:

$$\hat{H}_0 = \sum_{i=1}^{N} f(i) = \sum_{i=1}^{N} h(i) + \sum_{i=1}^{N} v^{HF}(i) \quad (1.23)$$

This HF Hamiltonian can be applied to the entire wave function rather than just the spin-orbital functions:

$$\hat{H}_0 |\Psi_0\rangle = E_0^{(0)} |\Psi_0\rangle \quad (1.24)$$

$$E_0^{(0)} = \sum_a \varepsilon_a \quad (1.25)$$

Using the Born-Oppenheimer approximation, the following is true:

$$\hat{H}_{elec} = -\sum_{i=1}^{N} \frac{1}{2}\nabla_i^2 - \sum_{i=1}^{N}\sum_{i=1}^{N} \frac{Z_A}{r_{iA}} + \sum_{i=1}^{N}\sum_{j>i}^{N} \frac{1}{r_{ij}} = \sum_{i=1}^{N} h(i) + \sum_{i=1}^{N}\sum_{j>i}^{N} \frac{1}{r_{ij}} \quad (1.26)$$

A perturbation (V) exists for the HF Hamiltonian defined by the following relationship:

$$\hat{H}_{elec} = \hat{H}_0 + V \tag{1.27}$$

$$V = \hat{H}_{elec} - \hat{H}_0 = \sum_{i=1}^{N} \sum_{j>i}^{N} \frac{1}{r_{ij}} - \sum_{i=1}^{N} v^{HF}(i) \tag{1.28}$$

The HF energy, which is used in HF *ab initio* calculations, is given by the following Equation [33]:

$$E_0 = \sum_a \varepsilon_a + \langle \Psi_0 | V | \Psi_0 \rangle \tag{1.29}$$

Using the HF operator, the associated *ab initio* calculation uses user-defined guess geometry for the initial calculation and through an iterative process it arrives at a converged value that satisfies the parameters of the given computation.

1.6.5. Basis Sets

A basis set is used to form a mathematical representation of the MOs. To exactly represent the MOs, the basis functions should form a complete set. This requires an infinite number of basis functions, while in practice, a finite number are used [34]. MOs are expressed as the linear combinations of a predefined set of one-electron functions known as basis functions. An individual MO is defined as:

$$\phi_i = \sum_{\mu=1}^{N} c_{\mu i} \chi_\mu \tag{1.30}$$

where $c_{\mu i}$ are known as MO expansion coefficients. The basis functions, X_i, ..., X_N, are usually chosen to be normalized. Gaussian and most other *ab initio* programs use Gaussian-type functions for their basis sets. These Cartesian Gaussian functions have the general form:

$$g(\alpha, \vec{r}) = c x^n y^m Z^l e^{-ar^2} \tag{1.31}$$

Where $\vec{r}$ is composed of x, y, and α is a constant determining the size (radial extent) of the function. The constant of normalization (c) is determined by:

$$\int_{all\,space} g^2 = 1 \qquad (1.32)$$

The normalization constant therefore depends on α, l, m, and n. Linear combinations of the primitive Gaussians as seen above are used to form the actual basis functions called the contracted Gaussians which have the form:

$$\mathrm{X}_{\mu} = \sum_{p} d_{\mu p} g_{p} \qquad (1.33)$$

where $d_{\mu p}$ are fixed constants within a given basis set. These functions are also normalized. Therefore the molecular orbitals for a basis set can be described as:

$$\varphi_i = \sum_{\mu} C_{\mu i} \mathrm{X}_{\mu} = \sum_{\mu} C_{\mu i} \left(\sum_{p} d_{\mu p} g_{p} \right) \qquad (1.34)$$

It is essential to understand basis sets because they are the foundation of modern *ab initio* techniques [28]. The size and quality of the basis set used in an *ab initio* calculation largely determines the quality of the final result. Many basis sets have been optimized and tested over the years. A minimal basis set has one Slater-Type Orbital (STO) per atomic orbital. Each STO is then approximated as a linear combination of *N* Gaussian functions, where the coefficients are chosen to give the best least-squares fit to the STO. Most commonly, *N* = 3, which gives the basis set STO-3G. Therefore the minimal basis set of STOs for a compound containing only first-row elements and hydrogen is denoted by (2s lp/ls) [34].

A basis set can be improved by increasing the number of basis functions per atom. Polarized basis sets allow for the addition of orbitals with angular momentum beyond what is required for the ground state description of each atom; this allows for flexibility in different bonding situations. The polarized basis set 6-31G* is a basis set that adds *d* polarization functions on each non-hydrogen atom. The 6-31G** basis set adds p functions to the hydrogens as well. The 6-31+G** basis set adds diffuse functions (+) to the non-hydrogen atoms, which are important for systems with lone

pairs, anions, and some excited states, as well as the polarization functions. The 6-31lG** basis set is commonly used for electron correlation calculations on molecules containing first-row atoms. The 6-311G** basis set, which is single zeta for the core and triple zeta for the valence atomic orbitals, contains five *d*-type Gaussian polarization functions on each non-hydrogen atom and three *p*-type polarization functions on each hydrogen atom [35]. Even larger basis sets are available which add multiple polarization functions per atom the triple zeta basis set [28] or additional functions for the valence shell.

1.6.6. Limitations of Hartree-Fock (HF) Theory

HF theory is useful for providing the initial predictions, but is limited by the fact that it does not take into account the instantaneous interactions between electrons. It is insufficient for modeling the energetic of reactions, bond dissociations, or excited states [28]. Energies calculated using the HF method is typically in error by 0.5% to 1% [34]. The region surrounding each electron in an atom, known as a *Coulomb hole*, is an area in which the probability of finding another electron is small. The HF method does include some correlation for the motions of electrons that have the same spin, but a method that includes electron correlation will consider the motions and interactions of electrons in more detail.

Improving the basis set will not necessarily improve the results for HF calculations. The calculated energy of a given molecule cannot improve past the Hartree-Fock limit. Due to the variational principle, the energy at the HF limit is above the exact energy. Larger and larger basis sets will keep lowering the energy until the HF limit is reached, and at this point, no further improvement may be made. Therefore it is necessary to move on to methods such as DFT and MP that include electron correlation and can improve on the HF method.

1.6.7. Electron Correlation

Desirable features of an *ab initio* method including electron correlation are listed below:

[1] The technique should be well defined and should lead to a unique energy and a continuous potential energy surface for any nuclear configuration.

[2] It should be size consistent. This means that the results for a system of molecules infinitely separated from one another must equal the sum of the results obtained for each individual molecule calculated separately [28].

[3] It should be exact when applied to a two-electron system.

[4] It should be efficient for large basis sets.

[5] It should be vibrational, resulting in a computed energy that is an upper bound to the correct energy.

[6] It should give an adequate approximation to the full configuration interaction result.

Full configuration interaction includes a mixing of al1 possible electronic states of a given molecule and is the most complete non-relativistic treatment of molecular systems possible within the limitations imposed by a chosen basis set [28].

No technique satisfies al1 of these criteria. Most methods introduce approximations with varying degrees of success [31, 35-37].

1.6.8. Density Functional Theory (DFT)

DFT has become one of the most frequently used tools in quantum chemistry for the description of atoms, molecules, and chemical reaction systems. An impressive number of applications of DFT have proven its usefulness and reliability [37]. The DFT approach is based upon a strategy of modeling electron correlation via general functional of the ED.

Computational methods based on DFT are attractive because they tend to be less resource intensive than conventional *ab initio* calculations and Quadratic Configuration Integral Spin Density (QCISD) while also taking into account the effects of electron correlation. DFT was established by W. Kohn and L. Sham [31] who showed that the electron density could be used as a fundamental quantity to develop a rigorous many-body theory. DFT is different from HF since it replaces the exchange-correlation energy by a one-electron integral involving the local electron spin densities or by an integral involving these spin densities and their gradients. When these functionals are used in conjunction with the Kohn-Sham (KS) procedure [31] and an expansion of the KS orbitals in terms of a basis set, then the techniques become analogous to conventional HF theories with the addition of electron correlation [38].

Formal DFT methods are based on the LDA given by the following equation, where ρ(r) is the electron density:

$$\mathrm{E}_{xc}^{LDA}[\rho(r)] = \int \rho(r)\varepsilon_{xc}(\rho(r))dr \qquad (1.35)$$

where ε_{xc} (n) is the accurately known exchange-correlation energy per particle of a uniform electron gas of density n. The LDA is exact for a homogeneous system and arbitrarily accurate for a system with varying density. Therefore LDA is the most basic approximation for E_{xc} since it requires only the energy (ε_{xc}) of the uniform electron gas and is found to yield only fair agreement with experimental molecular properties. The local spin-density approximation (LSDA) is an improvement on LDA since it uses different orbitals and different densities for electrons with different spin [34]. A better functional would exhibit effects of the in homogeneity of the ED, since atoms and molecules do have inhomogeneous EDs, but this effect is ignored in the LDA model. The addition of gradient corrections to the LDA model allows for better

modeling of the ED [39]. A gradient-corrected DFT method calculates not only the magnitude of the density, but also considers how rapidly the density is changing about a point in space. The more common *hybrid* DFT methods incorporate some HF exchange with the ED calculation [40] which includes gradient corrections.

The functionals that are used in DFT are separated into exchange and correlation parts. The exchange part can be either Slater (S), which corresponds to a free-electron gas, or Becke (B), which includes a gradient correction. The correlation part can be either ignored or treated with the VWN [41] parameterization for exact uniform gas results or treated with the gradient corrected functional of Lee, Yang, and Parr (LYP) [42]. A common gradient corrected DFT method uses the Becke Yang Parr (BLYP) function, which combines *a* local exchange functional with the gradient correction from Becke and uses the LYP correlation functional. The Becke's three parameter hybrid functionals B3LYP method differs from the BLYP method because it utilizes a functional that is a hybrid of exact (HF) exchange with local and gradient-corrected exchange and correlation terms [43]. DFT methods are appealing for many types of molecules because they can provide results that are as accurate as conventional methods, but DFT is much less resource intensive than such methods as MP, CC, and QCISD [28]. Current evidence [39, 44] suggests that vibrational frequencies calculated using DFT is close to those found by experiment.

All electronic structure calculations can be performed using Gaussian 16 [45] electronic structure program, which brings a variety of new methods, property predictions and performance enhancements and Gauss View 6, provides support for all major Gaussian 16 features is capable of predicting many properties of molecules and reactions. They are:

[1] Molecular Energies and Structures;

[2] Energies and Structures of Transition States;

[3] Bond and Reaction Energies;

[4] Molecular orbitals;

[5] Multipole moments;

[6] Atomic Charges and Electrostatic Potential;

[7] Vibrational Frequencies and

[8] IR and Raman Spectra.

The Gaussian 16 program accepts molecular specifications in several different formats, like Cartesian coordinates, Z-matrix format (internal coordinates) and mixed internal and Cartesian coordinates. All molecular specifications require the charge and spin multiplicity.

1.6.9 Molecular docking

Molecular docking is of great importance in the field of structural molecular biology, Pharmacogenomics and computer-assisted drug design. Docking can be used to execute virtual screening on large libraries of compound, rank the results, and propose structural propositions of the predominant binding modes of a ligand to the target, which is invaluable in lead optimization. The information attained thus forms a database for further experimental analysis of the selected molecule as a potential drug. Experimentally analysing a wide array of compounds is time consuming and not feasible. However, employing a virtual screening process like molecular docking ensures a foster mode of drug designing and also provides every conformation possible based on the receptor and ligand molecule.

1.6.9 Antimicrobial studies by disk-diffusion methods

Agar disk-diffusion testing developed in 1940, is the official method used in many clinical microbiology laboratories for routine antimicrobial susceptibility testing. Nowadays, many accepted and approved standards are published by the Clinical and Laboratory Standards Institute (CLSI) for bacteria and yeasts testing. Although not all fastidious bacteria can be tested accurately by this method, the standardization has been made to test certain fastidious bacterial pathogens like streptococci, *Haemophilus influenzae*, *Haemophilus parainfluenzae*, *Neisseria gonorrhoeae* and *Neisseria meningitidis*, using specific culture media, various incubation conditions and interpretive criteria for inhibition zones . In this well-known procedure, agar plates are inoculated with a standardized inoculum of the test microorganism. Then, filter paper discs (about 6 mm in diameter), containing the test compound at a desired concentration, are placed on the agar surface. The Petri dishes are incubated under suitable conditions. Generally, antimicrobial agent diffuses into the agar and inhibits germination and growth of the test microorganism and then the diameters of inhibition growth zones are measured shows the growth media, temperature, period of incubation and inoculum size required by CLSI standards.

References

[1] D.H. Williams, L. Fleming, Spectroscopic Methods in Organic Chemistry, Tata McGraw Hill Publishing Company Ltd, V edition, (1988).

[2] C.N. Banwell, Elaine M. McCash, Fundamentals of Molecular Spectroscopy, Tata McGraw Hill Publishing Company Ltd, IV edition, (1995).

[3] G. Aruldhas, Molecular Structure and Spectroscopy, Prentice-Hall of India Private Limited, I edition, (2000).

[4] Pavia Lampman Kriz, Introduction to Spectroscopy, John Wiley, New York, III Edition, (2003).

[5] Bernhard Schrader, Infrared and Raman Spectroscopy, VCH Pub., Inc., New York, (1995).

[6] L.J. Bellamy, The Infrared Spectra of Complex Molecules, Vol. 1. III Edition, Chapman and Hall, London, (1975), p.93.

[7] N.B. Colthup, L.H. Daly, Stephen E. Wiberly, Introduction to Infrared and Raman Spectroscopy, Academic Press, New York, (1964), p. 74, 221, 226.

[8] Mans Chandra, Atomic structure and the chemical bond. Tata McGraw Hill Publishing Company Ltd, IV edition, (2000).

[9] H.A. Szymanski, Interpreted Infrared Spectra. Vols, 1-3, Plenum Press, New York, (1964), (1966), (1967).

[10] G.M. Barrow, Introduction to Molecular Spectroscopy, McGraw-Hill, Kogakusha Ltd., International Student edition, (1962).

[11] P.R. Griffiths, J.A. De Haseth, Fourier Transform Infrared Spectroscopy, Wiley, New York, (1986).

[12] C. Mile, M. Guiliano, H. Reymond, H. Dou, Analysis of Hydrocarbons by Fourier Transform Infrared Spectroscopy, Intern. J. Environ. Anal. Chem. 21 (1985) 239.

[13] H. Kuzmnay, Solid Spectroscopy, Springer, New York, (1998).

[14] A. Crookell, P.J. Hendra, H.M. Mould, A.J. Turner, Fourier transform Raman spectroscopy in the near-infrared region, J. Raman Spectrosc. 21 (1990) 85.

[15] J. Cones, P. Cones, Near-Infrared Planetary Spectra by Fourier Spectroscopy. I. Instruments and Results, J. Opt. Soc. Am. 56 (1966) 896.

[16] M. Urban, ATR of Polymers, ACS, Washington, D.C. (1996).

[17] D.N. Kendall, Applied Infrared Spectroscopy, Chapman and Hall, London (1966).

[18] Ferraro, K. Nakamoto, Introductory Raman Spectroscopy; Academic Press, Inc.: San Diago (1994).

[19] S.E. Parker, K. Williams, A.J. Turner, P.J. Hendra, Fourier Transform Raman Spectroscopy Using a Bench-Top FT-IR Spectrometer, Appl. Spectros. 42 (1988) 796.

[20] P.J. Hendra, Int. J. Vibr. Spec. / www. ijvs. com /, 5, 5, 2 (2001).

[21] D.J. Cutleer, The Development of Fourier Transform Raman Spectroscopy, Spectrochim. Acta 46A (1990) 123.

[22] T. Hirschfeld, B. Chase, FT-Raman Spectroscopy: Development and Justification, Appl. Spectrosc. 40 (1986) 133.

[23] Teacher Notes on: NMR Spectroscopy, Free Radical Chemistry Biotechnology, www.freeradical.org.au.

[24] Skoog, Principles of Instrumental Analysis, 6th ed. Thomson Brooks/Cole. (2007), p. 169.

[25] Jensen, “Introduction to Computational Chemistry”, John Wiley & Sons, N.Y, (1999).

[26] C.J. Cramer, “Essentials of Computational Chemistry Theories and Models”, 2nd edition, John Wiley & Sons, Ltd., (NY), (2004).

[27] Ira.N. Levine, Levin "Quantum Chemistry", 5th edition, Person Education (Singapur) Pte. Ltd., (2004).

[28] J.B. Foreman, A. Frisch, "Exploring Chemistry with Electronic Structure Methods", Gaussian, Inc., Pittsburg, (1993).

[29] W.J. Hehre "*Ab Initio* Molecular Orbital Theory", John Wiley & Sons, N.Y, U.S.A (1986).

[30] P. Hohenberg, W. Kohn, Inhomogeneous Electron Gas, Phys. Rev. B 136 (1964) 864.

[31] Kohn, L.J. Sham, Self-Consistent Equations Including Exchange and Correlation Effects, Phys. Rev. A 140 (1965) 1133.

[32] A. Szabo, N.S. Ostland, Modern Quantum Chemistry: Introduction to Advanced Electronic Structure Theory, Dover Publications Inc., Mineola, N.Y., 1st ed., (1996).

[33] P. F. Bernath, Spectra of Atoms and Molecules, 1st ed, Oxford University Press, New York, (1995).

[34] I.N. Levine, Quantum Chemistry, Prentice-Hall Inc., Englewood Cliffs, New Jersey, 4th ed. (1991).

[35] J. Cizek, On the Correlation Problem in Atomic and Molecular Systems. Calculation of Wavefunction Components in Ursell-Type Expansion Using Quantum-Field Theoretical Methods, J. Chem. Phys. 15 (1960) 4256.

[36] C. Moller, M.S. Plesset, Note on an Approximation Treatment for Many-Electron Systems, Phys. Rev. 16 (1934) 618.

[37] J.A. Pople, M. Head-Gordon, K. Raghavachari, J. Chem. Phys. 87 (1987) 5968.

[38] B.G. Johnson, P.M.W. Gill, J.A. Pople, The performance of a family of density functional methods, J. Chem. Phys. 98 (1993) 5612.

[39] R.G. Parr, W. Yang, Density-Functional Theory of Atoms and Molecules, Oxford University Press, Oxford, (1989).

[40] University of Minnesota, "An *Ab initio* Handbook and Glossary of Terms", http://pollw.chem.umn.edu/ sullivan/8003/handouts/, (1997).

[41] S.H. Vosko, I. Wilk, M. Nusair, Accurate spin-dependent electron liquid correlation energies for local spin density calculations: a critical analysis, Can. J. Phys., 58 (1980) 1200.

[42] C. Lee, W. Yang, R.G. Parr, Development of the Colle-Salvetti correlation-energy formula into a functional of the electron density, Phys. Rev. B 37 (1988) 785.

[43] P.J. Stephens, F.J. Devlin, C.F. Chablowski, M.J. Frisch, *Ab Initio* Calculation of Vibrational Absorption and Circular Dichroism Spectra Using Density Functional Force Fields, J. Phys. Chem. 98 (1994) 11623.

[44] A.P. Scott, L. Random, Harmonic Vibrational Frequencies: An Evaluation of Hartree Fock, Møller-Plesset, Quadratic Configuration Interaction, Density Functional Theory and Semiempirical Scale Factors, J. Phys. Chem. 100 (1996) 16502.

[45] Gaussian, Inc. 340 Quinnipiac St, Bldg. 40, Wallingford, CT 06492 USA,custserv@gaussain.com.

Chapter -II

AIM AND PLAN OF WORK

Aim:

In recent years it was found that microbial infections and drug resistivity of microbes have been increased enormously. Infection caused by bacteria, fungi and other microorganism pose a serious challenge to the medical community. The widespread use of antibacterial and fungal infections has led to serious health hazards. The Continuous increase in bacterial resistance to existing drug leading to development of new drugs with antimicrobial activity against drug resistance microorganisms. Antibiotic resistance occurs when bacteria change in response to the use of antibiotics used to treat bacterial infections (such as urinary tract infections, pneumonia, bloodstream infections) making them ineffective. In view of the rapid increase in the multi-drug resistant, it is necessary to develop a new and effective antimicrobial drug.

Benzimidazoles are five membered heterocyclic aromatic organic compounds containing two hetero atoms. Both hetero atoms are belongs to nitrogen, which are present at non-adjacent position. Heterocyclic compounds are occupied prominent location among a various types of aromatic organic compounds. Benzimidazole and its derivatives are chosen for investigation. Benzimidazole and its derivatives are the building blocks of bioactive and clinical operations [1 & 2]. Benzimidazole derivatives are naturally occurring isostere of nucleotides [3] , which shows a large number of biological activities towards antioxidant [4] , Antimicrobial activity [5] , antiflammatory – analgestic [6] , anticancer [7] , CNS depressant [8] , androgen receptor antagonist [9] , antitubercular [10] , antihelmintic [11] and diabetic drugs [12], anti-ulcer [13] , anticonvulsant [14], antiviral-antifungal [15] and antiprotozoal [16] and used in treatment of cardiovascular disease, neurology, and endocrinology. In

addition the benzimidazole have played a very important role in the development of theory in heterocyclic chemistry and also extensively in organic synthesis. Benzimidazole nucleus is present in vitamin-B12.

In this present study some novel halogenoderivatives of benzimidazole compound have been synthesized and their antibacterial and antifungal activity has been studied. The halogenoderivatives of benzimidazole compound in 6-position is scare in the literature. Introduction of halogenations substitution in 6-position of benzimidazole gives characterizing drug are used in clinical medicine as anti-ulcer, anti-tumor and anti-viral agents.

Basic Properties of Benzimidazole

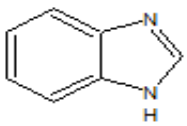

Formula	:	$C_7 H_6 N_2$
Molecular weight	:	118.17
Toxicity	:	Oral rat LD50:2910mg/Kg
Molar Refractivity	:	36.61±0.3 cm^3
Molar Volume	:	95.01 ± 3.0 cm^3
Index of Refraction	:	1.696 ± 0.02
Surface Tension	:	60.1 ± 3.0 dyne/cm^3
Density	:	1.242 ± 0.069 g/cm^3
Polarizibility	:	14.51 ± 0.5 cm^3

Synonyms : 1H-Benzimidazole; 1,3-benzodiazole;benzoglyoxaline;.

Physical and Chemical properties:

Melting point : 176° C

Boiling point : 360° C

Specific gravity : 1

Solubility in water : slightly soluble

Auto ignition : 538° C

Stability : Stable under normal temperature and condition.

PLAN OF THE WORK

1. Synthesis of 6-nitro-2-(4-nitrophenyl) -1H-benzimidazole
2. Synthesis of 6 amino-2-(4 nitrophenyl) -1H-benzimidazole
3. Synthesis of 6-chloro-2-(4 aminophenyl) - 1H-benzimidazole
4. Synthesis of 6 bromo -2-(4 chlorophenyl) -1 H benzimidazole
5. Experimental Studies using UV- visible spectroscopy, FT-IR spectra in the region of 4000-400 cm^{-1} and 1H NMR technique.
6. HOMO-LUMO energy band gap determination
7. Electrostatic Potential (MEP) Analysis
8. Natural Bond Orbital (NBO) Analysis
9. Computation methods - HF and DFT (B3LYP, B3PW91) methods with 6-31+G (d, p) and 6-31++G (d, p) basis sets.
10. Atomic Orbital (GIAO) analysis
11. Molecular Docking
12. Ramachandran Plot
13. Evaluation of anti-bacterial and anti-fungal activity

References:

[1] B. Narasimhan, D. Sharma, P. Kumar (2010) Benzimidazole: a medicinally important heterocyclic moiety, Med. Chem. Res., 21, 269–283.

[2] P. Singla, V. Luxami, K. Paul (2014) Benzimidazole-biologically attractive scaffold for protein kinase inhibitors, RSC Adv., 4, 12422-12440.

[3] J. A. Horig, P. Renz (1980) Biosynthesis of vitamin B12. Some properties of the 5,6-dimethylbenzimidazole-Forming system of Propionibacteriumfreudenreichiiand Propionibacteriumshermanii, Eur.J. Biochem., 105, 587–592.

[4] Z. Ates-Alagoz, B. Can-Eke, T. Coban, M. Iscan, E. Buyukbingol (2004) Antioxidant properties of novel benzimidazoleretinoids, Arch. Pharm. (Weinheim), 337, 188–192.

[5] a) Kumar, B. V. S., Vaidya S. D., Kumar R.V., Bhirud S. B., Mane R. B. 2006) Synthesis and anti-bacterial activity of some novel 2-(6- fluorochroman-2-yl)-1-alkyl/acyl/aroyl-1Hbenzimidazoles, Eur. J. Med. Chem., 41, 599. b) Fahmy H. H., Abdelwal S. H. (2000) Synthesis and antimicrobial activity of some new benzimidazole derivatives, Molecules, 5, 1429.

[6] Evans D., Hicks, T. A., Williamson W. R. N., Dawson W., Meacock S. C. R., Kitchen E. A., (1996) Synthesis of a group of 1H-- benzimidazoles and their screening for antiinflammatory activity, Eur. J. Med. Chem., 31, 635; Taha, Mamdouh A. M. (2005) J. Indian chem. Soc., 82,180.

[7] Demirayak S., Mohsen U. A., Karaburun A. C., (2002) Synthesis and anticancer and anti-HIV testing of some pyrazino [1, 2-a] benzimidazole derivatives, Eur. J.Med. chem., 37, 255.

[8] Sharma P., Mondloi A., Pritmani S. (1999) Synthesis of new 2-(substituted benzothiazolecarbamonyl)benzimidazoles as potential CNS depressants, Ind. J. Chem., 38B, 1289.

[9] Raymond A. N., Guan J., Vernon C. A., James C. l., George A., Tifanie S., Olivia L., Scott G. L., Zhihua S. (2007) Synthesis and SAR of potent and selective androgen receptor antagonists: 5,6- Dichloro-benzimidazole derivatives, Biorg. Med. Chem. Lett., 17, 784.

[10] Foks H., Pancechowska-kesepko D., Kuzmierkiewicz, W., Zwolska Z., Kopec E. A., Janowiec M. (2006) Synthesis and tuberculostatic activity of new benzimidazole derivatives, Chem. Heterocycl. Compd., 42, 611.

[11] X. J. Wang, M. Y. Xi, J. H. Fu, F.R. Zhang, G. F. Cheng, D. L. Yin, et al. (2012) Synthesis, biological evaluation and SAR studies of benzimidazole derivatives as H1-antihistamine agents, Chin. Chem. Lett., 23, 707–710.

[12] Vinodkumar R., Vaidya S. D., Kumar B. V. S., Bhise U. N., Bhirud S. B., Mashelkar U. C. (2008) Synthesis, anti-bacterial, anti-asthmatic and anti-diabetic activities of novel Nsubstituted-2-(4-phenylethynyl-phenyl)-1Hbenzimidazoles and N-substituted 2[4-(4,4- dimethyl-thiochroman-6-yl-ethynyl)-phenyl)-1Hbenzimidazoles, Eur. J. Med. Chem., 43, 986.

[13] Bariwal J. B., Shah A. K., Kathiravan M. K., Somani R. S., Jagtap J. R. (2008) Synthesis and antiulcer activity of novel pyrimidylthiomethyl and Pyrimidylsulfinylmethylbenzimidazoles as potential reversible proton pump inhibitors, Indian Journal of Pharmaceutical Education and Research, 42(3), 225-231.

[14] A. Chmirri, A. D. Sarro, G. D. Sarro, R. Gitto, M. Zapalla (1989) Synthesis and anticonvulsant properties of 2,3,3a,4-tetrahydro-1H-pyrrolo[1,2- benzimidazol-1-ones, J. Med. Chem., 32, 93.

[15] Bishnoi, A., Pandey, V.K., Saxena, R., (1978) Synthesis and characterization of benzimidazolylphenothiazine derivatives and a study of their antiviral and antifungal activities, Ind. J. Chem., 41B, 1978.

[16] Gomez, H. T., Nunez, E. H., Rivera, I. L., Alvarez, J. G., Rivera, R. C., Puc, R. M., Ramos, R. A., Guttirez, M. C. R., Bacab, M. J. C., Vazquez, G. N. (2008) Design, synthesis and in vitro antiprotozoal activity of benzimidazole-pentamidine hybrids, Bioorg. Med. Chem. Lett., 18, 3147.

[17] J. M. Kauffman, A. Khalej, P. T. Litak, J. A. Novinski, G. S. Bajwa (1994) Synthesis and photophysical properties of fluorescent 2-aryl-1,3-dialkyl benzimidazolium ions and al-alkyl-2-aryl benzimidazole with excited state intramolecular proton-transfer, J. Heterocycl. Chem., 31, 957- 965.

[18] Frankel S., Reitman S., Sonnenwirth A. C. Gradwol's (1970) Clinical Laboratory Methods and Diagnosis', A textbook on a laboratory procedure and their interpretation C. V. Mosby Company, Germany, 7th edition, 2, 1406.

[19] B. S. Furniss, A. J. Hannaford, P. W. G. Smith, A. R. Tatchell (Eds.), Vogel's Text Book of Practical

Chapter III

LITERATURE REVIEW

Kumaraswamy et al.,[1] synthesized a new analogs of benzimidazole fused heterocyclic compounds such as triazinane and oxadiazinanes by classical amino methylationwith different aryl-N,N unsymmetrical thiureas. The antibacterial activity of triazinane and oxadiazinanescompounds have been assessed with zone of inhibition by well diffusion method using a panel of selected gram positive and gram negative bacterial strains and which have showed good activity. The synthesized molecules were subjected to molecular docking studies with two proteins, namely topoisomerase and DNA gyrase subunit b. were more active towards bacteria than fungi.

Deshmukh et al., [2] synthesized and investigated 2-(4-Bromophenyl)-1 H-benzimidazole derivatives using o-phenylenediamine, 4-bromo benzoic acid in poluphosphoric acid at temperature 180˚Cwith 90% yield having m.p.296-298˚C. Newely synthesized derivatives have been evaluated on the basis of spectral and analytical data like melting point, IR 1H-NMR and Mass spectroscopy. All the synthesized compounds were screened for their antimicrobial activity shows good antimicrobial activity.

Navneet Singh et al., [3] developed and investigated In-vitro antibacterial activity of Benzimidazole derivatives from some amino acids. Synthesized compounds were characterized by using 1H-NMR, FT-IR, CG-MS and DART-MS. All the compounds evaluated for antibacterial activity against pathogenic bacteria *Staphylococcus aureus,*

Streptococcus pneumonia, Streptococcus pyogenes, and seudonomonas aeruginosa causes respiratory tract infections.

Muhammed Tariq Khan et al., [4] synthesized and characterized 2-Phenyl substituted benzimidazoles. The synthesized were characterized by physical data and FTIR spectroscopic technique and finally screened for their antihypertensive activity by tail cuff method of measurement of blood pressure by NIBP apparatus using Chart 5.0 software. The synthesized compounds have shown antihypertensive activity by taking Losartan as lead compound.

Virendraa R. et al.,[5] synthesized azo linked substituted benzimidazole, nenzoxazole and benzothiazole derivatives and characterized by ^{1}H-NMR, FT-IR, and UV-Vis spectroscopy. The synthesized compounds were evaluated for invitro antibacterial activity against Staphylococcus aureus and Escherichia Coli strains by Resazurin microtiter assay method. The computational studies were also performed to correlate HOMO-LUMO gap with antibacterial activity. The comparative molecular docking studies revealed better insights into binding mechanisms.

Kumaraswamy et al.,[6] carried out anti bacterial activity of 2-(4-aminophenyl) Benzimidazole based pyramidine derivatives from p-amino benzoic acid and benzene 1,2 diamine and EAA with thiourea . All the synthesized compounds have been characterized by 1H-NMR, IR spectral data and prepared compound were tested for antibacterial activity.

Rashmi Arora et al.,[7] designed a noval Pyrazole derivatives of Benzimidazole compounds. The synthesized compound was evaluated for analgesic activity at 7.36±0.05, 7.50±0.08, 8.43±0.12, 12.78±0.02 and 7.64±0.08 at 90 min when compared standard i.e 9.45±0.28 at 90 min, respectively. The synthesized compounds showed excellent siginificant analgesis and anti-inflammatory activites.

Garudachari et al.,[8] synthesized a series of quinoline incorporated benzimidazole derivatives from substituted aniline and istin through multi-step reaction. All the newely synthesized compounds were screened for in-vitro antibacterial and antifungal activity by well plate method. The results revealed that all the compounds were showed moderate to good antimicrobial activity as compared to the standard drugs against all tested microbial strains.

Muhammad Taha [9] Synthesized and investigated a series of novel derivatives of 4-methylbenzimidazole and evaluated towards biological activity. The synthesized novel derivatives of 4-methylbenzimidazole having benzoylhydrazide moiety, excellent antiglycation, antioxidant and cytotoxity activites.

Malathi Raghunath [10] designed a noval series of 6-substituted benzimidazole -2-carbamic acid derivatives by reacting substitute's benzyl chlorides with 4-hydroxy -2-aniline in the presence of anhydrous K_2CO_3 in acetone. All synthesized compounds shosed moderate to good antibacterial and antifungal activity and were nearly effiective as the standared antibacterial and antifungal drugs used for comparision, The exhibited good activity against gram negative bacterial strains like *K. pneumonia* and *P. aeruginosa* as well as against fungal strain *C.albicans.* The 6-substituted

benzimidazole -2-carbamates compounds also synthesized and evaluated for pharmacological activity are promising as antimicrobial agents and are amenable for further optimization.

Priya Jain etal., [11] synthesized a series of noval 2-substituted -5-nitro benzimidazole derivatives to find new chemical entities with enhanced atimicrobial activity, and investigated the antimicrobial activity of the compounds by disc diffusion using Gram-positive and Gram-negative bacteria. Some derivatives showed remarkable activity comparable to that of stabdard against Gram-positive and Gram-negative bacteria.

Yellajyousula lakshmi Narasimha Murthy et al.,[12] synthesized some new 2-diazo-benzimidazole deriviatives and their Ni(II), CU(II), and Ag(I) complexes and characterized by elemental analysis, IR, ^{1}H-NMR, ESR, UV-visible spectral techniques and along with thermal studies. The antimicrobial activity of the ligands [IIII a ($C_2H_{11}N_5O_2$) and III b ($C_{10}H_6N_2$)] and their metal complexes against bacterial strains and fungal strains were compared with standard compounds.

Kuldeep Kumar and Pathak [13] developed some new 2-substituted benzimidazole derivatives from microwave irradiation method by condensation of 2-nitroabiline with different carboxylic acids (aliphatic, aromatic and heterocylic).The synthesized compounds were identified by ^{1}HNMR , and FT-IR spectroscopic techniques and screened for their in vitro antimicrobial activities against the standard strains: Escherichia coli, pseudomous aeruginosa, bacillus subtilis, bacillus pumilus, Candida

albicans, Aspergillus niger. Among the synthesized compounds, 2-Pyridine -3-yl-1H-benzimidazole was found to be the most active antimicrobial compound in the series.

Yusaf Ozkay et al., **[14]** invistigated 12 novel benzimidazole compounds bearing hydrazone moiety to study the antimicrobial and antifungal activity. structures of the synthesized compounds were elucidated by spectral data. six different Gram - negative and four Gram positive bacterial strains were used in antibacterial activity tests. Antifungal activity tests were also performed against three different fungal strains. They also investigated relation between some electronic parameters and antimicrobial activity of the target compounds. Toxicity of the most effective compounds was also established by performing Brine-Shrimp lethality assay.

Abbas Ahmadi and Baback Nahri [15] synthesized and characterized some noval benzimidazole derivatives of 1-bromo-2,4-dinitrobenzene and their antifungal activities using elemental anaiysis and different spectroscopic techniques (IR, NMR and mass spectroscopy). Some of these compounds showed potential antifungal activities. The biological activity of these compounds as fungicides was tested against candida albicans, patient isolate Candida glabrata and Candida krusei. They found that the biological activity of four compounds was comarable to that of the commercially available fungicides wuth a minimum inhibitory concentration of 12.5 μg /ml.

Ahamdi [16] synthesized some novel benzimnidazole derivatives to investigated structures of the synthesized compounds by IR, 1H -NMR , Mass spectroscopy and CHN elemental analyzer and screened for antibacterial activity against Candida albicans for antifungal activities.

Baviskar et al., **[17]** invistigated some noval benzimidazole chalcones by condensation of N-(4(1H-benzo[d] imidazole-2-phenyl) acetamide with aromatic aldehydes in presences of aqueous potassium hydroxide solution room temperature. All the synthesized compounds were characterized on the basis of their ^{1}HNMR , and FT-IR spectroscopic techniques and elemental analysis and screened for antimicrobial activity by the cup-plat method.

Alam et al., [18] synthesized benzimidazole derivatives containing schiff base by two step reactions. In the first step, o-phenylmediamine was condensed with p-amino benzoix acid in xylene and poly phospheric acid to give 2-amino benzimidazole. In the second step, 2-amino benzimidazole is treated with different substituted aldehydes and ketones to form substituted benzimidazole having imine linkage. they evaluated all the synthesized compounds for antimicrobial activity against staphylococcus aureus and Escherichia coli by tube dilation method.

Elinima et al., [19] investigated in vitro antibacterial and antifungal activities of six benzimidazole and benzoxazole derivatives against standard strains and 59 clinical isolates. Of the six compounds, only compounds II and III were active, whereas the rest were devoid of any activity. Considerable growth inhibition of all of the standard strains, including fungi and gram-positive and gram-negative bacteria, resulted when they were treated with these compounds. Fifty-nine clinical isolate of Escherichia coli, Pseudomonas aeruginosa and Staphylococcus aureus were tested for susceptibility to the two compounds. The most susceptibility was the S. aureus isolates.

Ansari K.F. *et al.*, [20] developed a series of 2-substituted-1-[{(5-substituted alkyl/aryl)-1, 3, 4-oxadiazol-2-yl} methyl]-1H-benzimidazole derivatives, the synthesized compounds were identified by spectral and elemental methods of analyses. All the synthesized compounds were screened for their anti-microbial activities. All of the derivatives showed good activity towards gram-positive bacteria and negligible activity towards gram-negative bacteria. Some of the synthesized compounds showed good activity against tested fungi.

OztekinAlgul *et al.*, [21] investigated the structure-activity relationship for some newly synthesized benzimidazole structures and they were synthesized 2-substituted benzimidazole derivatives. The synthesized compounds were examined for anti-bacterial activity against both gram-positive (*Enterococcus faecalis*, *Staphylococcus epidermis*) and gram-negative (*Escherichia coli*, *Pseudomonas aeurginosa*) organisms and anti-fungal activity against *Candida albicans*, *Candida kruesi*, *Candida glabrata*, *Candida tropicalis* and *Candida parapsilosis*. All of the compounds were more active towards bacteria than fungi.

Goel P.K. *et al.*, [22] investigated the quantitative structure activity relationship (QSAR) of a set of twenty 1H- benzimidazole derivatives with anti-protozoal activity against *Entamoeba histolytica.* The studies used various combinations of thermodynamic, electronic, and spatial descriptors. By assuming the significance of the contributed descriptors for the inhibition of amoebic activity, they were synthesized six new compounds (BZ_1 to BZ_6) for the better inhibitory activity with less toxicity.

Podunacvac-Kuzmanovic *et al*., [23] synthesized a set of benzimidazole derivatives and they were tested for their inhibitory activities against the gram negative bacterium *Pseudomonas aeruginosa* and minimum inhibitory concentration were determined for all the compounds. Quantitative structure activity relationship (QSAR) analysis was applied to the synthesized derivatives using a combination of various physicochemical, steric, electronic, and structural molecular descriptors. From the QSAR result, they concluded that the 2-amino and 2-methyl benzimidazole derivatives (Fig-10) are effective *in vitro* against the gram negative bacteria *Pseudomonas aeruginosa.*

Gupta S.K. *et al*., **[24]** synthesized 2-alkyl benzimidazole and 2-aryl benzimidazole derivatives by using different acids namely acetic acid, o-chloro benzoic acid, benzoic acid and cinnamic acid. These were further treated with tosyl chloride and benzoyl chloride to get N-substituted benzimidazole derivatives. Final derivatives were tested for anti-microbial activity against *Escherichia coli, Pseudomonas aeruginosa* and *staphylococcus aureus*. Compound showed very potent activity against *Pseudomonas aeruginosa,* while 3a and 3d exhibited average activity against the same organism.

Raghvendra Dubey *et al*., **[25]** synthesized 2-alkyl and 2-Aryl substituted benzimidazole derivatives (Fig-26) by both conventional and microwave method in the presence of polyphosporicacid. They compared the physical properties of derivatives synthesized by both conventional and microwave method and also studied the effect of salt form of reactant for completion of the reaction. The microwave method is more beneficial, in respect of yield and time than conventional method of synthesis.

Ricardo ***et al.*****,[26]** synthesized and characterized 2-methylbenzimidazole with primary and secondary alkyl halides using a strong base as a catalyst. The comparative analysis of vibrational modes of benzimidazole and its alkyl derivatives show that regions of absorption are very similar in all of them. However, changes are produced at low frequencies specifically in the C–H out of plane deformations, ring breathing and ring skeletal vibrations. The ring out-of plane bending modes shift by 10–15 cm^{-1} in some cases as results of alkyl substitution. The theoretical calculated spectra, using Density Functional Theory (DFT) approximation, and experimental results were consistent with each other. The GIAO method was used to calculate absolute shielding, which agree consistently with those measured by ^{1}H and ^{13}C NMR. The consistency and efficiency of the GIAO ^{13}C and ^{1}H NMR calculations were thoroughly checked by the analysis of statistical parameters concerning computed and experimental ^{13}C and ^{1}H NMR chemical shift values of the studied compounds.

João Pina et al., [27] synthesized and characterized four novel triphenylamine–benzimidazole derivatives in solution (ethanol and methyl cyclohexane) at room temperature. This includes the determination of the absorption, fluorescence, and triplet–triplet absorption spectra, together with quantum yields of fluorescence, internal conversion, intersystem crossing, and singlet oxygen. From the overall data the radiative and radiationless rate constants could be obtained, and it is shown that the compounds are highly emissive with the radiative decay dominating, with more than 70% of the quanta loss through this deactivation channel. The basic structure of the triphenylamine–benzimidazole derivatives (1a) was modified at position 5 of the heterocyclic moiety with electron-donating (OH (1b), OCH3 (1c)) or electron-

withdrawing groups (CN, (1d)). It was found that the photophysical properties remain basically unchanged with the different substitutions, although a marked Stokes shift was observed with 1d. The presence and nature of a charge-transfer transition is discussed with the help of theoretical (DFT and TDFT) data. All compounds displayed exceptionally high thermal stability (between 399 and 454 °C) as seen by thermogravimetric analysis.

Michal et al., [27] studied tetrahydro-2-methylthio furan-2-yl] methyl phosphate dianion (1). The available conformational space was explored using DFT quantum chemical methods by means of two-dimensional potential-energy maps calculated as a function of φ, ψ, ω dihedral angles at the B3LYP/6-31+G** level. The calculated PESs revealed the existence of several low-energy domains. Simulations of IR and Raman spectra of 2-(methylthio) benzonitrile based on scaled DFT force fields were studied by Krishnakumar et al., [16]. The spectra were interpreted with the aid of normal coordinate analysis following full structure optimizations and force field calculations based on DFT using standard B3LYP/6-311G* and B3LYP/6-311+G** method and basis set combinations. Simulation of IR and Raman spectra utilizing the results of these calculations led to excellent overall agreement with the observed spectral patterns, especially with the higher level basis set.

Rice et al., [28] determined the structure and conformation of bis(methylthio) methane by gas-phase electron diffraction and *ab initio* methods. The entropy differences between the two conformers are also obtained from MP3/6-311+G(d) calculations. *Ab initio* HF and DFT study on 2, 4-pyrimidinedithiol were performed by Leszek et al., [21]. The IR and UV spectra of the photo product are reported. This

comparison results in the assignment of bands observed in the IR spectrum of 2,4-pyrimidinedethiol to the theoretically predicted normal modes.

Horak et al., [29] performed the molecular conformation and vibrational spectral studies of p-halogenoderivatives of anisole. The Raman and the IR spectra of P-haogeno derivatives of anisole have been analyzed in the light of the molecular conformation predicted by the consideration of steric hindrance and the conjugation in the system.

Wiles et al., [30] investigated the C=S stretching vibration in the infrared spectra of some thio semicarbozones. Examination of the spectra of N-methyl substituted thiosemicarbazones indicates that, even in this 830 to 805 cm^{-1} region, C=S strtching is coupled with other vibrations perhaps N-C-N stretching.

Mooney et al., [31] reported the IR spectra of chloro and bromo benzene derivatives of anisole and phenetoles. C-Chlorine and C-bromine vibrational frequencies were assigned to substituted halogenobenzenes and also showed how these vibrations are modified by nature and orientation of the substituent groups.

References

[1] kumaraswamy Gullapelli, Brahmeshwari G, Ravichander G & Uma Kusums, Egyptian Journal of Basic and Applied sciences, 4[2017], 303-309

[2] Deshmukh S.K. & Sanjay Dashrath Vaidya, J. Bio. Chem. Ghron. 2019,5(1), 85-90

[3] Navneet Singh, Prashant Arya, Rajendra Singh, Prachi K.M., International Research Journal of Chemistry, 17[2017], 1-15

[4] Muhammad Tariq Khan, Muhammad Tahir Razi, Syed Umer Jan, Muhammad Mukhtiar and Imran Rabbani. Pak. J. Pharm, Sci. 31[2018] 1067-1074

[5] Virendraa R, Chaitannya W, Suraj N, Shahnwaz I., Computational Biology and Chemistry, 78[2019] 330-337.

[6] Kumaraswamy Gullapelli, Murali Krishna thupurani and Brahmeshwari G, International Journal of Pharma and Bio Sciences 5[2014] 682-690

[7] Rashmi Arora, Amandeep Kaur,and Naresh Singh Gill, Current Research in Chemistry 4 [2012] 76-87

[8] Garudachari B, Satyanarayana M.N, Thippeswamy, Arun Isloor M, European Journal of Medicinal Chemistry, 54[2012] 900-906

[9] Muhammad Taha , Nor hadiani Ismail, waqas Jamil, Hesham Raswan, European Journal of Medicinal Chemistry, 84[2014] 731-738

[10] Malathi Raghunath and Viswanathan C.L, International Journal of Pharmacy and Pharmaceutical Sciences 6[2014]

[11] Priya Jain, Vaibhav Jain, Abhishek K Jain, Pradee K Singour, Internationmal Journal of Drug Design and Discovery, 2[2011],633-636.

[12] Yellajyosula lakshmi Narasimha Murthy, Gudru Durga, Anjali. J, Medicinal Chemistry 22[2013] 2266-2272.

[13] Kuldeep kumar and D.P. Patthak, The Pharma innovation, 1[2012], 44-51

[14] Yusuf Okay, Yagmur Tunah and Hulya Karaca, European Journal of Medicinal Chemistry, 45[2010],3293-3298

[15] Abbas Ahmadi and Babak Nahri, E-Journal of Chemistry, 8[2011]

[16] A. Ahmadi, Bulgarian chemical Communications, 46[2014], 245-252

[17] Baviskar B.A, Bhagyesh Baviskar, M. R. Shiradkar, U A Deokate, E-Journal of Chemistry 6[2009], 196-200

[18] Alam S.A.M.F. Ahmed T, Nazmuzzaman M, Rahman S., Ray S.K., International Journal of Research studies in Biosciences , 5[2017], 18-24.

[19] Ansari K.F., Lal C. Synthesis, physicochemical properties and antimicrobial activity of some new benzimidazole derivatives, *European Journal of Medicinal Chemistry*. 44[2009], 4028–4033.

[20] OztekinAlgul., Nizami Duran., Gulay Gulbol. Synthesis and evaluation of anti-microbial activity of some 1,5 (6)–H or Methyl-2-subtituted benzimidazole derivatives, *Asian Journal of Chemistry.*, 19 (2007), 3085-3092.

[21] Goel P.K., Jatav R.K., Kawathekar N. QSAR and synthesis of 1H-benzimidazole derivatives as potent anti protozoal agents, *Indian Drugs.* 44 (2007), 664-671.

[22] Podunavac-kuzmanovic S., Dragoljub D. Cvetkovic., and Dijana. J. Barna. QSAR analysis of 2-amino or 2-methyl-1-substituted benzimidazoles against *Pseudomonas aeruginosa*, *International Journal of Molecular Sciences.*, 10[2009], 1670-1682.

[23] Gupta R.R., Kumar M and Gupta V. Heterocyclic Chemistry, Five membered heterocycles. 2nd edn, Springer (India) Pvt. Ltd, New Delhi, **2005**, 375-376.

[24] Raghvendra Dubey., Narayana Subbiah., Hari Narayana Moorthy. Comparative studies on conventional and microwave assisted synthesis of benzimidazole and their 2-substituted derivative with the effect of salt from the reactant, *Chem. Pharm. Bull.*, 55 (2007), 115-117.

[25] RicardoInfante-CastilloLuis A.Rivera-MontalvoSamuel P.Hernández-Rivera, *Journal of Molecular Structures* 877[2008], 10-19

[26] João Pina ,J. Sérgio Seixas de Melo, Rosa M. F. Batista, Susana P. G. Costa, *J . Org. Chem*, 78[2013], 11389-11395

[27] Michal Raab, Stanislav Kozmon, Igor Tvaroška, Potential transition-state analogs for glycosyltransferases. Design and DFT calculations of conformational behavior, Carbohydr. Res. 340 (2005) 1051.

[28] E.M. Rice, D.A, Aarset, K., Hagen, K. Genge, Structure and conformation of bis(methylthio)methane, (MeS)(2)CH_2, determined by gas-phase electron diffraction and *ab initio* methods, J. Phys. Chem. 104A (2000) 6672

[29] M. Horak, E.R. Lippincott, R. K. Khanna, Molecular conformation and vibrational spectra of P-halogeno derivatives of anisole, Spectrochim. Acta 23A (1967) 1111.

[30] D.M. Wiles, B.A. Gingras, T. Suprunchuk, The C=S strtching vibration in the infrared spectra of some thiosemicarbazones, Can. J. Chem. 45 (1967) 469.

[31] E.F. Mooney, The infrared spectra of chloro- and bromobenzene derivatives-I Anisoles and Phenetoles, Spectrochim. Acta 19A (1963) 877.

Chapter -IV

Synthesis and Theoretical Investigations on the Molecular Structure, Vibrational Spectra, Infrared, Raman, UV and NMR Spectral Analysis and Antimicrobial Studies of 6-nitro-2-(4-nitrophenyl)-1H-benzimidazole

Abstract

The synthesis of 6-nitro-2-(4-nitrophenyl)-1H-benzimidazole has been reported and characterized by FT-IR spectra in the region of 4000-400 cm^{-1}.UV-visible spectroscopy, ^{1}H NMR experimental techniques. The theoretical studies such as molecular structure parameter, vibrational frequencies, electronic absorption spectra has been investigated using gas and solvent phase, HOMO-LUMO, molecular ele

ctrostatic potential (MEP) and natural bond orbital (NBO), of the title compound has been computed using the HF and DFT (B3LYP, B3PW91) methods with 6-31+G (d, p) and 6-31++G (d, p) basis sets.^{1}H –NMR Gauge Including Atomic Orbital (GIAO) chemical were calculated using 6-311++ G (d, p) basis set. The vibrational wave number and the chemical shifts values were compared with the obtained experimental data of the title compound. The electronic properties were evaluated by TD-DFT methodology in different solutions and in gas-phase method using integral equation formalism of the polarisable continuum model (IEF-PCM) at B3LYP/6-311++G (d,p) basis set. HOMO-LUMO energy band gap has been determined. The intermolecular electronic interaction and the stabilization energy was determined using NBO analysis. In addition to this the antimicrobial evaluation of 6-nitro-2-(4-nitrophenyl)-1H-benzimidazole was also performed against some bacteria and fungi using Disc–diffusion method. The inhibition zone of growth was also determined for bacterial and fungal strain.

4.1 Introduction

Benzimidazole is one of the most significant and promising heterocyclic compound. It is the N-containing organic compound fused with benzene and imidazole. Benzimidazole has the wide range of biological and pharmacological activities [1-2].It is present in various drugs compound such as astemizole, emedastine difumarate, mebendazole and omeprazole [3]. Benzimidazole moiety fulfills the structural requirement and the scientist from the worldwide have reported that the substitute compound have remarkable activity such as antiviral, antiproliferative, antihypertensive, anthelminitic, humanglucagonreceptor, antagonitand anti-infective activities [4-9].

The substituted benzimidazole molecules have prodigious importance in drug discovery owing to their unique and precise binding abilities for the biological targets with respect to their chemical formalization [10]. Considering the above facts the intent of this study is to perform an experimental and computational work on benzimidazole fusing with aryl group. In this study we describe the vibrational frequencies, ^{1}H chemical shifts and excitation energies have been investigated on 6-Nitro-2-(4-nitrophenyl)-1H-benzimidazole. The optimized geometric parameters and vibrational frequencies have been calculated using HF method with basis sets 6-31+G (d, p), 6-311++G (d, p) and similarly with DFT methods (B3LYP, B3PW91) methods along with basis sets 6-31+G (d, p), 6-311++G (d, p). HOMO-LUMO analysis have also been investigated using TD-DFT/B3LYP the6-311++G (d, p) basis set by applying the integral equation formalism of the polarizable continuum model (IEF-

PCM) along with this molecular electrostatic potential (MEP) and natural bond analysis (NBO).In addition we report the evaluation of the antimicrobial activities.

4.2 Materials and methods

4.2.1 General

The compound 2-(4-nitrophenyl)-1H-benzimidazole was purchase from the Sigma Aldrich Company with a state of 98% purity. The three necked round bottom flask fitted with a mechanical stirrer was taken and 7.5 ml concentrated Nitric acid (HNO_3) was added. The flask was immersed in ice cold water and concentrated sulfuric acid (H_2SO_4) of 7.5 ml was added slowly down the condenser along stirring. The compound 2-(4-nitrophenyl)-1H-benzimidazole of 6.70 gm were added in a portion of 1 hour at such a rate that the temperature did not exceed 35° C. It is stirred continuously for 12 hour then the reaction mixture was poured very slowly over crushed ice with intense stirring. The obtained product was filtered, washed with cold water and recrystallized from ethanol [11-12].The FT-IR spectrum of the compound was measured in the region of 4000 -400 cm^{-1} using KBr pellets. A UV-Vis spectrum was carried out in the wavelength region of 500- 200 nm. The ^{1}H nuclear magnetic resonance was recorded on Bruker advanced 500 NMR Spectrometer.

4.2.2 Computational method

The theoretical calculations were carried out with GAUSSIAN 16W program packages [13].The calculated results were visualized by means of Gauss view 6.0[14]. In the present work we have calculated the vibrational frequencies and the geometric parameters of a 6-Nitro-2-(4-nitrophenyl)-1H-benzimidazole, in the ground state to compare the fundamentals from the experimental vibration frequencies and geometric

parameters, by using the Hartree-Fock (HF) [15], Density functional theory using Becke's three parameter hybrid functionals [16] with Lee, Yang, and Parr correlation functional methods (B3LYP) [17], Becke's three parameter exchange functional with Perdew-Wang exchange functional with Perdew and Wang's gradient correlated functional(B3PW91) [16-18] with the standard 6-31+G(d,p) and 6-311++G(d,p) basis sets. The optimized molecule structure is used for the computation of vibrational frequencies. The integral equation formalism –polarized continuum model (IEF-PCM) [19] dealing with solvent effect was selected in electronic transition calculation. ^{1}H and ^{13}C NMR chemical shift values for 6-Nitro-2-(4-nitrophenyl)-1H-benzimidazole were computed by the same method in the solvent by using gauge-independent atomic orbital (GIAO). The IEF-PCM model provided by Gaussian 16W was used to evaluate the solvent effects (chloroform, ethanol, DMSO). Along with this we also investigated the atomic charges, molecular electrostatic potential (MEP), Natural bond analysis (NBO) properties and HOMO-LUMO pictures were also obtained.

4.3 Result and discussion

4.3.1 Geometry optimization

For meeting the requirements of both accuracy and computing economy, theoretical methods and basis sets should be considered. DFT has proved to be extremely useful in treating electronic structure of molecules. The density functional three parameter hybrid model (DFT/B3LYP) at 6-311G (d,p) and 6-311++G(d,p) basis sets along with HF/6-311++G(d,p) method was adopted to calculate the properties of the target molecule in this work. All the calculations were performed using the Gaussian 16W program package with the default convergence criteria

without any constraint on the geometry. The results obtained at this level of theory, were used for the detailed interpretation of the IR and Raman spectra. TED was calculated by using the SQM program and the fundamental vibrational modes were characterized by their TED.

The geometry optimization of the 6-Nitro-2-(4-nitrophenol)-1H-benzimidazole have been carried out using the HF and DFT (B3LYP/B3PW91) methods with the 6-31+G(d,p) and 6-311++G(d,p) basis sets. The title compound belongs to C1 point group symmetry and the optimized geometric structure is shown in Fig 4.1, while the optimized structural parameters are presented in the Table 4.1. It is seen from the Table 4.1, most of the optimized bond lengths agree with each other for the three methods .The crystal data of closely related molecule [20-22] is compared with the title compound. The imine length is shorter than amine length as expected imine N6-C10 is 1.3178 and amine has 1.3807 as expected [20].The bond length of O4-N8 and O3-N8 are almost equal to 1.23Å [22].The intra molecular C-C bond lengths are in range 1.38-1.40Å except C10-C12 which is 1.4649.The N6-C10-C12 and C21-N8-O4 bond angles of the title compound are 124.23^0 and 117.55^0 respectively. The highest bond angle of 132.58^0 was obtained for C13-C9-N5.The dihedral angle N6-C10-C12-C16 and C15-C13-C9-N5 are 179.99 and -179.99, respectively.

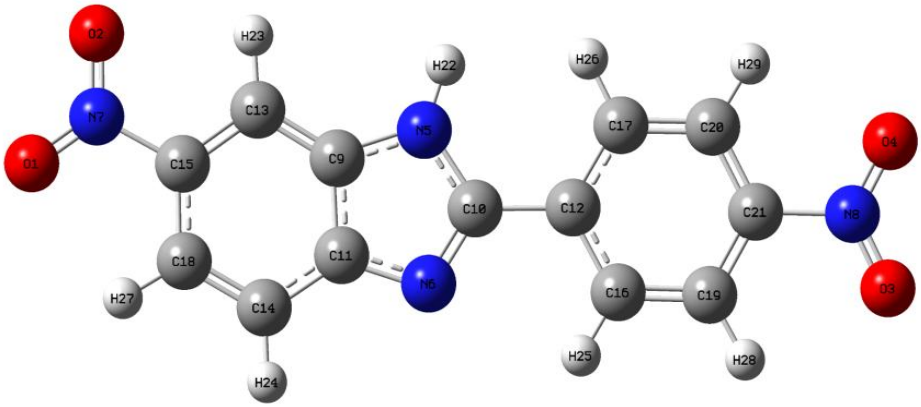

Fig 4.1. The optimized geometric structure of the molecule
6-Nitro-2-(4-nitrophenol)-1H-benzimidazole

TABLE 4.1: Optimized geometrical parameters of 6-Nitro-2-(4-nitrophenol)-1H-benzimidazole: bond length (Å), bond angles (º) and selected dihedral angles (_).

Parameters	Exp.[a]	**B3LYP 6311++G (d, p)**	**B3PW91 6311++G (d, p)**	**HF 6311++G (d, p)**	**B3LYP 6311+G (d, p)**	**B3PW91 6311+G (d, p)**	**HF 6311+G (d, p)**
Bond length (Å)							
O1-N7	1.223	1.224	1.218	1.186	1.232	1.226	1.193
O2-N7	1.223	1.226	1.220	1.189	1.234	1.228	1.196
O3-N8	1.230	1.223	1.218	1.186	1.231	1.225	1.193
O4-N8	1.237	1.224	1.218	1.187	1.232	1.226	1.194
N7-C15	1.491	1.475	1.470	1.463	1.469	1.465	1.458
C15-C13	1.395	1.390	1.387	1.377	1.393	1.390	1.379
C15-C18	1.402	1.406	1.403	1.397	1.410	1.407	1.399
C18-H27	1.080	1.080	1.082	1.070	1.082	1.083	1.071
C18-C14	1.374	1.383	1.381	1.374	1.387	1.384	1.376
C14-C11	1.402	1.401	1.399	1.392	1.404	1.402	1.394
C11-N6	1.378	1.374	1.370	1.374	1.376	1.371	1.372
N6-C10	1.321	1.317	1.315	1.288	1.322	1.319	1.291
C10-N5	1.387	1.380	1.375	1.362	1.381	1.376	1.361
C10-C12	1.475	1.464	1.461	1.476	1.466	1.463	1.477
C12-C17	1.391	1.403	1.400	1.389	1.406	1.403	1.391
C17-C20	1.389	1.388	1.386	1.382	1.391	1.388	1.383
C20-C21	1.383	1.390	1.387	1.379	1.394	1.391	1.381
C21-N8	1.467	1.479	1.473	1.467	1.473	1.468	1.462
N5-H22	0.956	1.006	1.006	0.991	1.008	1.007	0.991
C17-H26	0.986	1.083	1.084	1.074	1.085	1.086	1.074
C20-H29	0.996	1.081	1.082	1.071	1.082	1.083	1.071
Bond angles (°)							
O1-N7-O2	124.35	124.48	124.67	124.60	124.25	124.50	124.50
O1-N7-C15	117.82	117.82	117.72	117.79	117.92	117.82	117.83
O2-N7-C15	117.93	117.69	117.59	117.60	117.81	117.67	117.66
C15-C18-H27	119.91	118.56	118.45	119.10	118.60	118.47	119.11
C15-C13-H23	120.70	120.50	120.41	121.06	120.57	120.48	121.06
C18-C14-C11	119.18	118.22	118.17	118.09	118.21	118.17	118.08
C13-C9-C11	120.30	122.81	122.86	122.78	122.88	122.92	122.08
C13-C9-N5	133.25	132.58	132.56	132.48	132.53	132.53	132.48
C9-N5-C10	108.32	107.25	107.25	106.60	107.28	107.27	106.78
N5-C10-N6	113.62	112.16	112.31	113.13	112.20	112.35	112.89
C10-N6-C11	106.32	105.84	105.65	105.67	105.71	105.53	105.79
N6-C10-C12	125.63	124.23	124.06	124.08	124.16	123.99	123.68
C10-C12-C17	123.62	122.30	122.39	121.54	122.26	123.37	122.10
C12-C17-C20	121.80	120.74	120.67	120.48	120.74	120.66	120.61
C12-C16-C19	118.70	120.58	120.54	120.28	120.59	120.56	120.41
C19-C21-N8	118.30	119.16	119.13	118.79	119.18	119.15	119. 04
C21-N8-O4	119.20	117.55	117.46	117.47	117.65	117.53	117.50
O4-N8-O3	122.20	124.88	125.08	125.03	124.68	124.92	124.97
C21-N8-03	119.12	117.55	117.45	117.48	117.65	117.54	117.52
C21-C19-H28	120.10	119.65	119.57	120.12	119.71	119.65	120.15

Torsional angle (°)							
O1-N7-C15-C13	-	-179.99	179.96	179.67	179.95	179.97	179.99
O1-N7-C15-C18	-	0.0068	-0.045	-0.260	-0.028	-0.0575	-0.004
O2-N7-C15-C13	-	0.0064	-0.035	-0.326	-0.0505	-0.0101	0.003
O2-N7-C15-C18	-	-179.94	179.95	179.73	-0.028	179.96	-179.99
O3-N8-C21-C20	-	179.99	-179.92	-179.93	-179.84	-179.80	179.99
O3-N8-C21-C19	-	-0.007	0.037	-0.135	0.102	0.1433	-0.001
O4-N8-C21-C20	-	-0.0084	0.076	0.106	0.163	0.1487	0.003
O4-N8-C21-C19	-	179.91	-179.95	179.90	-179.89	-179.90	-179.99
N5-C10-C12-C16	-	-179.99	179.95	159.74	174.08	173.61	179.98
N5-C10-C12-C17	-	0.020	-3.126	-20.71	-6.078	-6.582	-0.0193
N6-C10-C12-C16	-	0.0235	-3.0612	-20.28	-5.812	-6.397	-0.0184
N6-C10-C12-C17	-	-179.97	176.85	159.25	174.02	173.40	179.98
C18-C14-C11-N6	-	179.99	179.91	179.71	179.88	179.85	180.00
C15-C13-C9-N5	-	-179.99	179.97	179.59	179.94	179.89	-179.99
H27-C18-C14-C11	-	-180.00	-179.980	-179.88	-179.99	-179.96	-180.00
C10-C12-C16-C19	-	-180.00	-179.92	-179.88	-179.91	-179.88	-179.99
C9-N5-C10-C12	-	-180.00	-179.94	-179.27	-179.84	-179.96	179.99
C17-C20-C21-N8	-	-179.99	-179.98	-179.86	-179.93	-179.94	180.00

4.3.2 Vibrational assignments

Horak et al., [23] performed the molecular conformation and vibrational spectral studies of p-halogenoderivatives of anisole. The Raman and the IR spectra of P-haogeno derivatives of anisole have been analyzed in the light of the molecular conformation predicted by the consideration of steric hindrance and the conjugation in the system. They also investigated the C=S stretching vibration in the infrared spectra of some thio semicarbozones. Examination of the spectra of N-methyl substituted thiosemicarbazones indicates that, even in this 830 to 805 cm^{-1} region, C=S strtching is coupled with other vibrations perhaps N-C-N stretching.

The theoretical vibrational spectra of 6-nitro-2-(4-nitrophenyl)-1H-benzimidazole were calculated at the HF and DFT (B3LYP/B3PW91) methods with

the 6-31+G(d,p) and 6-311++G(d,p) basis sets. FT-IR spectrum was recorded for both the experimental and theoretical methods as presented in the Fig 4.2 – 4.3, and calculated frequency was scaled with 0.961 for B3LYP, 0.957 for B3PW91 and 0.892 for HF [24] both the frequencies are represented in the Table 4.2. The vibrational bands assignments have been made by using both the animation option of Gauss view 6.0 graphical interface for Gaussian program16 W [14] and VEDA 4 program [25]. All the calculated and experimental data are in good agreement.

The FT-IR spectra of the title compound contains some characteristic bands of vibrations such as C-H, N-H, C=N, C-N and C=C, groups. The N-H Stretching occurred in the region of 3518cm^{-1}[26]. The characteristic vibrations for C-H stretching of heterocyclic aromatic compounds are expected to appear in 3000 and 3100 cm^{-1}[27].The C-H Symmetric stretching vibration of the title compound observed in and around the region of 3100 cm^{-1} for all the DFT and HF basic sets and 3114 cm^{-1}experimentally. The asymmetric C-H was observed at 3061cm^{-1} experimentally whereas for DFT /B3LYP [6-311++G(d,p)/6-31+ G(d,p)] we observed 3098cm^{-1} /3117cm^{-1} for DFT /B3PW91 [6-311++G(d,p)/6-31+G(d,p)] 3092 cm^{-1}/3112cm^{-1} and for HF [6-311++G(d,p)/6-31+G(d,p)] 3031cm^{-1}/3052cm^{-1}[28].

The characteristic region of the benzimidazole derivative spectrum is 1500-1650 cm^{-1}.The vibrational frequencies and intensity differ in this region based on the substituent and its position [26]. The title compound shows vibrational frequency at 1513cm^{-1} which is good agreement with the obtained results. The band appearing at 1596cm^{-1} and 1313cm^{-1} are assigned to C=N and C-N [29]. In this study the N-O vibration is observed in the region around1100cm^{-1}and in experimental spectrum

in1013 cm^{-1}. The out of bending OCON torsion ONCC and C-C stretching observed at 1105cm^{-1}, 1046cm^{-1} and 1011cm^{-1}.The vibrational spectra of 2-substituted benzimidazole show a very intensive band around the 741 cm^{-1}. The title compound shows C-H and C-C vibration around 790 – 680 cm^{-1}along with their torsion HCCN, bending CCC, bending and torsion HCC is observed in this region.

.

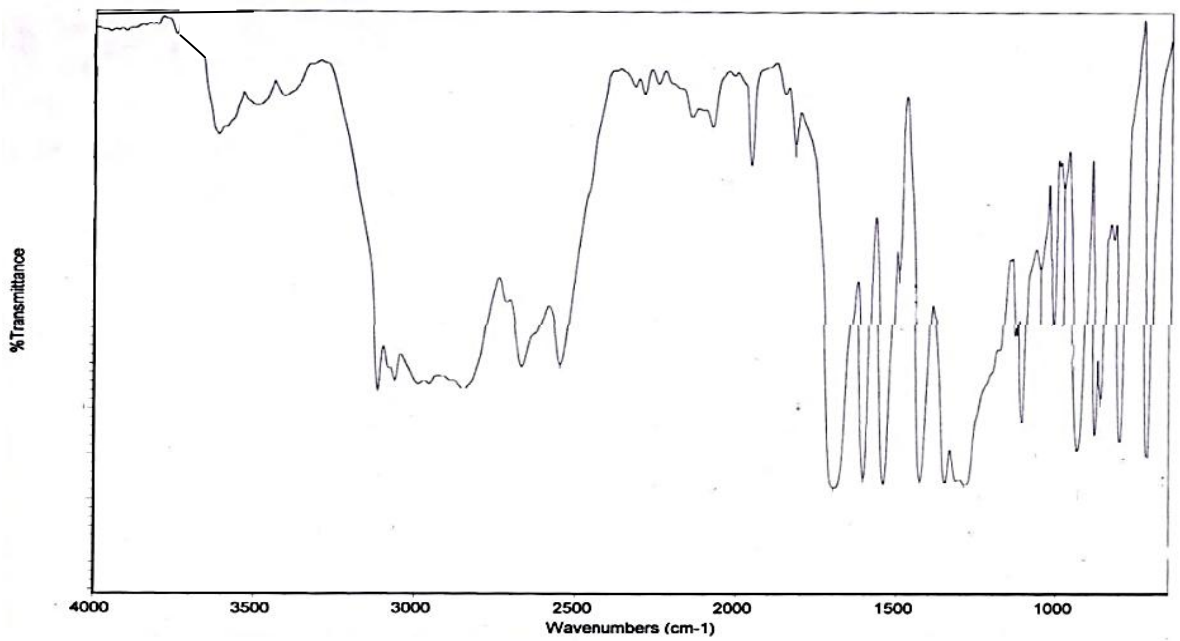

Fig 4.2 Experimental FT-IR spectra of
6-nitro-2-(4-nitrophenyl)-1H-benzimidazole

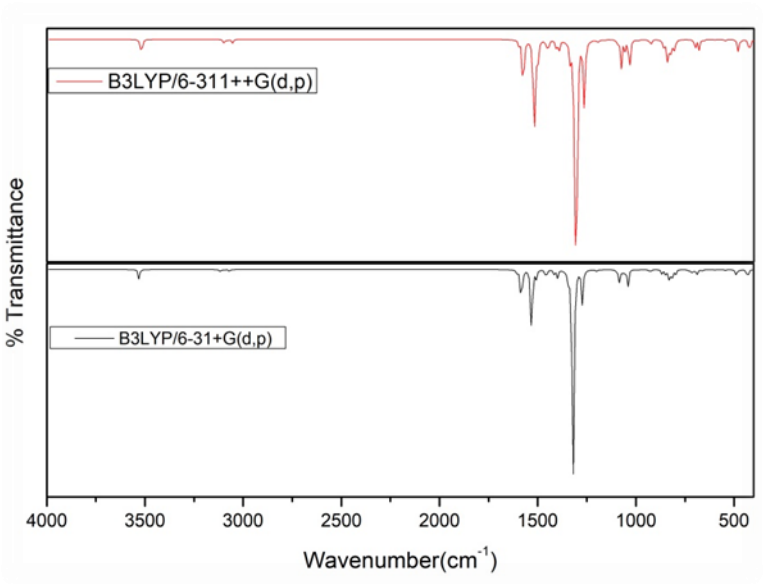

Fig 4.3 calculated FT-IR spectra of
6-nitro-2-(4-nitrophenyl)-1H-benzimidazole for **B3LYP/6-31+G(d,p)** basis set

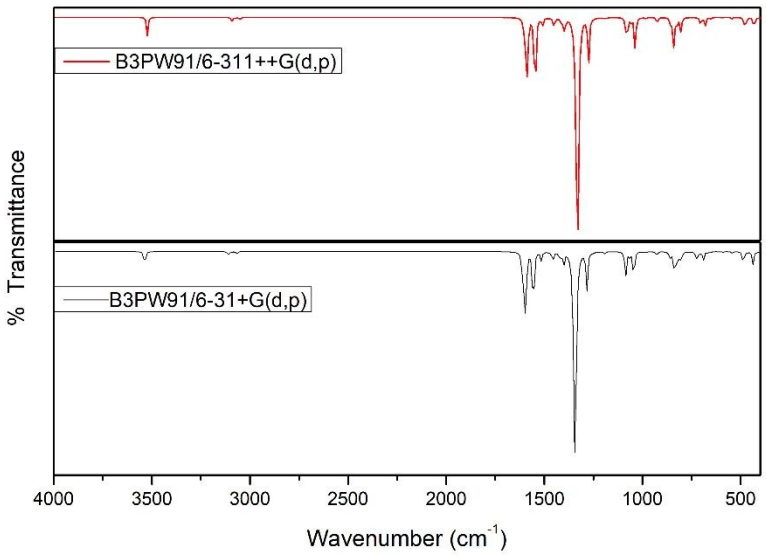

Fig 4.4 calculated FT-IR spectra of
6-nitro-2-(4-nitrophenyl)-1H-benzimidazole for **B3PW91/6-31++G (d,p)** basis set

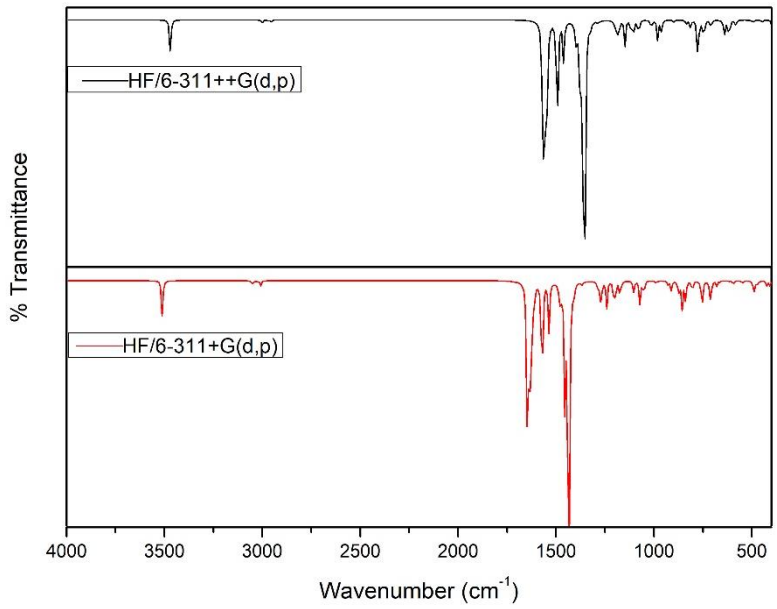

Fig 4.5 calculated FT-IR spectra of
6-nitro-2-(4-nitrophenyl)-1H-benzimidazole for **HF/6-31++G (d,p)** basis set

Table 4.2: Experimental and calculated vibrational; frequencies of6-nitro-2-(4-nitrophenyl)-1H-Benzimidazole

Assignments [a]	**B3LYP**	**B3LYP**	**B3PW91**	**B3PW91**	**HF**	**HF**	**Exp.**
	6311++ G (d, p)	6311+ G (d, p)	6311++ G (d, p)	6311+ G (d, p)	6311++ G (d, p)	6311+ G (d, p)	
ν(N-H)	3518.79	3530.49	3522.60	3536.49	3485.75	3511.35	3613.84
ν(C-H) s	3100.78	3119.97	3094.71	3114.41	3031.29	3053.13	3114.32
ν(C-H) as,	3098.88	3117.6	3092.93	3112.38	3031.25	3052.97	3061.87
ν(C-H) as,	3094.63	3112.41	3089.57	3107.91	3026.07	3046.19	2980.15
ν(C=N)	1596.37	1604.08	1607.03	1613.45	1635.43	1645.78	1698.28
ν(C=N)	1576.75	1585.77	1594.32	1604.13	1625.43	1634.79	1604.29
ν(C=C)	1513.81	1527.48	1543.93	1553.40	1563.81	1571.12	1541.35

ν(C-N)	1313.12	1326.75	1337.90	1349.45	1360.26	1366.51	1349.69
ν(C-N)	1249.76	1255.93	1249.16	1254.94	1197.10	1205.84	1289.22
O-N	1116.93	1109.51	1144.1	1208.46	1240.67	1205.13	1129.71
o(OCON)	1105.54	1109.51	1090.92	1083.27	1083.52	1075.11	1108.57
τ (ONCC)	1046.09	1048.49	1007.79	1084.27	971.34	971.94	1055.21
ν(CC)	1011.25	1038.48	965.47	966.82	964.91	961.07	1013.4
ν (CH)+ τ (HCCN)	790.88	790.34	720.21	717.46	711.51	706.49	799.59
β (CCC)+(CC)	754.16	744.33	685.01	685.92	680.79	681.83	715.94
ν(CH)+ β (HCC) + τ (HCCC)	555.87	539.87	502.23	510.98	506.01	502.48	--

ν, stretching; δ, twisting; β, bending; τ, torsion; θ, breathing; s, symmetric; as, asymmetric;

4.3.3 Natural bond orbital (NBO) analysis.

NBO analysis gives the accurate possible natural Lewis structure picture of ø, because all orbitals are mathematically chosen to include the highest possible percentage of the ED. Interaction between both filled and virtual orbital spaces information is correctly explained by the NBO analysis and it could enhance the analysis of intra and inter-molecular interactions. The second order Fock matrix was carried out to evaluate donor (i) – acceptor (j) i.e. donor level bonds to acceptor level bonds interaction in the NBO analysis. The result of interaction is a loss of occupancy from localized NBO of the idealized Lewis structure into an empty non-Lewis orbital. For each donor (i) and acceptor (j), the stabilization energy E (2) associates with the delocalization i → j is estimated as:

$$E(2) = \Delta E_{ij} = q_i \frac{F(i,j)^2}{\varepsilon_j - \varepsilon_i} \qquad (2.2)$$

where q_i is the donor orbital occupancy, ε_j and ε_i are diagonal elements; and F(i, j) is the off diagonal NBO Fock matrix element. NBO analysis provides an efficient method for studying intra and inter-molecular bonding and interaction among bonds, and also provides a convenient basis for investigating charge transfer or conjugative interaction in molecular systems. Some electron donor orbital, acceptor orbital and the interacting stabilization energy resulted from the second-order micro-disturbance theory are reported [58, 59]. The larger E (2) value the more intensive is the interaction between electron donors and acceptors i.e. the more donation tendency from electron donors to electron acceptors and the greater the extent of conjugation of the whole system [60]. Delocalization of ED between occupied Lewis – type (bond or lone pair) NBOs and formally unoccupied (anti bond or Rydeberg) non Lewis NBOs correspond to a stabilizing donor-acceptor interaction.

The Natural bond orbital calculation [31] of the 6-nitro-2-(4-nitrophenyl)-1H-benzimidazole was performed using the DFT/B3LYP method with the 6-311++ G(d, p) basis set provided by Gaussian 16 W. NBO analysis is an effective method for studying intra and intermolecular bonding and also provides a convenient basis for investigating charge transfer or conjugative interaction in the molecular systems. The hyper conjugative interaction energy was deduced from the second order perturbation approach of Fock matrix in the NBO basis between electron donor and electron acceptor orbitals [32] and the possible intensive interaction are given in the Table 4.3. The intensive interaction between the electron donors and electron acceptor scan be identified by large E (2) values. The intramolecular hyper conjugative interaction was observed for the bonding orbital σ (C12-C16) which distributes to the anti-bonding orbital σ^* (C16-C19) with the stabilization energy of 65.75 Kcal/mol. The

intramolecular hyper conjugative interaction was observed for the bonding orbital σ (C10-C12) which distributes to the anti-bonding orbital σ^* (C16-C19) with the stabilization energy of 32.78 Kcal/mol. The intramolecular hyper conjugative interaction was observed for the bonding orbital σ (C20-H29) which distributes to the anti-bonding orbital σ^* (C15-C18) with the stabilization energy of 188.89 Kcal/mol and for the bonding orbital σ (N8-C21) which distributes to the anti-bonding orbital, σ^* (C15-C18) and σ^* (C16-C19) with the stabilization energy of 59.46 and 158.11 Kcal/mol. The intramolecular hyper conjugative interaction was observed for the bonding orbital σ (O4-N8) which distributes to the anti-bonding orbital σ^* (C15-C18) and σ^* (C16-C19) with the stabilization energy of 37.14 and 94.67 Kcal/mol. The increased occupancy of the localized π^* (C13-C15) in the idealized non -Lewis structure and decreased occupancy of π (C13-C15) in the idealized Lewis orbital and their subsequent impact on their molecular stability and geometry also related with their pure p character of the two carbons C13 and C15 .The intramolecular hyper conjugative interaction was observed for the bonding orbital π(C14-C18), which distributes to the anti-bonding orbital π^* (C13-C15) with the stabilization energy of 20.11 Kcal/mol. This leads to strong stabilization of benzimidazole moiety [33]

Table 4.3 Significant donor acceptor interaction of 6-Nitro-2-(4-nitrophenol)-1H-benzimidazole and their second order perturbation energies calculated at B3PW91/6-311++G (d, p) basis set.

Donor Orbital(i)	Type	ED/e	Acceptor orbital (j)	Type	ED/e	E (2) (kcal/mol) [a]	E(j)-E(i) (a.u.) [b]	F(i,j) (a.u.) [c]
O1-N7	σ	1.99566	N7 - C15	σ*	0.10488	0.84	1.38	0.031
O1-N7	σ	1.99566	C13-C15	σ*	0.02093	0.63	1.64	0.029
O1-N7	π	1.98549	C13-C15	π*	0.38497	4.33	0.46	0.044
O2-N7	σ	1.99576	N7-C15	σ*	0.10488	0.76	1.38	0.03
O2-N7	σ	1.99576	C15-C18	σ*	0.02249	0.53	1.22	0.023
03-N8	σ	1.9958	N5-C10	σ*	0.04258	1.06	1.31	0.034
03-N8	σ	1.9958	N5-H22	σ*	0.01847	1.25	1.41	0.038
03-N8	σ	1.9958	C15-C18	σ*	0.02249	11.3	1.24	0.106
03-N8	σ	1.9958	C16-C19	σ*	0.01454	23.31	0.77	0.12
O4-N8	σ	1.99581	N5-C10	σ*	0.04258	7.76	1.31	0.091
O4-N8	σ	1.99581	C14-H24	σ*	0.01342	12.89	1.37	0.119
O4-N8	σ	1.99581	C15-C18	σ*	0.02249	37.14	1.23	0.192
O4-N8	σ	1.99581	C16-C19	σ*	0.01454	94.67	0.76	0.24
N5-C9	σ	1.98376	N5-C10	σ*	0.04258	2.53	1.04	0.046
N5-C9	σ	1.98376	C10-C12	σ*	0.03737	3.58	1.26	0.06
N5-H22	σ	1.98863	N6-C10	σ*	0.01435	2.35	1.26	0.049
N6-C10	σ	1.97811	C11-C14	σ*	0.02359	5.47	1.41	0.078
N7-C15	σ	1.98843	C14-C18	σ*	0.01216	1.37	1.4	0.039
N8-C21	σ	1.98846	C15-C18	σ*	0.02249	59.46	0.97	0.215
N8-C21	σ	1.98846	C16-C19	σ*	0.01454	158.11	0.5	0.25
C9-C11	π	1.55232	C13-C15	π*	0.38497	21.82	0.28	0.071
C9-C11	π	1.55232	C14-C18	π*	0.26876	16.16	0.3	0.065
C10-C12	σ	1.97143	C16-C19	σ*	0.01454	32.78	0.36	0.097
C11-C14	σ	1.97713	C14-C18	σ*	0.01216	2.61	1.3	0.052
C12-C16	σ	1.97011	C16-C19	σ*	0.01454	65.75	0.37	0.139
C13-C15	π	1.69595	O1-N7	π*	0.6253	25.96	0.15	0.061
C14-C18	π	1.70486	C13-C15	π*	0.38497	20.11	0.27	0.068
C15-C18	σ	1.97499	C14-H24	σ*	0.01342	2.64	0.98	0.046
C16-H25	σ	1.97728	C16-C19	σ*	0.01454	13.21	0.18	0.044
C18-H27	σ	1.97485	C14-H24	σ*	0.01342	0.53	0.79	0.018
C19-H28	σ	1.97514	C12-C16	σ*	0.02276	3.61	1.06	0.055
C20-H29	σ	1.97512	C15-C18	σ*	0.02249	188.89	0.64	0.31

[a] $E^{(2)}$, energy of hyperconjugative interactions.

[b] Energy difference between donor and acceptor i and j NBO orbitals

[c] F_{ij} is the Fock matrix element between i and j NBO orbitals

4.3.4 ^{1}H NMR Spectra Analysis

In order to provide an unequivocal assignment of ^{1}H NMR spectra of the 6-nitro-2-(4-nitrophenyl)-1H-benzimidazole compound, we consider series of NMR calculation using GIAO method [30]. All the calculation are performed using DFT/B3LYP method with the 6-311++ G (d, p) basis set and the results are Tabulated in the Table 4.4. The integral equation formalism –polarized continuum model (IEF-PCM) provided by Gaussian 16W is considered to describe the influence exerted by the solvents (DMSO, Ethanol, Chloroform) on the NMR spectra of the given compound and the calculated values are also listed in the Table 4.4

The ^{1}H NMR experimental chemical shifts of title compound were observed 7.74-8.63 ppm as shown in Fig 4.6. These chemical shift was calculated at 7.79-9.2 ppm for DMSO , 7.77-9.25 ppm for ethanol and 7.55-9.24 ppm for chloroform. Thus the GIAO method shows the significant difference in chemical shift in the Table3, with respect to experimental and theoretical evaluation. It was observed that the chemical shifts in all solvents are almost equal.

Table 4.4 Experimental and calculated (GIAO)^{1}H NMR chemical shifts for of 6-nitro-2-(4-nitrophenyl)-1H-benzimidazole

Atom		B3LYP/6-311++G(d,p)		
^{1}H	Exp.	DMSO	Ethanol	Chloroform
H23	8.63	8.5406	8.5267	8.4225
H24	7.96	8.0997	8.0981	8.0775
H25	7.74	8.8796	8.8815	8.8898
H26	7.74	8.108	8.0935	7.9796
H27	8.19	8.3656	8.3693	8.3930
H28	8.25	9.2604	9.2596	9.2481
H29	8.25	7.9966	7.9935	7.9685

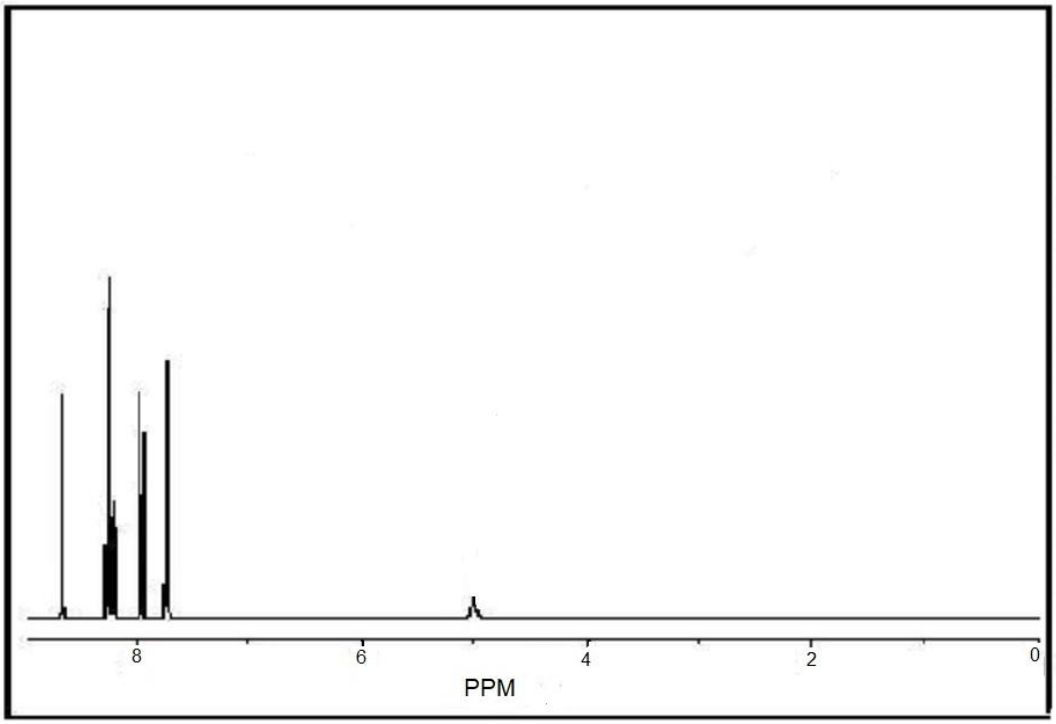

Fig 4.6.^{1}H- NMR spectra of 6-nitro-2-(4-nitrophenyl)-1H-benzimidazole

4.3.5 Electronic properties

The electronic transition of 6-nitro-2-(4-nitrophenyl)-1H-benzimidazole were calculated using B3LYP/6-311++G (d, p) basis set of DFT in gas phase and in solvents such as DMSO, Chloroform and water. The effect of solvent was evaluated by applying the integral equation formalism of the polarizable continuum model (IEF-PCM). The UV-vis spectral data for both the gas and solvents phase were illustrated in Table 4.5, by using Gaussian 3.0 [34].The absorption wavelength values in the UV study of the title compound are almost equal in both the gas and solvents phase. According to calculated electronic data shows the absorption band in the range of 300-430 nm in all the states. We know very well that the $n \longrightarrow \pi^*$ transition is not seen in

benzimidazole compound but it has a lone pair of electron on nitrogen atom [35-36]. The broad band we observed is due to the $\pi \rightarrow \pi^*$ transition in the benzimidazole ring.

HOMO and LUMO are the very important parameters for quantum chemistry. We can determine the way the molecule interacts with other species; hence, they are called the frontier orbitals. HOMO, which can be thought the outermost orbital containing electrons, trends to give these electrons such as an electron donor. On the other hand; LUMO can be thought the innermost orbital containing free places to accept electrons. The HOMO and LUMO energy calculated by B3LYP/6-311G (d,p)/6-311++G(d,p) and HF/6-311++G(d,p) method are shown in Table - 4.5 This electronic transition absorption corresponds to the transition from the ground to the first excited state and is mainly described by an electron excitation from the HOMO to the LUMO.

The longest wavelength corresponding to electronic transition from HOMO to the LUMO (74%) and the wavelength is 423 nm for gas whereas for DMSO HOMO to the LUMO (96%) and the wavelength is 417 nm, chloroform HOMO to the LUMO (93%) and the wavelength is 408 nm and for water HOMO to the LUMO (95%) and the wavelength is 416nm.The large λ indicates that more electrons are pushed into the aromatic ring structure.

The energies of the frontier molecular orbitals (FMOs) for the title compound are shown in Figure 4.7. The observed HOMO and LUMO energies and the energy gap (ΔE), the ionization potential (I), the electron affinity (A), the electronegativity (χ), global hardness (η), global softness (S) and the Electrophilicity index (ω) for the title compound have been calculated using B3LYP/6-311++G(d,p) basis set. The HOMO-LUMO energy gap is very important parameter for the stability of the structure [37]

and also it reflect the biological activity of the compound. The energy value of the band gap is 3.4155 eV for HOMO to LUMO and 3.7232 for HOMO to LUMO +1.This ensure that the compound is stable. The global hardness is another good indicator of chemical stability. The global hardness of the title compound is 1.7075 as shown in Table 4.6, which indicates the good chemical stability and the compound is stable, electronegativity (χ) is calculated as 5.5157 which is a measure of attraction of an atom to electron. The extremely low global softness of 0.2928 theoretical value shows the compound is nontoxic. The Electrophilicity index (ω) was found to be 8.9086 this ensures that there is strong energy transformation between HOMO and LUMO, this electrophilicity index act as a pre-cursor to analyze the biological activity in terms of docking where the title compound act as legend and its docked to a suitable protein [38].

Table-4.5 Calculated electronic transition states for the 6-nitro-2-(4-nitrophenyl)-1H-Benzimidazole with the TD-DFT/IEF-PCM method.

MEDEIUM	DFT/B3LYP with 6-311++G (d,p)				
	λ (nm)	Band gap (eV)	Oscillator Strength	Major contributions	
Gas	423	2.9284	0.0000	HOMO-3->LUMO (74%),	HUMO-3->LUMO+1 (21%)
	421	2.9458	0.0003	HOMO-2->LUMO (37%),	HUMO-2->LUMO+1 (59%)
	378	3.2814	0.6044	HOMO->LUMO (97%),	
	344	3.6074	0.0389	HOMO-1->LUMO (29%),	HOMO->LUMO+1 (58%)
	335	3.6978	0.1032	HOMO-1->LUMO (62%),	HOMO->LUMO+1 (35%)

	317	3.9105	0.0005	HOMO-10->LUMO (72%),	HOMO-10->LUMO+1 (21%)
DMSO	417	2.9718	0.6595	HOMO->LUMO (96%)	
	397	3.1239	0.0003	HOMO-4->LUMO (70%),	HOMO-4->LUMO+1 (26%)
	393	3.1534	0.002	HOMO-3->LUMO (41%),	HOMO-3->LUMO+1 (55%)
	380	3.2650	0.0722	HOMO-1->LUMO (20%),	HOMO->LUMO+1 (67%)
	364	3.4092	0.1217	HOMO-1->LUMO (69%),	HOMO->LUMO+1 (26%)
	348	3.5670	0.0992	HOMO-2->LUMO (69%),	HOMO-1->LUMO+1 (21%)
Chloroform	408	3.0383	0.6743	HOMO->LUMO (93%)	
	404	3.0679	0.0081	HOMO-4->LUMO (70%),	HOMO-4->LUMO+1 (25%)
	401	3.0929	0.0165	HOMO-3->LUMO (40%),	HOMO-3->LUMO+1 (55%)
	370	3.3516	0.0619	HOMO-1->LUMO (21%),	HOMO->LUMO+1 (67%)
	356	3.4816	0.1203	HOMO-1->LUMO (69%),	HOMO->LUMO+1 (27%)
	338	3.6695	0.087	HOMO-2->LUMO (68%),	HOMO-1->LUMO+1 (22%)
Water	416	2.9773	0.6354	HOMO->LUMO (95%)	
	396	3.1271	0.0003	HOMO-4->LUMO (70%),	HOMO-4->LUMO+1 (26%)
	393	3.1570	0.002	HOMO-3->LUMO (41%),	HOMO-3->LUMO+1 (55%)
	380	3.2646	0.073	HOMO-1->LUMO (20%),	HOMO->LUMO+1 (67%)
	364	3.4094	0.1201	HOMO-1->LUMO (69%),	HOMO->LUMO+1 (27%)
	348	3.5647	0.1006	HOMO-2->LUMO (69%),	HOMO-1->LUMO+1 (21%)

Table 4.6. Global chemical reactivity descriptors of 6-nitro-2-(4-nitrophenyl)-1H-benzimidazole	
Properties	B3LYP/6-311++G(d,p)
E_{HOMO}(eV)	-7.2232
E_{LUMO}(eV)	-3.8082
Ionisation potential (I)	7.2232
Electron affinity(A)	3.8082
Chemical potential (μ)	-5.5157
Electronegativity (χ)	5.5157
Global hardness(η)	1.7075
Global softness (S)	0.2928
Electrophilicity index (ω)	8.9086

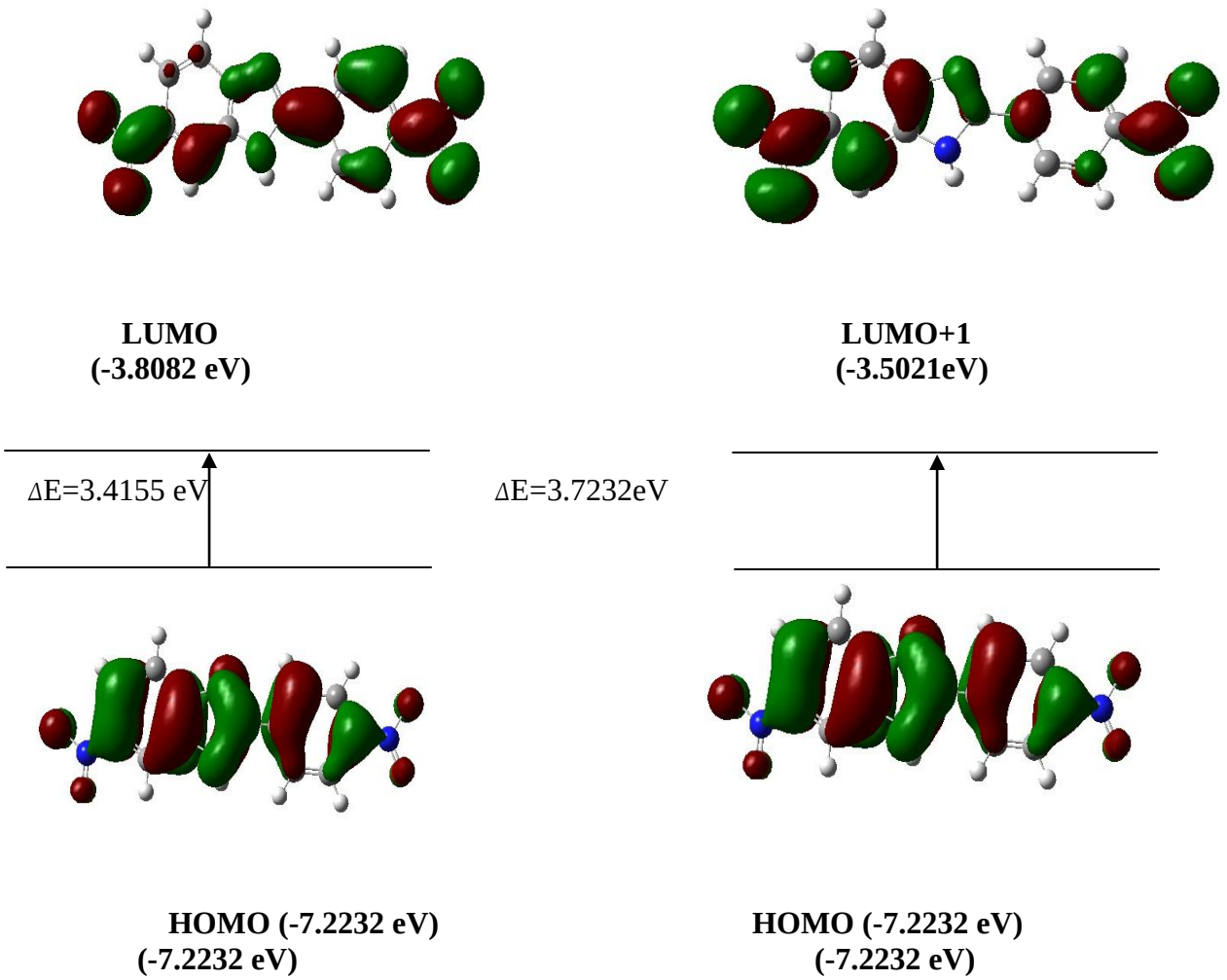

Fig 4.7 The molecular orbital of 6-nitro-2-(4-nitrophenyl)-1H-benzimidazole using DFT/B3LYP with 6-311++G (d, p) and the selected electronic transition in DMSO phase.

4.3.6 Molecular Electrostatic Potential (MEP)

MEP is related to the ED and is a very useful descriptor in understanding sites for electrophilic and nucleophilic reactions as well as hydrogen bonding interactions. The electrostatic potential *V(r)* is also well suited for analyzing processes based on the "recognition" of one molecule by another, as in drug-receptor, and enzyme-substrate interactions, because it is through their potentials that the two species first "see" each other. To predict reactive sites of electrophilic and nucleophilic attacks for the investigated molecule, MEP at the B3LYP/6-311++G(d,p) optimized geometry was calculated. The negative (red and yellow) regions of MEP were related to electrophilic reactivity and the positive (blue) regions to nucleophilic reactivity. From the MEP it is evident that the negative charge covers the nitro group and the positive region is over the methyl group. The more electro negativity in the nitro group makes it the most reactive part in the molecule.

Molecular electrostatic potential is associated to the electron density and is a very useful descriptor in discerning sites for electrophilic and nucleophilic reactions as well as hydrogen bonding interactions [39-40].The electrostatic potential is a real physical property, which can be determined experimentally as well as computationally [41]. MEP map was generated to predict the reactive sites for electrophilic and nucleophilic attack. It is generated using the optimized geometry of the 6-nitro-2-(4-nitrophenyl)-1H-benzimidazole by DFT/B3LYP with 6-311++G (d, p) basis set using Gauss View 6.0 program. The red colour (negative) region represents the electrophilic reactivity and the blue colour (positive) region represents the nucleophilic reactivity as shown in Fig 4.8. It can be seen from the figure negative region is localized near the nitrogen atom of the benzimidazole ring and the maximum positive region is

associated with the H atoms of the imidazole indicating possible site for nucleophilic attack. This result extends information about the intermolecular interaction and molecular bonding.

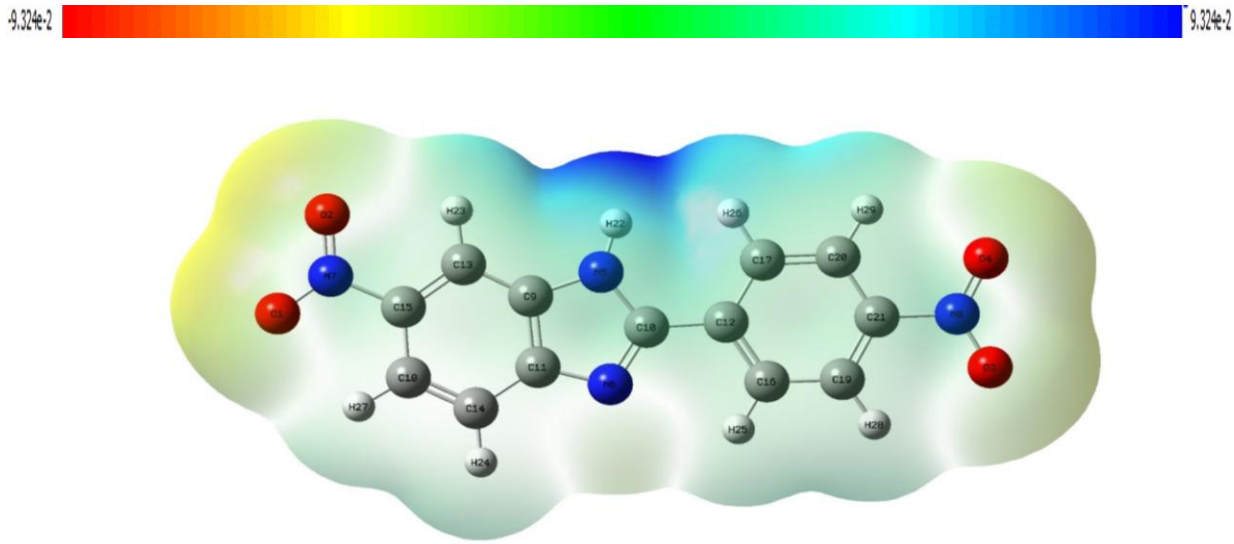

Fig 4.8.The molecular electrostatic potential of 6-nitro-2-(4-nitrophenyl)-1H-benzimidazole using DFT/B3LYP with 6-311++G (d, p)

4.3.7 Molecular docking

Molecular docking is of great importance in the field of structural molecular biology, Pharmacogenomics and computer-assisted drug design. Docking can be used to execute virtual screening on large libraries of compound, rank the results, and propose structural propositions of the predominant binding modes of a ligand to the target, which is invaluable in lead optimization. The information attained thus forms a database for further experimental analysis of the selected molecule as a potential drug. Experimentally analysing a wide array of compounds is time consuming and not feasible. However, employing a virtual screening process like molecular docking ensures a foster mode of drug designing and also provides every conformation possible based on the receptor and ligand molecule.

In the recent past the drug design plays an important role in pharma industry. This title compound called ligand interacts with suitable protein selected using online drug target prediction Swiss ADME-Target prediction. By using Auto dock software, 6-nitro-2-(4-nitrophenyl)-1H-benzimidazole molecules are docked with 3EQA protein. The ligand of 6-nitro-2-(4-nitrophenyl)-1H-benzimidazole molecules binds at the active site of the substrate are shown in Fig 6. The molecular docking binding energy (kcal/mol) was also obtained to be -5.36 kcal/mol. The bonded residues corresponding to 3EQA protein is SER 483, ARG 184 and THR 486 and observed bond length is enlisted in Table 4.7. This low value of binding energy shows the bio-active nature of the molecule.

Table 4.7 Hydrogen bonding and molecular docking for protein target-3EQA

Protein ID	Bonded residue	No of bonds	Bond distance	Binding energy (Kcal/mol)	Ref RMSD (Å)
3EQA	SER 483	1	2.5	-5.36	32.46
	ARG 184	2	1.9		
	THR 486	1	3.3		
	ASP 177	1	2.4		

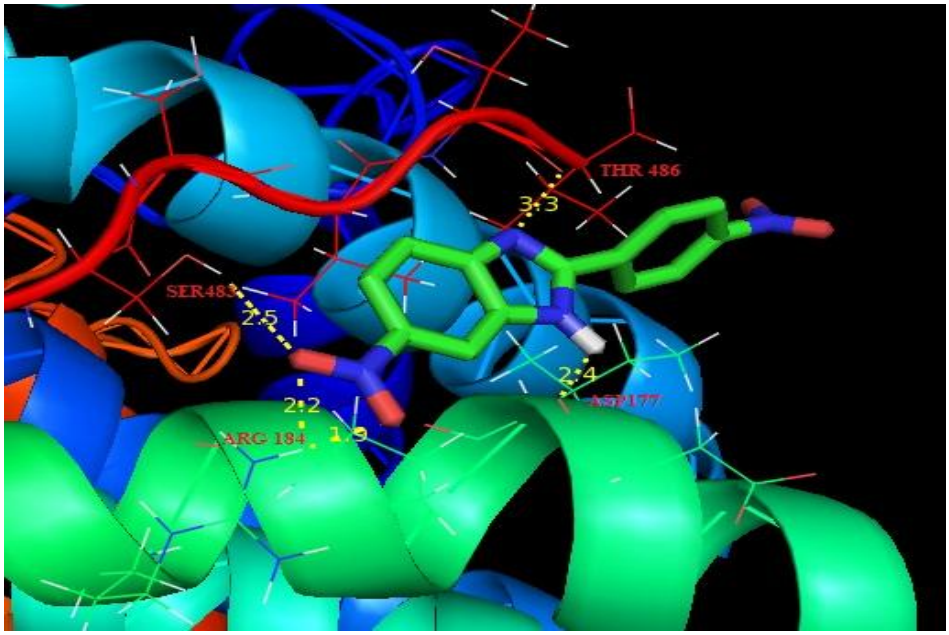

Fig-4.9. Ligand 6-nitro-2-(4-nitrophenyl)-1H-benzimidazole embedded in the active site of 3EQA protein

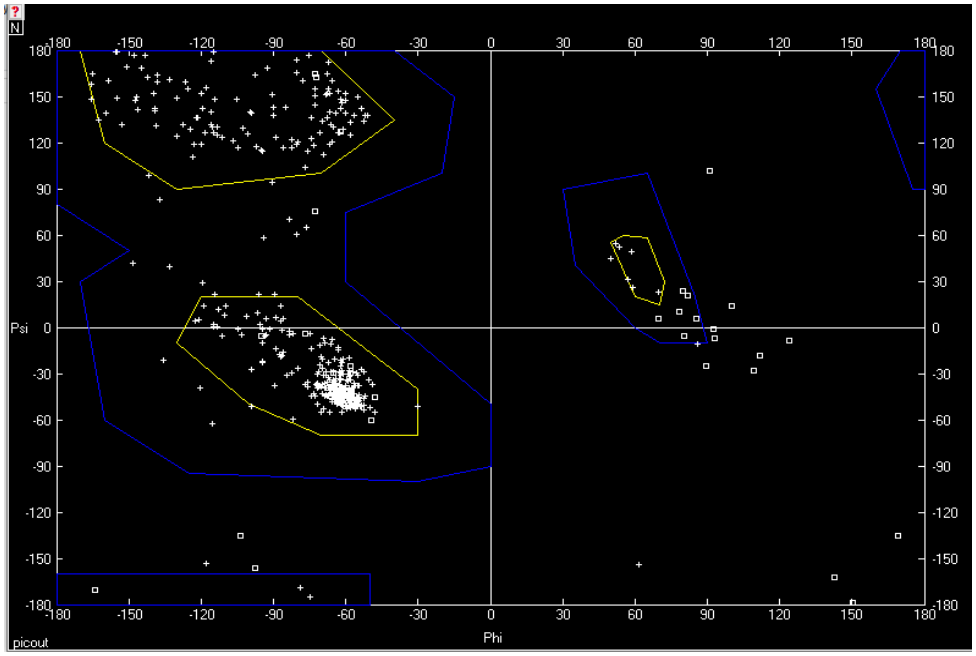

Fig. 4.10 Ramachandran Plot of the protein 3EQA with binding residues SER 483, ARG 184 and THR 486

On observing the Ramachandran Plot, the energetically allowed regions of the binding residue SER 483, ARG 184 and THR 486 has the torsion angle psi (ψ) against phi (ϕ) lying in the most allowed blue region as shown in Fig. 4.10. From the plot, it is concluded that the selected protein has majority of the residues in allowed region thus indicating the 3EQA protein to be a stable protein.

4.3.8 Anti-microbial activity:

The antimicrobial activities were carried for total of four bacterial strains viz. *Staphylococcus aureus (*MTCC-3160), *Enterococcus faecalis* (MTCC-3159) as Gram –positive bacteria and *Pseudomonas aeruginosa* (MTCC-4030), *Escherichia coli* (MTCC-1667) as Gram-negative bacteria and two fungal strains viz. *Aspergillusniger* (MTCC 282),*Candida albicans* (MTCC 227) were used in the investigation.

Table-4.8 Antimicrobial activity of the 6-nitro-2-(4-nitrophenyl)-1H-benzimidazoleby Disc diffusion method

Microbial Compound	**Diameter of the Inhibition Zone (mm)**			
Gram Positive	25 µg/ml	50 µg/ml	100 µg/ml	Ciprofloxacin 25µg/ml
*Staphylococcus aureus (*MTCC-3160)	20±2.4	23±2.7	29±3.4	19±2.2
Enterococcus faecalis(MTCC-3159)	10±1.1	14±1.5	20±2.2	18±1.9
Gram -Negative				
Pseudomonas aeruginosa (MTCC-4030)	17±1.5	19±1.7	23±2.1	29±2.6
Escherichia coli (MTCC-1667)	13±1.1	20±1.6	23±1.8	39±3.1
Fungal Compound				
Aspergillusniger(MTCC 282),	18±1.9	26±2.8	29±3.1	27±2.9
Candida albicans(MTCC 227)	14±1.2	18±1.6	24±2.1	16±1.4

They were chosen based on their clinical and pharmacological importance. The bacterial and fungal strains obtained from Microbial Type Culture Collection, Institute of Microbial Technology, Chandigarh, were used for evaluating antimicrobial activity. The bacterial strains were grown in Mueller-Hinton agar (MHA), whereas the fungal strains were grown in potato dextrose agar.

Antimicrobial activity of 6-nitro-2-(4-nitrophenyl)-1H-benzimidazolecompound was determined by Disc diffusion method according to National Committee for Clinical Laboratory Standards (NCCLS). Inoculum of each microbial culture to be tested was spread on agar plates with a sterile swab moistened with the microbial suspension. Subsequently, discs of 6 mm diameter were kept into the agar medium and filled with 20 μl (25, 50, 100 μg/ml) of 6-nitro-2-(4-nitrophenyl)-1H- benzimidazole compound and allowed to diffuse at room temperature for 2 h. The plates were then incubated in the upright position at 37°C for 24 h for bacterial culture and 28^0C for 48 h for fungal culture. Disc containing the same volume of ethanol served as negative controls while standard antibiotic Ciprofloxacin 25 mg (50 μl) were used as the positive controls. After incubation, the growth inhibition zones were measured in mm dia. Three replicates were carried for a compound against each of the test organism. Data were expressed as mean ±standard deviation.

The zone of inhibition ranged from 20±2.4 to 29±3.4,10±1.1 to 20±2.2,17±1.5 to 23±2.1,13±1.1 to 23±1.8,18±1.9 to 29±3.1and 14±1.2 to 24±2.1 are in mm diameter for *Staphylococcus aureus, Enterococcus faecalis, Pseudomonas aeruginosa, Escherichia coli, Aspergillusniger* and *Candida albicans.* This indicates the diameter increases with increase in concentration of the title compound. Maximum activity was

shown against *Staphylococcus aureus* and *Aspergillusniger* with inhibitory zone of 20±2.4 to 29±3.4 and 18±1.9 to 29±3.1 at the concentration of 100µg/ml whereas least activity was shown against *Enterococcus faecalis (*10±1.1 to 20±2.2). From the Table 7 it clearly indicates that the 6-nitro-2-(4-nitrophenyl)-1H-benzimidazolecompound has the capacity of inhibiting the metabolic growth of the investigated bacteria and fungi to some extent especially *Staphylococcus aureus* and *Aspergillusniger* as shown in Fig 6. It is well evident that most number of drugs would be active against Gram-positive than Gram-negative bacteria [42]. In this present study the title compound as shown that it is active against both types of the bacteria and fungi, which may indicate broad spectrum of properties this remarkable activity of this title compound may be arising from the benzimidazole ring, which plays an vital role in the anti-microbial activity [43] and also due to nitro group attached to the benzimidazole ring hence it is noted that there is direct relationship between the biological activity and electron withdrawing group[44].However the title compound shows the lower antimicrobial potencies than the compared control drug except in *Staphylococcus aureus* which is also providing the little higher activity than the compared control drug. It is evident from this work that some more exploration of benzimidazole derivative at the para position will lead to development of the some very potent antimicrobial agent.

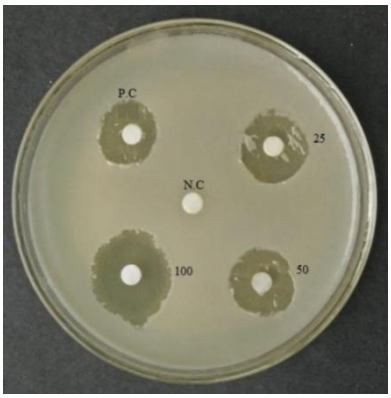

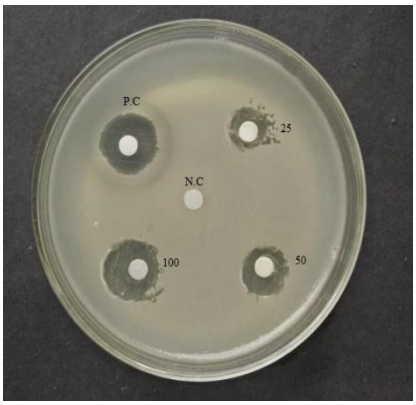

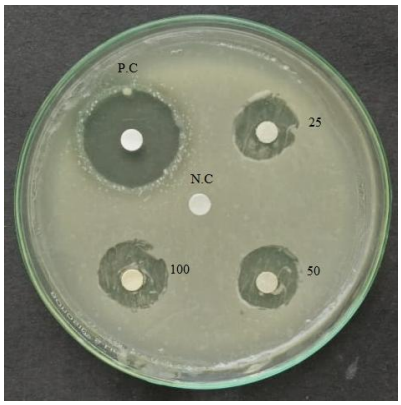

Staphylococcus aureus *Enterococcus faecalis* *Pseudomonas aeruginosa*

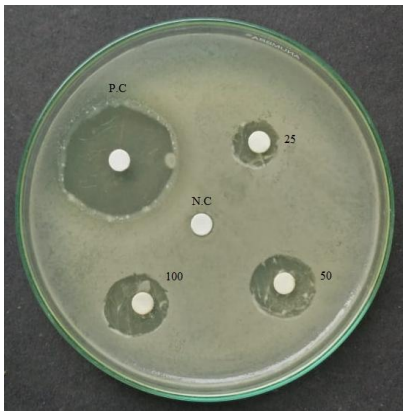

Aspergillus niger *Candida albicans* *Escherichia coli*

Fig 4.11 Anti-bacterial activity of the 6-nitro-2-(4-nitrophenyl)-1H-benzimidazole

Conclusion

In this study we synthesized the 6-nitro-2-(4-nitrophenyl)-1H-benzimidazolecompound. We thoroughly investigated the FT-IR spectra, UV- Vis, ^{1}H proton NMR, Natural Bond Orbital (NBO) and Molecular Electrostatic Potential (MEP) in detail manner for the first time .The calculated geometrical parameter are in good agreement with the literature data. A FT-IR spectra analysis shows that the calculated vibrational frequencies are in good agreement with the experimental values. From NBO analysis, the intermolecular interaction and the stabilization energy have been determined. The chemical shifts values for different

solutions were determined and compared with experimental data which shows a very good agreement for ^{1}H Proton NMR.

The energy gap of 3.4155 eV of the present compound and electrophilicity index value was determined using HOMO and LUMO energies. The high electrophilicity index value indicates that the title compound is biological active. The MEP map indicates that the hydrogen atom attached to the benzimidazole ring is more positive. These sites give us the information about the intermolecular interaction and the metallic bonding of the title compound. The synthesized compound is screened for antimicrobial activity against the bacteria and fungi. This compound has shown moderate activity against the entire gram positive and gram negative bacteria and fungi except *Staphylococcus aureus* where it shows comparable highly active then the reference compound. The present study has revealed the antibacterial activity of the title compound and it can also be seen as potential source of useful drugs. Further studies have to be carried out by substituting the electron with drawing group at the different position of the benzimidazole ring for further enhancement of the antimicrobial activity.

References:

[1] Z. Z. Chen, S. Q. Li, W. L. Liao, Z. G. Xie, M. S. Wang, Y. Cao, J. Zhang, Z. G. Xu, Efficient method for the synthesis of fused benzimidazole-imidazoles via deprotection and cyclization reactions, Tetrahedron. 71 (2015) 8424-8427.

[2] C. S. Digwal, U. Yadav, A. P. Sakla, P. V. S. Ramya, S. Aaghaz, A. Kamal, VOSO4 catalyzed highly efficient synthesis of benzimidazoles, benzothiazoles, and quinoxalines, Tetrahedron. Lett. 57 (2016) 4012-4016.

[3] T. Sakai, T. Hamada, N. Avada, J.Watanabe, Pharmaobiol. Dyn.12 (1989) 530.

[4] C. W. Evans, C. Atkins, A. Pathak, B. E. Gilbert, J. W. Noah, Benzimidazole analogs inhibit respiratory syncytial virus G protein function, Antiviral. Res. 121 (2015) 31-38.

[5] M. Hranjec, G. Pavlovic, G. K. Zamola, Synthesis, crystal structure determination and antiproliferative activity of novel 2-amino-4-aryl-4,10-dihydro[1,3,5]triazino[1,2-a] benzimidazoles, J. Mol. Struct. 1007 (2012) 242-251.

[6] M. C. Sharma, S. Sharma, N. K. Sahu, D. V. Kohli, 3D QSAR kNN-MFA studies on 6-Substituted benzimidazoles derivatives as nonpeptide angiotensin II receptor antagonists: A rational approach to Anti-hypertensive agents, J. Saudi. Chem. Soc. 17 (2013) 167-176

[7] A. T. Mavrova, D. Wesselinova, N. Vassilev, J. A. Tsenov, Design, synthesis and antiproliferative properties of some new 5-substituted- 2-iminobenzimidazole derivatives, Eur. J. Med. Chem. 63 (2013) 696-701.

[8] C. G. Opez, F. V. Albores, V. G. Prieto, M. Ruocco, M. Lorito, Changes in Trichoderma asperellum enzyme expression during parasitism of the cotton root rot pathogen Phymatotrichopsis omnivore, Fungal. Biol. 119 (2015) 264-273.

[9] Z. Zhang, K. K. Ojo, S. M. Johnson, E. T. Larson, P. H. J. A. Geiger, A. C. Gonzalez, A. C.White, M. Parsons, E. A. Merritt, D. J. Maly, C. L. M. J. Verlinde, W. C. V. Voorhis, E.Fan, Benzoylbenzimidazolebased selective inhibitors targeting cryptosporidium parvumand toxoplasma gondii calcium-dependent protein kinase-1, Bioorg. Med. Chem. Lett. 22(2012) 5264-5267.

[10] S. Dhole, M. Selvaraju, B. Maiti, K. Chanda, C.M. Sun, Microwave controlledreductive cyclization:aselective synthesis of novel benzimidazole-alkyloxypyrrolo[1,2-a]quinoxalinones, ACS Comb. Sci. 17 (2015) 310-316.

[11] Singh J, Grover P, Pathak DP. Synthesis and Comparative QSARstudy of some novel benzimidazole derivatives. Acta. Pharm. Sci.(2010) 52: 510-521.

[12] M.Sugumaran, M.Yokesh Kumar Synthesis and Biological Activity of Novel 2, 5 Disubstituted Benzimidazole Derivatives International Journal of Pharmaceutical Sciences and Drug Research 2012; 4(1): 80-83

[13] M. J. Frisch, G. W. Trucks, H. B. Schlegel, G. E. Scuseria, M. A. Robb, J. R. Cheeseman,G.Scalmani, V. Barone, G. A. Petersson, H. Nakatsuji, X. Li, M. Caricato, A. V. Marenich,J.Bloino, B. G. Janesko, R. Gomperts, B. Mennucci, H. P. Hratchian, J. V. Ortiz, A.F. Izmaylov, J. L. Sonnenberg, D. Williams-Young, F. Ding, F. Lipparini, F. Egidi, J. Goings, B. Peng, A. Petrone, T. Henderson, D. Ranasinghe, V. G. Zakrzewski,

[14] Roy Dennington, Todd A. Keith, and John M. Millam, Gauss view Version 6.Semichem Inc., Shawnee Mission, KS, 2016.

[15] C. Moller, M.S. Plesset, Phys. Rev. 46 (1934) 618.

[16] A.D. Becke, J. Chem. Phys. 98 (1993) 5648

[17] C. Lee, W. Yang, R.G. Parr, Phys. Rev. B 37 (1988) 785.

[18] P. Predew, Y. Wang, Phys. Rev. B 45 (1992) 244

[19] J. Tomasi, B. Mennucci, R. Cammi, Quantum mechanical continuum salvation models, Chem. Rev. 105 (2005) 2999-3094.

[20] Namik O¨ zdemir, Bilge eren, Muharremdincer,YunusBekdemir.Quantum-Chemical, IR, NMR,and X-ray Diffraction Studies on 2-(4-Chlorophenyl)-1-methyl-1H-benzo[d]imidazole, International journal of Quantum Chemistry. Vol 111(2011), 3112-3124

[21] Olga V. Dorofeeva et al..Molecular structure and conformation of nitrobenzene reinvestigated by combined analysis of gas-phase electrondiffraction, rotational constants, and theoretical,StructChem (2007) 18:739–753

[22] RajendranGandhimathi et al..Geometry optimization, HOMO and LUMO energy, molecular electrostatic potential, NMR, FT-IR and FT-Ramananalyzes on 4-nitrophenol, Eur. Phys.Appl. Phys. (2015) 69: 10202

[23] M. Horak, E.R. Lippincott, R. K. Khanna, Molecular conformation and vibrational spectra of P-halogeno derivatives of anisole, Spectrochim. Acta 23A (1967) 1111.

[24] J.P.Merrick, JD.Moran,L.Radom, J.Phy, ChemA111 (2007)11683-11700

[25] M.H. Jamr´oz, Vibrational Energy Distribution Analysis VEDA-4,Warsaw,2004.

[26] D.J. Rabiger, M.M. Joullie, J. Org. Chem. 29 (1964) 476.

[27] M.Evecen,H.Tanak, Material science-Poland 34,(2016),886-904.

[28] HakanArslan, OztekinAlgul Vibrational spectrum and assignments of 2-(4-methoxyphenyl)-1H-benzo[d]imidazole by ab initio Hartree–Fock anddensity functional methods SpectrochimicaActa Part A 70 (2008) 109–116.

[29] N. Sundaraganesan, S. Ilakiamani, P. Subramani, B.D. Joshua, Spectrochim. Acta Part A 67 (3–4) (2007) 628.

[30] F.J. Luque , J.M. Lopez , M. Orazco , Perspective on Electrostatic interactions of a solute with a continuum. A direct utilization of ab initio molecular potentials for the prevision of solvent effects, Theor. Chem. Acc. 103 (2000) 343–345.

[31] F. Weinhold, J.E. Carpenter, The Structure of Small Molecules and Ions, Plenum, New York, 1988, pp. 227

[32] I. Fleming, molecular Orbitals and Organic Chemical Reactions, Wiley, London, 2010.

[33] Nour T. Abdel Ghani, Ahmed M. Mansour,Molecular structure of 2-chloromethyl-1H-benzimidazole hydrochloride: Single crystal, spectral, biological studies, and DFT calculations,SpectrochimicaActa Part A 86 (2012) 605– 613

[34] N.M.O.Boyle,A.L.Tenderholt and K.M.langner, Gausssum 3.0 J.Comp.chem.29 (2008),839-845.

[35] M. Krishnamurthy, P. Phaniraj, S.K. Dogra, Absorptiometric and fluorimetricstudy of solvent dependence and prototropism of benzimidazole homologues,J. Chem. Soc. Perkin Trans. II (1986) 1917-1925.

[36] A.K. Mishra, S.K. Dogra, Photoluminescence of 2-(o-aminophenyl)benzimidazole, J. Photochem. 31 (1985) 333-344.

[37] R.G. Pearson, Absolute electronegativity and hardness correlated with molecular orbital theory, Proc. Natl. Acad. sci. 83 (22) (1986) 84 40–84 41.

[38] H. Tandon , A. Shalini , T. Chakraborty , Molecular electrophilicity index-a promising descriptor for predicting toxological property, J. Bioeqiv. Availab. 9 (6) (2017) 518–527.

[39] Luque, F. J.; Lo´pez, J. M.; Orozco, M. TheorChemAcc 2000, 103, 343-345.

[40] Okulik, N.; Jubert, A. H. Internet Electron. JMol Des 2005, 4, 17-30.

[41] Politzer, P.; Truhlar, D. G., Eds. Chemical Applications of Atomic and Molecular Electrostatic Potentials; Plenum Press: New York, 1981.

Chapter V

Synthesis, Spectral Property, DFT Studies and Anti-Microbial Evaluation of 6 amino-2-(4 nitrophenyl)-1H-benzimidazole

Abstract

6 amino-2-(4 nitrophenyl)-1H-benzimidazole was synthesized and characterized by FT-IR, UV visible spectroscopy, ^{1}H NMR and ^{12}C NMR spectral analysis. The optimized molecular structure geometry and vibrational wave numbers of the title compound were calculated using the HF and DFT (B3LYP, B3PW91) methods with 6-311 G (d, p) and 6-311++ G (d, p) basis sets and compared with experimental data. HOMO and LUMO energies are calculated. Electronic absorption spectra and ^{1}H and ^{13}C NMR has been calculated in gas and solvents (DMSO, chloroform, water) by using TD-DFT methodology(Integral formalism of the polarizable continuum model(IEF-PCM)) at DFT/B3LYP 6-311++G (d, p) basis set. Natural bond orbital (NBO) analysis has performed to understand the stability, hyper conjugative interaction and delocalization. Molecular electrostatic potential (MEP) reveals the electrophilic and nucleophilic sites for reaction. The title compound has been screened for antimicrobial activity using Disc-diffusion method.

5.1 Introduction

Benzimidazole is an important heterocyclic aromatic organic compound. The derivatives of this compound show extensive biochemical, pharmacological and antimicrobial activities [1-2]. The substituted benzimidazole derivatives have wide applications such as drugs, enzyme inhibitors, dyes and polymers [3]. Moreover, benzimidazole based drugs available such as esomeprazole, lansoprazole, telmisartan, bendazol and bendamustine [4] and playsa significant role in pharmacophore. The efficiency of these effective compounds encourages for developing the more number of significant compounds.

Marinescuet al., [5] reported the synthesis of six benzimidazole compound and characterized it. Density functional theory analysis of the molecular structure has been done. They conclude that the electronic and structural parameters of the benzimidazole compounds are well correlated to their antimicrobial activity. Saral et al., [6] reported the synthesis of 1-Methyl-2-(2’-hydroxy-4’-chlorophenyl) benzimidazole and 1-Methyl-2-(2’-hydroxy-4’-methoxyphenyl) benzimidazole compounds and calculated geometric parameters, vibrational frequencies, electronic excitation energies and their NMR chemical shifts of both compounds using B3LYP methods with 6-31G(d, p) basis set, also compared the experimental value with theoretical data. Quantum-Chemical, IR, NMR and X-ray Diffraction Studies on 2-(4-Chlorophenyl)-1-methyl-1H-benzo[d] imidazole was carried out by Ozdemir et al., [7] and compared the theoretical studies using HF and DFT/B3LYP methods using 6-31G (d, p) basis set with experimental data.

Literature survey shows that the HF, DFT and experimental studies on 6 amino-2-(4 nitrophenyl)-1H-benzimidazole has not been reported so far. Looking the importance of nitrogen containing heterocyclic moiety and number of patents concerning this moiety in last few years. It was thought that it would be lucrative to report the synthesis and detailed spectroscopic investigation of 6 amino-2-(4 nitrophenyl)-1H-benzimidazole using HF and DFT. The present study deals with optimized geometric parameters and describe the vibrational frequencies of the title molecule using HF and DFT (B3LYP/B3PW91) methods with basis sets 6-311 G (d, p)and 6-311++ G (d, p) using Gaussian 16 W and Gauss View 6.0. Highest Occupied Molecular Orbital (HOMO) and Lowest Unoccupied Molecular Orbital (LUMO) has also been investigated using IEF-PCM (TD-DFT/B3LYP6-311++G(d, p)), Fukui function calculations has been performed to obtain local reactivity descriptive , natural bond analysis (NBO) was calculated to obtain redistribution of electron density (ED) and E(2) energies. The UV and NMR spectral studies have been carried out using B3LYP/6-311++G (d, p), Molecular electrostatic potential also performed to know the information about the charge transfer within the molecule. Antimicrobial activity of the title molecule is valuated.

5.2 MATERIALS AND METHODS

5.2.1 GENERAL

A round bottom flask was taken and 15 ml of rectified sprit was poured in it. The synthesized 6-nitro-2-(4-nitrophenyl)-1H-benzimidazole compound [8-10] of 0.5 gram is added to it. Zinc dust powder was purchased from Sigma Aldrich Company with a state of 99%purity. 2.5 gram of zinc dust powder and 5 ml of 20% Sodium

Hydroxide was added to the solution. The solution was refluxed until the colour of the solution changes from dark red to a colourless it takes nearly for 5 hours then they obtained colourless solution of hot mixture is filtered. The residue of zinc which was obtained is returned back to the flask and it is again extracted by adding the hot rectified sprit the extracts were combined, the solvent which was obtained under vacuum was recrystallized from methanol [11-12].

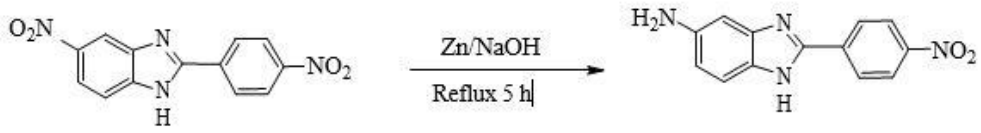

6-nitro-2-(4-nitrophenyl)-1H-benzimidazole 6-amino-2-(4-nitrophenyl)-1H-benzimidazole

The FT-IR spectrum of this compound was recorded in the region of 4000-400 cm^{-1} using KBr pellet technique. The ultraviolet absorption spectrum of the title compound is examined in the region of 500-200 nm. ^{1}H NMR spectrum was recorded on Bruker advanced 500 NMR Spectrometer.

5.2.2 Computational method

The molecular structure of 6 amino-2-(4 nitrophenyl)-1H-benzimidazole has been explicated theoretically with Gaussian 16 W Program packages [13]. The calculated results were visualized by means of Gauss view 6.0 [14].The optimized structure of the title compound is used for the computation of vibrational frequencies in ground state and it is compared with the experimental vibrational frequencies by using Hartree-Fock [15], Density functional three parameter hybrid model (DFT/B3LYP) [16], Becke`s three parameter exchange function (DFT/B3PW91) [17] with the

standard basis sets 6-311 G (d, p) and 6-311++ G (d, p).The electronic transition calculation was performed by Integral equation formalism polarized continuum model (IEF-PCM) with different solvent. NMR chemical shift of ^{1}H and ^{13}C were computed by same method with different solvents by using gauge- independent atomic orbital (GIAO) by applying B3LYP/6-311++ G(d,p). NBO analysis of the title compound was performed in the Gaussian 16 W to understand the intra and inter molecular bonding and also to know the charge transfer in the molecular system. The visualization of HOMO-LUMO is obtained. Molecular electrostatic potential was also carried out to know the reactive sites of the title compound.

5.3 RESULTS AND DISCUSSION

5.3.1 Geometry optimization

The comparative optimized bond length, bond angles and torsion angle of the 6 amino-2-(4 nitrophenyl)-1H-benzimidazole molecule are listed in Table 5.1 The optimized geometry was executed using the B3LYP, B3PW91 and HF methods with the 6-311G (d, p) and 6-311++G (d, p) basis sets (Figure 1). It belongs to C1 group point symmetry. The crystal data of the closely related molecule [7] is compared with the title molecule [18-19]. Due to overlapping, strong bonds are formed. In resultant the bond length reduces, hence short bond length will have strong bonds [20]. Strong bonds are formed between N3-H20, C15-H24, C8-H27 and O1-N6 for the title molecule because they have shorter bond lengths than other. The imine length is shorter than amine length as expected imine N4-C8 is 1.321 Å whereas amine N3-C8 is 1.389 Å as expected [7].The bond length of O1-N6 and O2-N6 are almost equal to 1.22 Å [19]. The N4-C8-C10 and O2-N6-C19 bond angles of the title compound are

124.65°and 117.65° respectively. The highest bond angle of N3-C7-C11 is 133.45°. The dihedral angle N3-C7-C9-C12 and N4-C9-C12-H22 are -179.95°and 179.98°respectively. Comparing all the different parameters in various basis sets shows good agreement with the literature values.

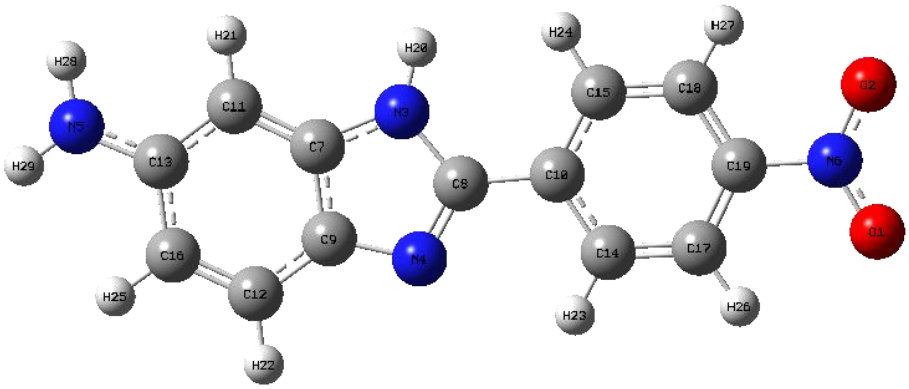

Fig. 5.1 Optimized structure of 6 amino-2-(4 nitrophenyl)-1H-benzimidazole

TABLE 5.1: Optimized geometrical parameters of 6-amino-2-(4-nitrophenol)-1H-benzimidazole: bond length (Å), bond angles (º) and selected dihedral angles (_).

Parameters	**Exp.**[a]	**B3LYP 6311++G (d, p)**	**B3PW91 6311++G (d, p)**	**HF 6311++G (d, p)**	**B3LYP 6311+G (d, p)**	**B3PW91 6311+G (d, p)**	**HF 6311+G (d, p)**
Bond length (Å)							
O1-N6	1.231	1.226	1.220	1.187	1.225	1.219	1.186
O2-N6	1.238	1.227	1.221	1.188	1.226	1.220	1.187
N3-C7	1.352	1.378	1.374	1.373	1.377	1.373	1.373
N3-C8	1.389	1.390	1.384	1.373	1.389	1.383	1.373
N3-H20	0.956	1.006	1.006	0.991	1.006	1.005	0.991
N4-C8	1.321	1.315	1.313	1.282	1.315	1.313	1.281
N4-C9	1.362	1.377	1.373	1.382	1.377	1.372	1.381
N5-C13	1.491	1.396	1.390	1.396	1.394	1.388	1.396
N6-C19	1.467	1.473	1.467	1.465	1.474	1.468	1.464
C8-C10	1.475	1.460	1.456	1.475	1.459	1.456	1.474
C9-C12	1.402	1.401	1.399	1.392	1.401	1.399	1.392
C10-C15	1.392	1.405	1.403	1.390	1.405	1.402	1.390
C11-C13	1.395	1.398	1.396	1.383	1.398	1.396	1.383
C15-H24	0.986	1.084	1.085	1.074	1.084	1.085	1.074
C18-C19	1.383	1.391	1.389	1.379	1.390	1.388	1.379
C18-H27	0.996	1.081	1.082	1.071	1.081	1.082	1.071

Bond angles (°)							
C7-N3-C8	108.32	107.45	107.47	106.80	107.47	107.50	106.81
C8-N4-C9	106.32	105.92	105.72	105.68	105.84	105.65	105.65
O1-N6-O2	122.20	124.51	124.71	124.80	124.71	124.86	124.90
O1-N6-C19	119.12	117.73	117.63	117.60	117.63	117.56	117.55
O2-N6-C19	119.20	117.75	117.65	117.60	117.66	117.58	117.55
N3-C7-C11	133.25	132.45	132.41	132.14	132.50	132.46	132.17
C9-C7-C11	120.30	123.06	123.16	123.14	123.07	123.17	123.13
N3-C8-N4	113.62	111.75	111.91	112.76	111.81	111.94	112.78
N4-C8-C10	125.63	124.65	124.47	124.41	124.52	124.35	124.35
C8-C10-C15	123.62	122.42	122.52	121.77	122.55	122.64	121.84
C13-C11-H21	120.70	120.82	120.85	121.05	120.76	120.80	121.01
C9-C12-C16	119.81	118.48	118.46	118.50	118.56	118.53	118.56
C10-C14-C17	118.70	120.78	120.75	120.46	120.76	120.73	120.45
C10-C15-C18	121.80	120.94	120.87	120.66	120.88	120.82	120.65
C10-C15-H24	121.63	120.95	121.01	120.86	120.94	121.00	120.85
C13-C16-H25	119.91	118.42	118.39	118.64	118.34	118.32	118.57
C19-C17-H26	120.10	119.55	119.48	120.07	119.35	119.31	119.96
N6-C19-C17	118.30	119.33	119.31	119.08	119.32	119.30	119.11

Torsional angle (°)							
C8-N3-C7-C11	-	-179.89	-179.91	179.17	-179.91	-179.88	179.22
H20-N3-C7-C9	-	-179.24	-179.13	-172.63	-178.85	-179.17	-172.41
C7-N3-C8-C10	-	-179.96	-179.96	-179.42	-179.92	-179.95	-179.40
H20-N3-C8-N4	-	179.25	179.14	172.58	178.86	179.19	172.33
H20-N3-C8-C10	-	-0.790	-0.910	-7.630	-1.210	-0.860	-7.840
C9-N4-C8-C10	-	179.98	179.98	179.84	179.97	179.97	179.82
C8-N4-C9-C7	-	0.020	0.020	-0.170	0.010	0.020	-0.200
C8-N4-C9-C12	-	179.99	-180.00	179.87	180.00	-179.99	179.83
H29-N5-C13-C11	-	158.56	158.56	-155.60	157.70	158.00	-154.82
H25-N5-C13-C16	-	-24.29	-24.26	27.09	-25.30	-24.92	27.84
O1-N6-C19-C17	-	-0.020	0.070	0.010	-0.010	-0.010	-0.090
O1-N6-C19-C18	-	-180.01	-179.92	-179.83	-179.98	-179.99	-179.89
O2-N6-C19-C17	-	179.97	-179.94	-179.95	179.99	179.99	179.95
N3-C7-C9-C12	-	-179.95	-179.95	-179.41	-179.91	-179.95	-179.37
C11-C7-C9-N4	-	179.87	179.89	-179.36	179.88	179.86	-179.39
N3-C7-C11-C13	-	179.90	179.90	179.68	179.87	179.89	179.59
C9-C7-C11-H21	-	179.69	179.69	-179.68	179.73	179.73	-179.75
N3-C8-C10-C14	-	179.09	178.78	162.48	178.69	179.10	163.83

[a] Reference taken from [7,18,19]

5.3.2 Vibrational assignments

Selected theoretical and experimental vibrational frequencies of the 6 amino-2-(4 nitrophenyl)-1H-benzimidazole molecule and their assignments are given in Table 6.2 The experimental and theoretical spectra FT-IR is shown in Figure 5.2 The calculated HF and DFT non-scale harmonic frequencies are usually higher than the corresponding experimental quantities due to lack of electron correlation, basis sets insufficiency and anharmonicity effects [21]. To overcome this effect, calculated scale frequencies were scaled with 0.892 for HF, 0.961 for B3LYP and 0.957 for B3PW91 [22]. The DFT calculated result is underestimated than the corresponding HF ones [23]. The vibrational bands assignments have been made by using Gauss view 6.0 molecular visualization program graphical interfaced for Gaussian 16 W [13] and also using VEDA 4 program [24].

All the heterocyclic compounds show υ (N-H) vibration in the region of 3500-3000 cm^{-1}. The N-H spectrum is obtained at 3509 cm^{-1} experimentally and 3520 cm^{-1} theoretically for benzimidazole [25]. We have observed υ(N-H) band at 3559 cm^{-1} experimentally while the DFT (B3LYP/B3PW91) calculations gives the gives the symmetric and asymmetric vibrations of the υ (N-H) bands in corresponding region 3428-3538 cm^{-1} and for HF it is in the region of 3375-3494 cm^{-1} .The C-H stretching vibration of the heterocyclic aromatic compound are expected to appear in the region of 3000-3100 cm^{-1} [26] .The υ(C-H) vibration of the 6 amino-2-(4 nitrophenyl)-1H-benzimidazole compound was observed at3091-3097 cm^{-1} for DFT (B3LYP/B3PW91) calculations and 3062 cm^{-1} from experimental spectra and for HF the bands are

observed in the region of 3030 cm^{-1} .This shows the strongly association of intermolecular hydrogen bonding of the benzimidazole compounds.

The characteristic region of the benzimidazole derivate spectrum is 1650-1500 cm^{-1} , which associates to the stretching vibrations of υ (C-N) and υ (C=C)and their vibrational frequencies and the intensities differ in this region based on their substituent and its position [27].The title compound shows a strong bond at 1400 – 1635 cm^{-1}, which is associated to the stretching of υ (C-N) and stretching of υ (N-O) and bending of β (N-H). This band has been computed at 1625 – 1450 cm^{-1} in DFT (B3LYP/B3PW91) and 1580 to 1482 cm^{-1} for HF. These bands are very intense due to conjugation of benzene and imidazole ring hence, in addition to this vibrational frequency will vary based on the electronegativity of the substitute [28]. The title compound shows good agreement with all this result. Differentiating the stretching of ν(C-N) and ν(C=N) is a difficult [29], since the association of other vibrations are possible in this region. However, with the help of the animation option of Gauss View 6.0 and VEDA 4 program, the ν(C-N) vibrations are identified and assigned. This value supports the reported literature result [30-31]. The N-O vibration of the title molecule is observed in the region of 1596 cm^{-1} and these bands has been computed for the region of 1550-1560 cm^{-1} by DFT(B3LYP/B3PW91) and 1575to 1579 cm^{-1} for HF. The τ (CNCN) and β (CCC) observed in the region of 1300-1430cm^{-1} both for experimental and HF and DFT calculations. The stretching of ν (C-C) along with β (N-C) of the title compound observed in the band region of 1150-1200 cm^{-1} and theoretically at 1065 cm^{-1}. The vibrational spectra of 2 –substituted benzimidazole shows a very intense band around the region of 700-800 cm^{-1}[32]. The title compound

shows the intense band around 790 cm^{-1}in both the experimental and theoretical studies it is due to effect of stretching and bending of ν (C-H) out of plane these values are closely related to the literature [32]. The small variation in experimental and theoretical method may be due to solid phase.

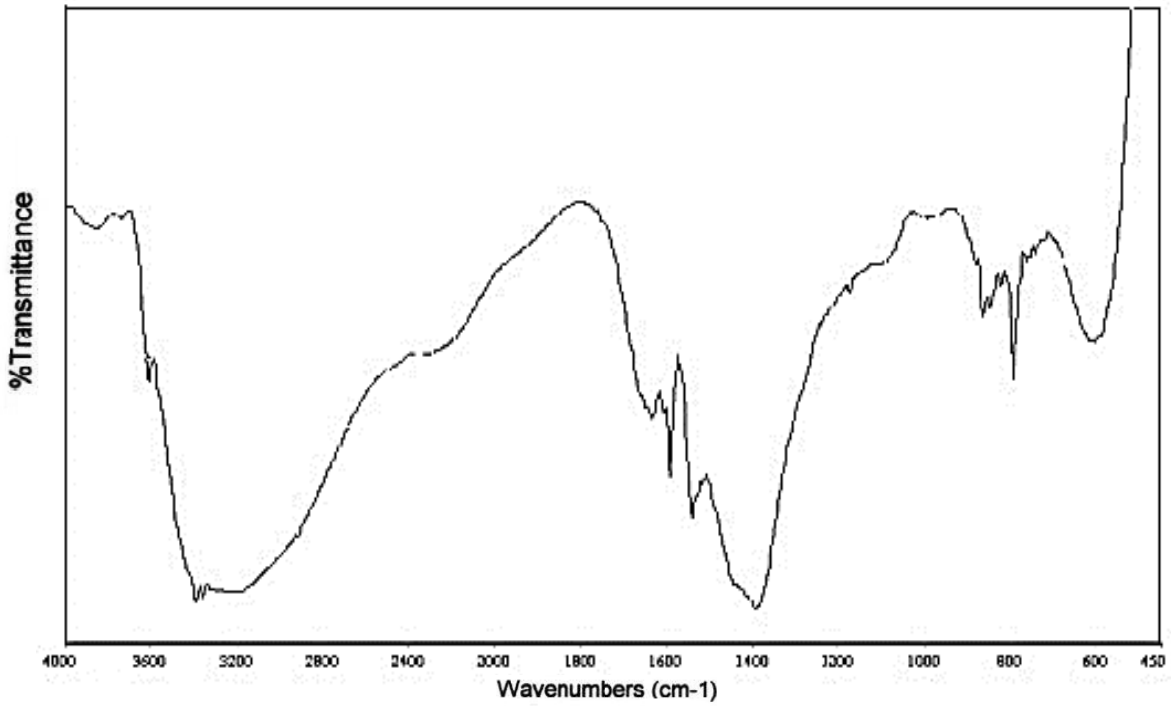

Fig. 5.2 The experimental FT-IR spectra of 6-amino-2-(4-nitrophenyl)-1H-benzimidazole

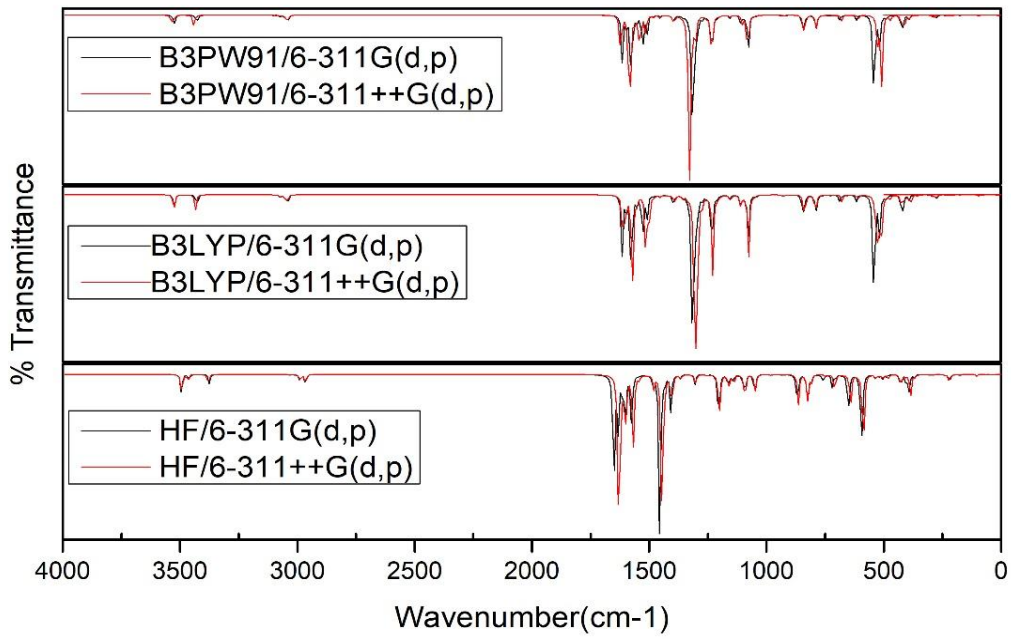

Fig 5.3 Calculated vibrational; frequencies of 6-amino-2-(4-nitrophenyl)-1H-benzimidazole

Table 5.2: Experimental and calculated vibrational; frequencies of 6-amino-2-(4-nitrophenyl)-1H-benzimidazole

Assignments	B3LYP 6-311++G (d, p)	B3LYP 6-311G (d, p)	B3PW91 6-311++G (d, p)	B3PW91 6-311G (d, p)	HF 6-311++G (d, p)	HF 6-311G (d, p)	Exp.
ν(N-H) as	3528.34	3525.65	3538.25	3535.07	3493.09	3494.15	3559
ν(N-H) s	3433.57	3428.06	3439.97	3436.89	3379.99	3375.47	3432
ν(C-H)	3097.66	3099.86	3091.69	3094.38	3030.18	3032.84	3062
β(N-H)	1610.76	1614.97	1620.91	1624.60	1632.30	1650.73	1632
ν(N-O)	1551.29	1552.54	1559.27	1560.24	1576.96	1579.19	1596
ν(N-C) as	1501.55	1508.81	1513.72	1516.38	1542.36	1546.39	1539
ν(N-C)	1452.05	1453.96	1452.40	1454.16	1478.90	1482.00	1400
τ(CNCN)	1392.89	1395.76	1394.97	1397.62	1432.67	1434.92	1393
β(CCC)	1304.43	1314.29	1328.80	1337.02	1301.92	1304.87	1290
ν(C-C) +β(N-C)	1206.62	1207.81	1205.38	1206.47	1162.14	1163.59	1065
ν(N-O) +β(CCC)	968.69	976.57	961.89	970.44	985.14	986.01	975
ν(C-C)	839.15	847.64	842.28	844.45	865.53	871.91	864
β(CCC)+β(CNC)	819.88	820.64	820.00	820.58	834.64	838.51	824
β(C-H)	779.06	781.30	774.49	778.59	809.03	810.16	795
ν(C-H)	609.78	612.30	606.65	607.69	607.02	608.25	606

ν, stretching; δ, twisting; β, bending; τ, torsion; θ, breathing; s, symmetric; as, asymmetric;

5.3.3 Natural bond orbital (NBO) analysis

Natural bond orbital (NBO) analysis gives the accurate possible natural Lewis structure of Ø because all orbits are mathematically chosen to include the highest possible percentage of the ED. The molecular wave function represents the Lewis structures, hybridization, donor-acceptor interaction etc. NBO analysis provides an information of gaining an intuition into inter and intra molecular bonding, rehybridization, charge transferor conjugative interaction in the molecular system [33-34] and also provides the information of the interaction of bond associated with anti-bonding orbital it will resultant in weaken the associated bonding inverse an interaction with bonding pair will strength the bond. It explains intra and intermolecular bonding, charge transfer or conjugative interactions in molecular systems. NBO analysis is used to evaluate the donor-acceptor interactions to measure the delocalization or hyper conjugation and interaction between virtual and both filled orbital spaces. The Natural bond orbital analysis [35] of the 6 amino-2-(4 nitrophenyl)-1H-benzimidazole was performed using Gaussian 16 W packages at B3LYP /6-311++ G (d,p) basis set. The hyper conjugative interaction was deduced from the second order perturbation approach of Fock Matrix in NBO basis between donor-acceptor orbitals [36] and the possible interaction are given in Table 5.3. The larger E (2) second order interaction energy values shows that the interaction between electron donor and electron acceptors are more intense hence strong intramolecular hyper conjugative interactions causes in increase in electron density (ED) and gives stabilization to the system. The result of NBO analysis shows that the σ(N5-C13) participates as donor and the σ* (N4-C8) as acceptor and the intermolecular hyper

conjugative interaction was observed with the stabilization energy of 173.23 Kcal/mol. This interaction weakens the N5-C13 with elongation of its bond length (1.491 Å). The intramolecular hyper conjugative interaction of the electrons occurs from π (C7-C9) to π* (C11-C13) with the stabilization energy of 16 Kcal/mol leads to stabilization of benzimidazole moiety [37].The lone pair interaction of e (N5) with anti-bonding π*(C14-C17) has large stabilization energy of160.59 Kcal/mol, which results the evidence for a charge transfer from nitrogen atom to the π*(C14-C17) and induces partial π character. The E (2) values and different types of transition is shown in Table 5.3

Table 5.3 Significant donor acceptor interaction of 6 amino-2-(4-nitrophenol)-1H-benzimidazole and their second order perturbation energies calculated at B3PW91/6-311++G (d, p) basis set.

Donor Orbital(i)	Type	ED/e	Acceptor orbital (j)	Type	ED/e	E (2) (kcal/mol) [a]	E(j)-E(i) (a.u.) [b]	F (i, j) (a.u.) [c]
O1-N6	σ	1.9957	N6-C19	σ*	0.1032	0.75	1.36	0.029
O2-N6	σ	1.9957	N6-C19	σ*	0.1032	0.74	1.36	0.029
N3-C7	σ	1.9846	C7-C9	σ*	0.0377	0.97	1.36	0.033
N3-C8	σ	1.9849	C7-C11	σ*	0.0188	4.56	1.38	0.071
N3-C8	σ	1.9849	C10-C14	σ*	0.0224	1.42	1.33	0.039
N3-H20	σ	1.9888	N4-C8	σ*	0.0139	3.88	0.84	0.051
N3-H20	σ	1.9888	C7-C9	σ*	0.0378	1.4	1.24	0.037
N4-C8	π	1.8393	C7-C9	π*	0.4888	18.33	0.33	0.076
N4-C8	π	1.8393	C10-C15	π*	0.387	10.99	0.32	0.056
N5-C13	σ	1.9917	N3-H20	σ*	0.0185	163.52	0.85	0.333
N5-C13	σ	1.9917	N4-C8	σ*	0.0139	172.23	0.96	0.363
N5-C13	σ	1.9962	C12-H22	σ*	0.0132	117.35	0.98	0.304
N5-C13	σ	1.9962	C14-C17	π*	0.2624	109.75	0.59	0.243
N5-H28	σ	1.9882	C12-H22	σ*	0.0132	84.61	0.83	0.237
N5-H28	σ	1.9882	C14-C17	π*	0.2624	108.61	0.44	0.208
N6-C19	σ	1.9885	C14-C17	σ*	0.0142	1.5	1.23	0.038
C7-C9	σ	1.9636	C7-C11	σ*	0.0187	4.47	1.24	0.067
C7-C9	π	1.5757	C11-C13	π*	0.3966	16	0.27	0.06
C7-C9	π	1.5757	C12-C16	π*	0.2967	20.01	0.28	0.069
C7-C11	σ	1.9737	C14-C17	σ*	0.0142	10.45	1.13	0.097
C8-C10	σ	1.9734	N4-C8	σ*	0.0433	5.01	0.83	0.058
C9-C12	σ	1.976	N3-H20	σ*	0.0185	5.19	0.72	0.055
C10-C15	σ	1.9729	C15-H24	σ*	0.0143	24.64	0.06	0.035
C10-C15	π	1.6184	C14-C17	π*	0.2624	127.3	0.04	0.064

C11-H21	σ	1.9793	N3-H20	σ*	0.0185	10.18	0.56	0.067
C12-C16	σ	1.9754	N3-H20	σ*	0.0185	20.04	0.73	0.108
C12-C16	σ	1.9754	C14-C17	σ*	0.0142	24.55	1.12	0.014
C13-C16	σ	1.9722	N4-C8	σ*	0.0138	76.47	0.83	0.225
C14-C17	π	1.6547	C10-C15	π*	0.3966	21.4	0.28	0.07
C16-H25	σ	1.9792	N3-H20	σ*	0.0185	55.45	0.54	0.155
C18-C19	π	1.6426	C14-C17	π*	0.2624	116.2	0.05	0.069
N5	e	1.843	C14-C17	π*	0.2624	160.59	0.07	0.096
C18-C19	π	1.6426	C12-H22	π*	0.0133	173.67	1.11	0.876

[a]$E^{(2)}$**,** energy of hyperconjugative interactions**.**

[b]Energy difference between donor and acceptor i and j NBO orbitals

[c]F_{ij} is the Fock matrix element between i and j NBO orbitals

5.3.4 NMR spectra analysis

The chemical shift calculations of ^{1}H and ^{13}C have been carried out using B3LYP/6-311++ G (d, p) basis set for the optimized geometry in GIAO method [38].Gaussian 16 W provides the Integral equation formalism polarized continuum model (IEF-PCM) model which is used to describe the influence effects exerted by solvents (DMSO, chloroform, water) on the NMR spectra of 6 amino-2-(4-nitrophenyl)-1H-benzimidazole compound, the results are tabulated in Table 5.4

^{1}H NMR result for the compound shows 1,2-disubstituted benzene system at the ring of benzimidazole nucleus and 1,4 disubstituted benzene system because of the 4-nitrophenyl group at 2 –position. The benzimidazole protons generally gave signal between the 7.71-7.17 ppm in DMSO solution [39]. The hydrogen atoms present in benzimidazole ring shows normal range aromatic hydrogen atoms NMR peaks in the range of 6.81-7.44 ppm. The chemical shift calculated at 6.93-8.82 ppm for DMSO, 6.79- 8.57 ppm for chloroform and 6.94 – 8.83 ppm for water. The proton attached to nitrogen gives a signal at 3.58 ppm experimentally, for all solvents it is in the range of 3.1-3.58 ppm this may be due to different chemical environment.

^{13}C chemical shift values for aromatic carbons gave signals in the range of 100-200 ppm [40-41]. The NMR chemical shift of benzimidazole ring carbon atoms of the title compound shows signal in the range of 111.09-152.32 ppm were based on the literature value [7].These chemical shifts were calculated at 94.66 -150.67 ppm in DMSO,93.87-150.13 ppm in chloroform, 94.71 150.70 in water. The C-13 has the greatest chemical shift in all the solvent this is due to binding of high electronegative oxygen atoms. The carbon C-8 atom gives the signal at 152.32 ppm and in all the solvents it is in the range of 150 ppm which supports the formation of benzimidazole group. It is clearly seen from the Table 5.4

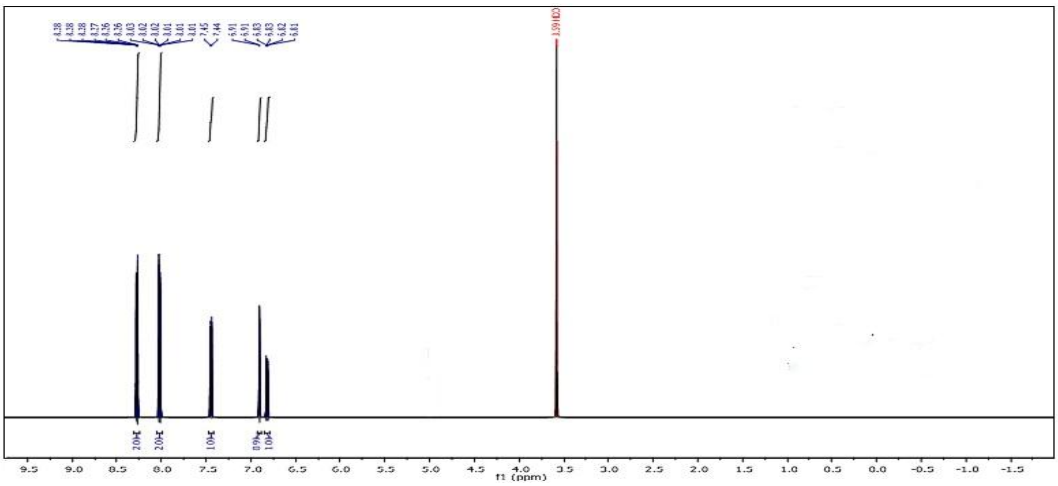

Fig 5.4 ^{1}H- NMR spectra of 6-amino-2-(4-nitrophenyl)-1H-benzimidazole.

Table 5.4 Experimental and calculated (GIAO)^{1}H and ^{13}C NMR chemical shifts for of 6-amino-2-(4-nitrophenyl)-1H-benzimidazole

Atom		**B3LYP/6-311++G (d, p)**			
^{1}H	**Exp.**	**Gas**	**DMSO**	**Chloroform**	**Water**
H21	6.91	6.5249	6.937659	6.7954	6.9456
H22	7.44	7.7934	7.776581	7.7953	7.7752
H23	8.28	8.4739	8.44962	8.4727	8.448
H24	8.02	7.5457	8.025789	7.8701	8.0343
H25	6.82	6.7147	6.947171	6.8779	6.9508
H26	8.28	8.5982	8.647768	8.6392	8.648
H27	8.02	8.4739	8.675031	8.6244	8.6779
H29	3.58	3.1314	3.582626	3.4581	3.5889
^{13}C	**Exp^{a}.**				
7-C	135.01	139.7803	140.7138	140.4163	140.73
8-C	152.32	149.2057	150.6713	150.1319	150.702
9-C	137.07	144.0983	143.2575	143.5699	143.239
10-C	131.52	141.6758	142.9386	142.6371	142.9529
11-C	111.09	92.6203	94.66782	93.8751	94.7148
12-C	119.5	131.9408	129.8337	130.6614	129.7845
13-C	123.01	147.634	148.8072	148.5441	148.8192
14-C	129.21	134.2269	133.7003	133.9769	133.682
15-C	129.21	128.6182	131.9283	130.8036	131.9912
16-C	122.53	114.7624	115.171	115.1038	115.1732
17-C	131.52	134.1188	134.2445	134.2521	134.2428
19-C	142.83	146.2517	146.9595	146.7072	146.9737

[a] Reference taken from [7]

5.3.5 Electronic properties

The electronic transition of the 6 amino-2-(4-nitrophenyl)-1H-benzimidazole compound have been investigated such as absorption wavelength, oscillator strength, band gap and transition strength were computed by Integral formalism of the polarisable continuum model (IEF-PCM) model using B3LYP/6-311++G (d, p) basis set of DFT which deals with solvent effects for the DMSO, chloroform and water as solvents. The contributions of the transition were designated with the help of Gauss sum3.0 [42]. The Ultraviolet spectra analysis data for both the gas and solvent phase is tabulated in the Table 4.6. The electronic spectra exhibit broad absorption bands in

the range of 300-635 nm in all the state. In DMSO solvent six absorption bands are found 633, 436, 363, 335, 326 and 317. These bands show that there is high energy π-π*transfer within the phenyl ring of the benzimidazole compound and this may be due to tautomeric structure [43-44]. It is well known that the system has lone pair of electrons in tertiary nitrogen beside this we do not see any n-π* transition [45-46]. The electron transition from the HOMO-2, HOMO-1 and HOMO to LUMO are mainly formed due to π-π*transition. Molecular orbital geometry computations show that the visible absorption band for the title compound corresponds to the electron transition between the HOMO and LUMO for the different solvent and gas phase. For gas phase the band at 532 nm are assigned to electronic transition, HOMO – LUMO with 100% contribution, whereas for solvents (DMSO, chloroform and water) the bands are at 633, 610 and 631 nm all are assigned to electronic transitions, HOMO – LUMO with 100% contribution. The large wavelength (λ_{max}) shows that more electrons are push towards the aromatic ring structure.

The frontier molecular orbital plays a vital role in electric, optical and chemical reactions [47]. The small frontier orbital gap ensures as that the molecule is polarizable, highly chemical reactive and has low kinetic stability. The distribution of energy levels of HOMO and LUMO is shown in Figure 5.4. The value of the energy separation between HOMO and LUMO is 2.8036 eV and 4.3793 eV for HOMO and LUMO+1. This low value shows that the title molecule is more reactive and less stable. In addition to this we have calculate the Ionization potential (I), electron affinity (A).electro-negativity (χ), global softness (S) global hardness (η) and the electrophilicity index (ω) and the results are tabulated in Table 5.6. The global

hardness of the title compound is 1.4018 this shows that the compound is less stable. It is the good indicator of chemical stability. Similarly, the electronegativity (χ) calculated as 4.3607 it shows the attraction of an atom to electron. The electrophilicity index (ω) is 6.7826, this high value shows that there is maximum flow between the donor and acceptor of the title compound. This ensures there is strong energy transformation between HOMO and LUMO [48]. Electrophilic reactivity gives the toxic potential of the substance [49].

Table 5.5. Global chemical reactivity descriptors of 6-amino-2-(4-nitrophenyl)-1H-benzimidazole.

Properties	**B3LYP/6-311++G(d,p)**
E HOMO (eV)	-5.7625
E LUMO (eV)	-2.9589
Ionisation potential (I)	5.7625
Electron affinity(A)	2.9589
Chemical potential (μ)	-4.3607
Electronegativity (χ)	4.3607
Global hardness(η)	1.4018
Global softness (*S*)	0.3567
Electrophilicity index (ω)	6.7826

Table 5.6 Calculated electronic transition states for the 6-nitro-2-(4-nitrophenyl)-1H-Benzimidazole with the TD-DFT/IEF-PCM method.

DFT/B3LYP with 6-311 ++ G(d,p)						
	Exp. λ (nm)	λ (nm)	Band gap (eV)	Oscillator Strength	Major contributions	Minor contributions
Gas		532	2.3305	0.3241	HOMO->LUMO (100%)	
		390	3.1791	0.0755	HOMO-1->LUMO (98%)	
		381	3.2542	0.0023	HOMO-4->LUMO (86%)	HOMO-5->LUMO (7%)
		321	3.8624	0.0192	HOMO->LUMO+1 (52%)	HOMO-2->LUMO (2%)
		309	4.0124	0.0008	HOMO-8->LUMO (86%)	HOMO-7->LUMO (4%)
		308	4.0255	0.3446	HOMO->LUMO+2 (55%)	
DMSO	297	633	1.9587	0.3784	HOMO->LUMO (100%)	
		436	2.8437	0.1125	HOMO-1->LUMO (99%)	
		363	3.4155	0.0001	HOMO-5->LUMO (96%)	HOMO-5->LUMO+1 (3%)
		335	3.7010	0.0324	HOMO-3->LUMO (79%)	HOMO->LUMO+2 (7%)
		326	3.8032	0.4894	HOMO->LUMO+1 (49%)	HOMO-3->LUMO (7%)
		317	3.9112	0.0136	HOMO->LUMO+2 (89%)	HOMO-3->LUMO (8%)
CHLOR OFORM		610	2.0325	0.3927	HOMO->LUMO (100%)	
		425	2.9173	0.1046	HOMO-1->LUMO (99%)	
		368	3.3691	0.0002	HOMO-5->LUMO (96%)	HOMO-5->LUMO+1 (3%)
		329	3.7685	0.0544	HOMO-3->LUMO (58%),	HOMO->LUMO+1 (6%)
		322	3.8504	0.4598	HOMO->LUMO+1 (53%)	HOMO-3->LUMO (9%)
		317	3.9112	0.0161	HOMO->LUMO+2 (64%)	HOMO->LUMO+1 (9%)
WATER		631	1.9649	0.3647	HOMO->LUMO (100%)	
		436	2.8437	0.1106	HOMO-1->LUMO (99%)	
		363	3.4155	0.0001	HOMO-5->LUMO (96%)	HOMO-5->LUMO+1 (2%)
		335	3.7010	0.029	HOMO-3->LUMO (80%)	HOMO->LUMO+2 (7%)
		326	3.8032	0.4825	HOMO->LUMO+1 (49%)	HOMO-3->LUMO (6%)
		317	3.9112	0.0144	HOMO->LUMO+2 (89%)	HOMO-3->LUMO (8%)

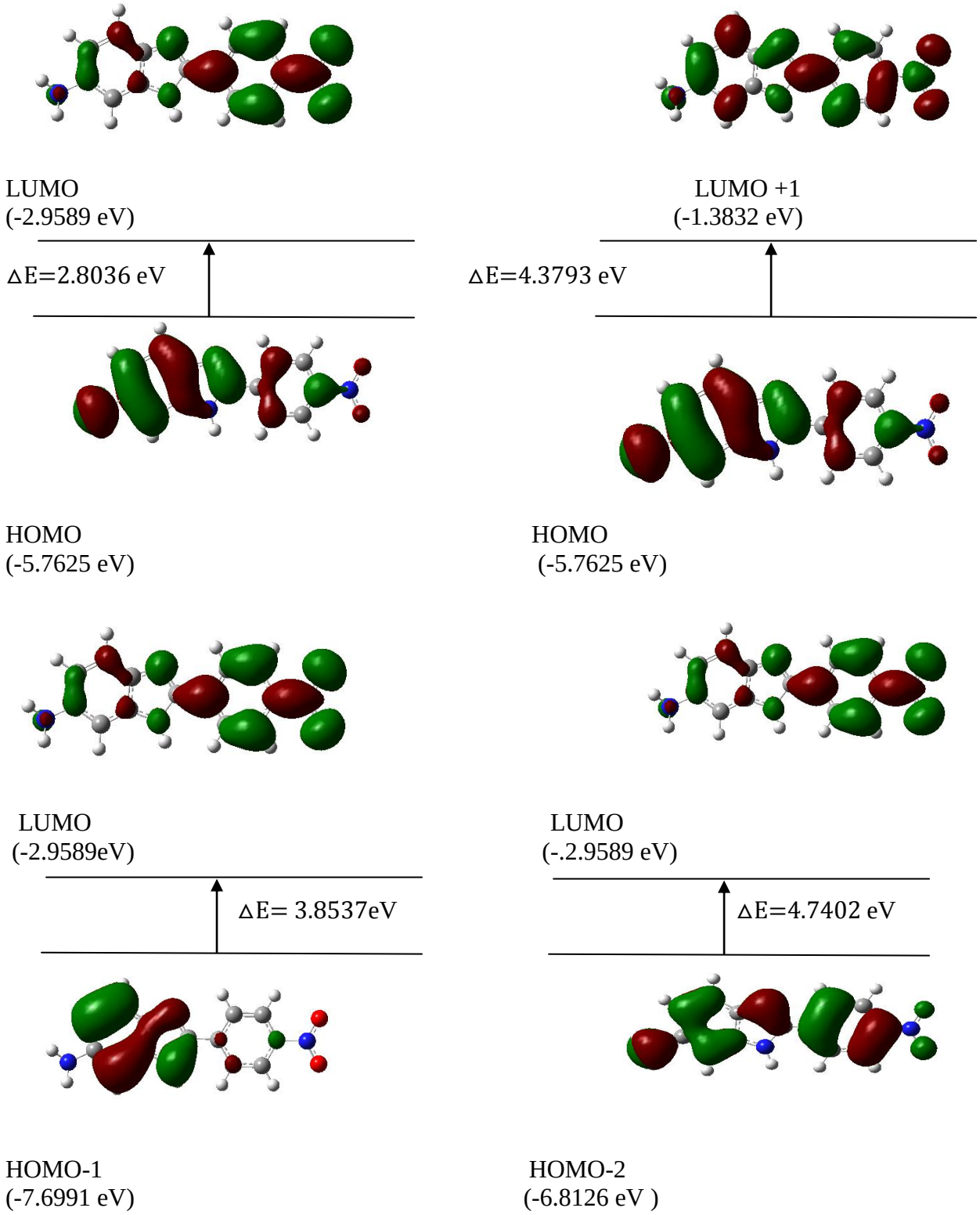

Fig 5.5 The molecular orbital of 6-amino-2-(4-nitrophenyl)-1H-benzimidazole using DFT/B3LYP with 6-311++G (d, p) and the selected electronic transition.

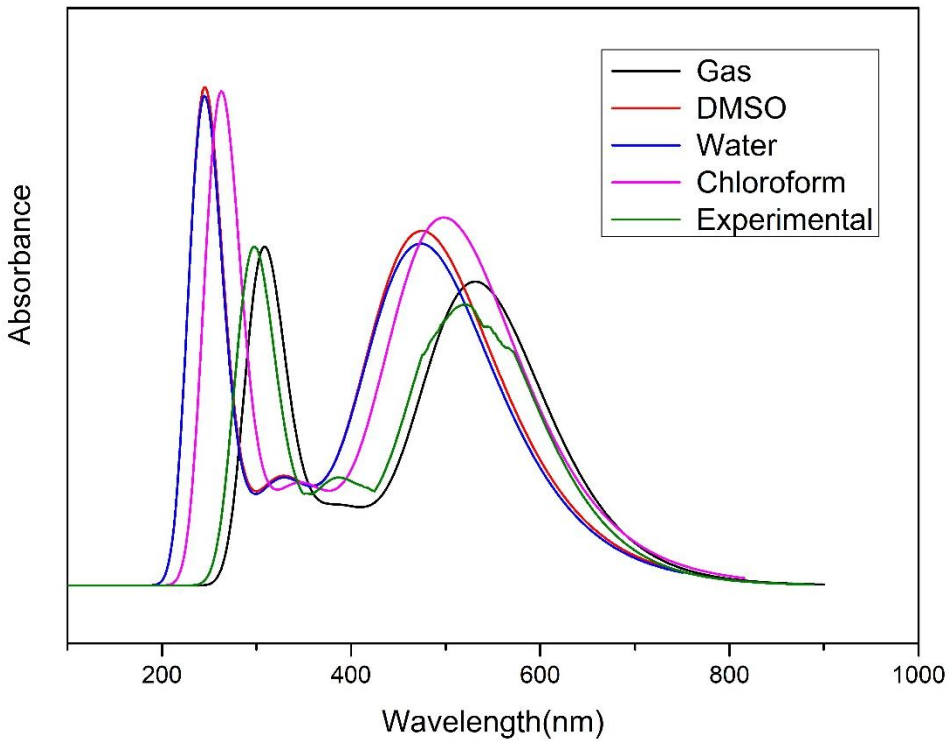

Fig 5.6 Experimental and theoretical UV-Vis spectra of 6-amino-2-(4-nitrophenyl)-1H-benzimidazole

5.4 Molecular electrostatic potential (MEP)

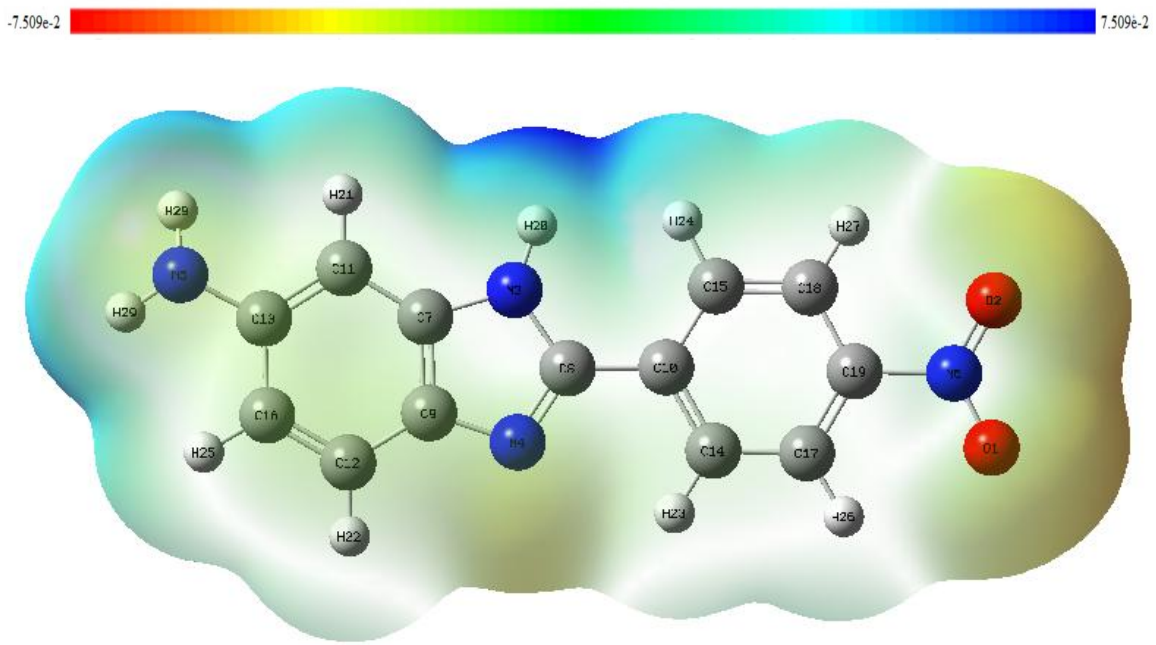

Fig 5.7 The molecular electrostatic potential of 6-amino-2-(4-nitrophenyl)-1H-benzimidazole using DFT/B3LYP with 6-311++G (d, p)

Molecular electrostatic potential (MEP) map was generated at the B3LYP/6-311++G(d, p) for the optimized geometry of 6 amino-2-(4-nitrophenyl)-1H-benzimidazole compound using Gauss view 6.0 program as shown in Figure 6. The electrophilic, nucleophilic reactions and hydrogen bonding interactions can be identified using molecular electrostatic potential [49-51].MEP map is useful for predicting the electrophilic attack and nucleophilic interaction. Electrostatic potential is represented by various colors for various values, red colour represents then negative region (electrophilic reactivity), blue colour represents the positive region (nucleophilic reactivity) and green colour represents that the region has zero potential. It can be seen from Figure 5.6 The negative region is localized on the oxygen atom of the nitrophenol ring N6, this is one of the possible sites for the electrophilic attack

similarly the positive region is localized around the H atoms of the benzimidazole ring this indicates the possible site for nucleophilic attack. It is maximum around the H20 atom of the imidazole ring.

5.5 Molecular docking

Molecular docking studies are used to determine the interaction of two molecules and to find the best orientation of ligand which would form a complex with overall minimum energy. The small molecule, known as ligand usually fits within protein's cavity which is predicted by the search algorithm. These protein cavities become active when they come in contact with any external compounds and are thus called as active sites. Docking is frequently used to predict the binding orientation of small molecule drug candidates to their protein targets in order to predict the affinity and activity of the small molecule. Hence docking plays an important role in the 158 rational drug designs. Given the biological and pharmaceutical significance of molecular docking, considerable efforts have been directed towards improving the methods used to predict docking

The title compound of the study 6-amino-2-(4-nitrophenyl)-1H-benzimidazole called ligand interacts with suitable protein selected using online drug target prediction Swiss ADME-Target prediction. By using Auto dock software, 6-amino-2-(4-nitrophenyl)-1H-benzimidazole molecules are docked with 3EQA protein. The ligand of 6-amino-2-(4-nitrophenyl)-1H-benzimidazole molecules binds at the active site of the substrate are shown in Fig 5.7 The molecular docking binding energy (kcal/mol) was also obtained to be -5.40 kcal/mol. The bonded residues corresponding to 3EQA protein is VAL 485, SER 484, ALA 110 and SER 107 and observed bond

length is enlisted in Table 5.7. This low value of binding energy shows the bio-active nature of the molecule.

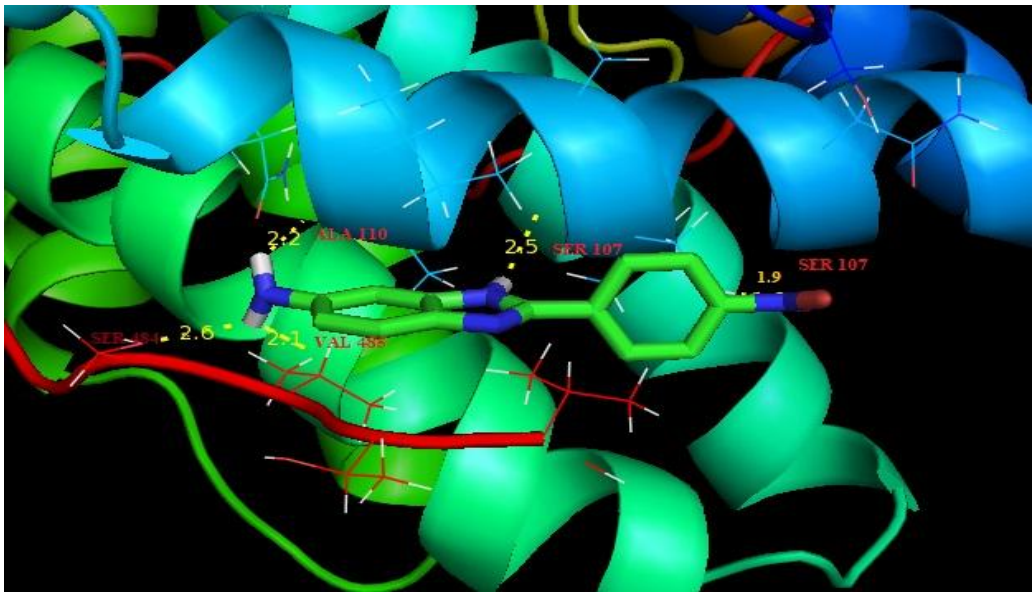

Fig-5.8 Ligand 6-amino-2-(4-nitrophenyl)-1H-benzimidazole embedded in the active site of 3EQA protein

Table 5.7 Hydrogen bonding and molecular docking for protein target-3EQA

Protein ID	Bonded residue	No of bonds	Bond distance	Binding energy (Kcal/mol)	Ref RMSD (Å)
3EQA	VAL485	1	2.1	-5.40	27.15
	SER 484	1	2.6		
	ALA 110	1	2.2		
	SER 107	2	2.5		

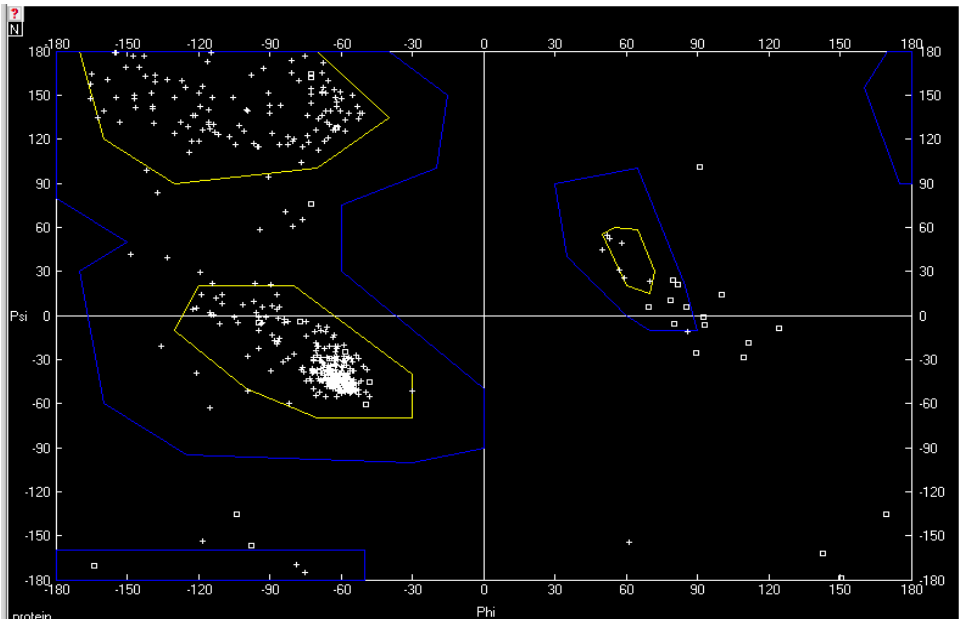

Fig. 5.9 Ramachandran Plot of the protein 3EQA with binding residues VAL 485, SER 484, ALA 110 and SER 107

A Ramachandran plot is a way to visualize backbone dihedral angles ψ against φ of amino acid residues in protein structure. A Ramachandran plot can be used in two somewhat different ways. One is to show in theory which values, or conformations, of the ψ and φ angles are possible for an amino-acid residue in a protein. On the basis of phi and psi angles, we decide that either this kind of rotation and torsion is possible theoretically in the periphery of structure biology. A second is to show the empirical distribution of data points observed in a single structure. On observing the Ramachandran Plot, the energetically allowed regions of the binding residue VAL 485,SER 484, ALA 110 and SER 107 has the torsion angle psi (ψ) against phi (ϕ) lying in the most allowed blue region as shown in Fig. 5.8 From the plot, it is concluded that the selected protein has majority of the residues in allowed region thus indicating the 3EQA protein to be a stable protein.

5.6 Anti-microbial activity:

The antimicrobial activity for 6 amino-2-(4-nitrophenyl)-1H-benzimidazole compound was tested against *Staphylococcus aureus (*MTCC-3160), *Enterococcus faecalis* (MTCC-3159) as Gram –positive bacteria and *Pseudomonas aeruginosa* (MTCC-4030),*Escherichia coli* (MTCC-1667) as Gram-negative bacteria and *Aspergillusniger* (MTCC 282),*Candida albicans* (MTCC 227) as two fungal strains. The evaluating microbial strains were obtained from Microbial Type Culture Collection, Institute of Microbial Technology, and Chandigarh. The Gram-positive bacteria *Staphylococcus aureus*, Enterococcus *faecalis*ca uses boils, skin infection. The Gram-negative bacteria *Pseudomonas aeruginosa*, *Escherichia coli* commonly causes urinary tract infection, respiratory infection. The fungus *Aspergillusniger*, *Candida albicans* causes bronchopulmons, urinary tract infection. Based on their clinical and pharmacological importance the above microorganisms were selected. Antimicrobial activity of 6-amino-2-(4-nitrophenyl)-1H-benzimidazole compound was determined by Disc diffusion method according to National Committee for Clinical Laboratory Standards (NCCLS). The process culture of bacteria used Mueller-Hinton agar (MHA), whereas the fungal strains were grown in potato dextrose agar. The agar was poured in Petri dishes and invigorates the microorganism individually on the agar plates through a sterile swab. The disc of 6 mm diameter were kept in the agar medium and filled with 20 μl (25, 50, 100 μg/ml) of title compound and allowed to diffuse at room temperature for 2 h. The plates were placed on leveled surface and incubated at 37°C for 24 h for bacterial culture and for fungal culture it is incubated for 48 h at 28°C.The plates were then placed on level surface and then

incubated at disc containing the same volume of ethanol served as negative controls while standard antibiotic Ciprofloxacin 25 μg (20 μl) were used as the positive controls. Soon afterwards, zone of inhibition was measured in mm dia. Three replicates were carried for a compound against each of the test organism. Data were expressed as mean ± standard deviation.

The diameter of inhibition zones of the title compound is presented in Table 5.7 The obtained results were compared with the ciprofloxacin as reference standard. It is clearly seen from the Table 5.7 that the title compound shows significant effects on both Gram-positive and Gram-negative bacteria. 6 amino-2-(4-nitrophenyl)-1H-benzimidazole compound shows it affects Gram positive bacteria more than the Gram negative bacteria. It shows strong antibacterial activity against the *Staphylococcus aureus* and *Enterococcus faecalis* this result is better than the reference compound, moderate activity is shown again the Gram-negative bacteria and fungi. This clearly indicates the title compound has the capacity of inhibiting the metabolic growth of the investigating bacteria and fungi to some extent. It is well evident that the more number of drugs are against Gram-positive than Gram-negative [52]. It is an evident from the result that the title compound exhibits potent capacity against the Gram-positive, Gram-negative and fungi. This remarkable property may be arising from the benzimidazole ring [53] and also due to amino attached to the benzimidazole ring hence we know that the electrons having drawing substituent have shown lower activity against Gram-positive and Gram-negative bacteria those having electron donating [54]. The compound shows weak activity against *Aspergillusniger* and *Candida albicans* respectively with compared reference drug ciprofloxacin however

the result is significant against the fungal activity and further investigations are required to optimize the anti-microbial activity. It is known that the antifungal of the compound depends on the suitable position of functional group in the benzimidazole ring [55]. Hence replacing the position of the functional group at the para position or changing the functional group in the benzimidazole will lead to develop a potent compound.

Table 5.8: Antimicrobial activity of the 6-amino-2-(4-nitrophenyl)-1H-benzimidazoleby Disc diffusion method

Microbial Compound	**Diameter of the Inhibition Zone (mm)**			
Gram Positive	25 µg/ml	50 µg/ml	100 µg/ml	Ciprofloxacin 25µg/ml
*Staphylococcus aureus (*MTCC-3160)	14±1.2	17±1.4	19±1.6	13±1.1
Enterococcus faecalis (MTCC-3159)	12±1.1	14±1.2	16±1.7	11±1.3
Gram –Negative				
Pseudomonas aeruginosa (MTCC-4030)	9±1.1	11±1.3	15±1.8	14±1.7
Escherichia coli (MTCC-1667)	6±0.7	11±1.4	13±1.6	13±1.6
Fungal Compound				
Aspergillusniger (MTCC 282),	5±0.6	9±1.1	13±1.6	11±1.3
Candida albicans (MTCC 227)	7±0.7	10±1.1	12±1.3	10±1.1

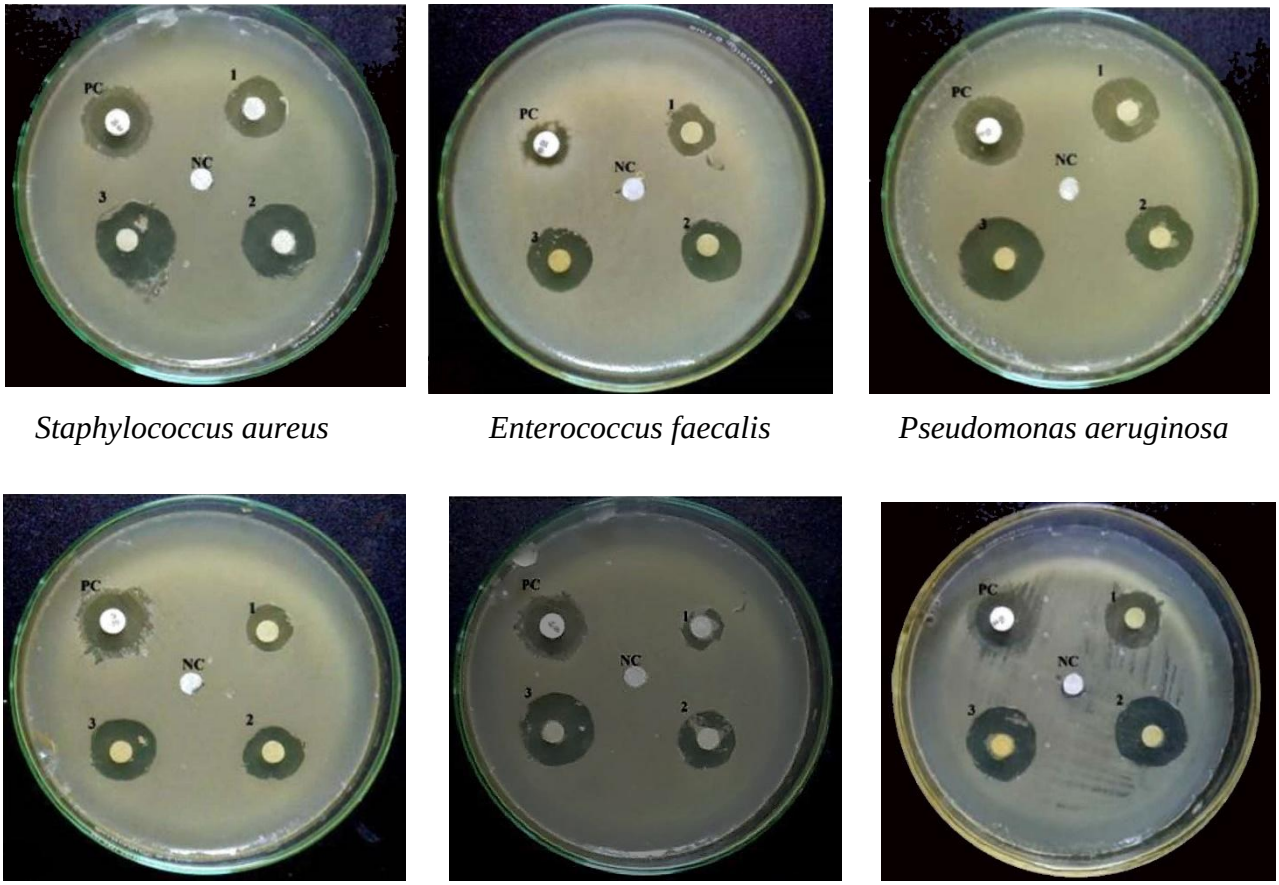

Staphylococcus aureus *Enterococcus faecalis* *Pseudomonas aeruginosa*

Escherichia coli *Aspergillus niger* *Candida albicans*

Fig 5. 10 Anti-bacterial activity of the 6-amino -2-(4-nitrophenyl)-1H-benzimidazole.

Conclusion:

6 amino-2-(4-nitrophenyl)-1H-benzimidazole has been synthesized and characterized by FT-IR, UV-Vis, ^{1}H and ^{13}C NMR spectral analysis. The optimized molecular structure geometry, vibrational wave numbers of the title compound were calculated using the HF and DFT (B3LYP, B3PW91) methods with 6-311 G (d, p) and 6-311++ G (d, p) basis sets and compared with experimental data. All the values are in good agreement with each other.TD-DFT calculations were performed for electronic experiments for gas phase and different solvents (DMSO, chloroform and water). HOMO- LUMO energy gap was determined to be2.8036 eV this shows the compound is less stable and more reactive. Global and local reactivity descriptor

provides that there is maximum flow of energy between donor and acceptor of the title molecule it is due to π-π*transition. The chemical shifts for ^{1}H and ^{13}C also calculated and compared with experimental data and it shows a very good agreement.NBO analysis reveals the intermolecular interaction and the stabilization energy of the molecule. MEP map provides the information on nucleophilic and Electrophilic sites of the molecule. The H20 of the compound is most active site for nucleophilic reaction. The synthesized compound exhibits antibacterial and antifungal activity. It is more active towards the Gram-positive bacteria than Gram-negative bacteria this is due to presence of NH_2 (electron donor) in benzimidazole ring. The compound shows weak antifungal activity.

Reference:

1. Kumar, B.V.S., Vaidya, S.D., Kumar, R.V., Bhirud, S.B., Mane, R.B.,2006. Eur. J. Med Chem. 41, 599.
2. Kazimierczuk, Z., Upcroft, J.A., Upcroft, P., Gorska, A., Starosciak, B., Laudy, A., 2002. Acta Biochim. Pol. 49, 185.
3. Yadav, G.; Ganguly, S. Eur. J. Med. Chem. 2015, 97, 419−443.
4. C. S. Digwal, U. Yadav, A. P. Sakla, P. V. S. Ramya, S. Aaghaz, A. Kamal, VOSO4 catalyzed highly efficient synthesis of benzimidazoles, benzothiazoles, and quinoxalines, Tetrahedron. Lett. 57 (2016) 4012-4016.
5. M. Marinescu, D.G. Tudorache, G.I. Marton, C.-M. Zalaru, M. Popa, M.-C.Chifiriuc, C.-E. Stavarache, C. Constantinescu, Density functional theory molecular modeling, chemical synthesis, and antimicrobial behaviour of selected benzimidazole derivatives, Journal of Molecular Structure (2016)
6. Hasan Saral, Ozgürozdamar, Ibrahim uçar synthesis, structural and spectroscopic studies of two new benzimidazole derivatives: A comparative study Journal of Molecular Structure 1130 (2017) 46-54

7. Namik ozdemir, Bilge eren, Muharremdincer, Yunusbekdemir. Quantum-Chemical, IR, NMR and X-ray Diffraction Studies on 2-(4-Chlorophenyl)-1-methyl-1H-benzo[d]imidazole, International Journal of Quantum Chemistry, Vol 111, 3112–3124 (2011)
8. Singh J, Grover P, Pathak DP. Synthesis and Comparative QSAR study of some novel benzimidazole derivatives. Acta. Pharm. Sci.(2010) 52: 510-521.
9. M.Sugumaran, M.Yokesh Kumar Synthesis and Biological Activity of Novel 2, 5 Disubstituted Benzimidazole Derivatives International Journal of Pharmaceutical Sciences and Drug Research 2012; 4(1): 80-83
10. F. Liakath Ali Khan, Fasiuddin G S Synthesis, spectroscopic studies, antimicrobial activity and theoretical studies of 6-nitro-2-(4-nitrophenyl)-1H-benzimidazole.", International Journal of Emerging Technologies and Innovative Research , Vol.6, (5) (2019) 249-261,
11. Raju B., Rahul R., Sivasankar B.N. A new reagent for selective reduction of amino group, Indian Journal of Chemistry. 2009, 45B, 1315-1318.
12. M. Sugumaran, M. Yokesh Kumar Synthesis and Biological Activity of Novel 2, 5-Disubstituted Benzimidazole Derivatives International Journal of Pharmaceutical Sciences and Drug Research 2012; 4(1): 80-83
13. M. J. Frisch, G. W. Trucks, H. B. Schlegel, G. E. Scuseria, M. A. Robb, J. R. Cheeseman, G. Scalmani, V. Barone, G. A. Petersson, H. Nakatsuji, X. Li, M. Caricato, A. V. Marenich, J. Bloino, B. G. Janesko, R. Gomperts, B. Mennucci, H. P. Hratchian, J. V. Ortiz, A.. Izmaylov, J. L. Sonnenberg, D. Williams-Young, F. Ding, F. Lipparini, F. Egidi, J. Goings, B. Peng, A. Petrone, T. Henderson, D. Ranasinghe, V. G. Zakrzewski, Zheng, W. Liang, M. Hada, M. Ehara, K. Toyota, R. Fukuda, J. Hasegawa, M. Ishida, T. Nakajima, Y. Honda, O. Kitao, H. Nakai, T. Vreven, K. Throssell, J. A. Montgomery, Jr.,

14. Roy Dennington, Todd A. Keith, and John M. Millam, Gauss view Version 6.Semichem Inc., Shawnee Mission, KS, 2016.
15. C. Moller, M.S. Plesset, Phys. Rev. 46 (1934) 618
16. C. Lee, W. Yang, R.G. Parr, Phys. Rev. B 37 (1988) 785.
17. P. Predew, Y. Wang, Phys. Rev. B 45 (1992) 244

18. Olga V. Dorofeeva et al..Molecular structure and conformation of nitrobenzenereinvestigated by combined analysis of gas-phase electrondiffraction, rotational constants, and theoretical, Struct Chem (2007) 18:739–753
19. Rajendran Gandhimathietal..Geometry optimization, HOMO and LUMO energy, molecular electrostatic potential, NMR, FT-IR and FT-Ramananalyzes on 4-nitrophenol, Eur. Phys. Appl. Phys. (2015) 69: 10202
20. M. Mitra, P. Manna, A . Das, S.K. Seth, M. Helliwelli, A. Bauza. S.R. Choudhury On the importance of unprecedented lone pair salt bridge interactions in Cu(II)- malonate-2-Amino- 5-Chloropyridine-percholate ternary system J. Physics chem..A 117(2013) 5802-5811.
21. (a) G. Rauhut, P. Pulay, J. Phys. Chem. 99 (1995) 3093–3100;
(b) J.A. Pople, H.B. Schlegel, R. Krishnan, J.S. Defrees, J.S. Binkley, M.J. Frisch,R.A. Whiteside, Int. J. Quantum Chem.: Quantum Chem. Symp. 15 (1981)269–278.
22. J.P.Merrick, JD.Moran,L.Radom, J.Phy, ChemA111 (2007)11683-11700
23. Zhou, W.; Lu, J.; Zhang, Z.; Zhang, Y.; Cao, Y.; Lu, L.;Yang, X. VibrSpectrosc 2004, 34,199
24. M.H. Jamr´oz, Vibrational Energy Distribution Analysis VEDA-4,Warsaw,2004.
25. T.D. Klots, P. Devlin and W.B. Collier, Spectrochim. Acta, 53A, 2445 (1997).
26. M.Evecen,H.Tanak, Material science-Poland 34,(2016),886-904
27. D.J. Rabiger, M.M. Joullie, J. Org. Chem. 29 (1964) 476.
28. Hakan Arslan, Oztekin Algul Vibrational spectrum and assignments of 2-(4-methoxyphenyl)- 1H-benzo[d]imidazole by ab initio Hartree–Fockanddensity functional methods Spectrochimica Acta Part A 70 (2008) 109–116.
29. N.P.G. Roeges, A Guide to the Complete Interpretation of Infrared Spectra of Organic Structures, John Wiley and Sons Inc., New York, 1994.
30. Y.S. Mary, P.J. Jojo, C.Y. Panicker, C.V. Alsenoy, S. Atael, I. Yildiz, Quantum mechanical and spectroscopic (FT-IR, FT-Raman, 1H NMR and UV) investigations of 2- (phenoxymethyl)benzimidazole, Spectrochim. Acta A 125 (2014) 12e24.
31. N. Sundaraganesan, S. Ilakiamani, P. Subramani, B.D. Joshua, Comparison of experimental and ab initio HF and DFT vibrational spectra of benzimidazole, Spectrochim. Acta 67 (2007) 628-635.
32. D.G.O. Sullivan, Spectrochim. Acta Part A 16 (1960) 762.
33. M. Snehaltha, C. Ravikumar, I.H.Joe, N.Sekar, V.S.Jayakumar,Spectrochim Acta Part A 72(3) (2009) 654-662.

34. H.Tanak, A.A.Agar, O.Buyukgungor,Spectrochim Acta Part A 118 (2014) 672-682.
35. F. Weinhold, J.E. Carpenter, The Structure of Small Molecules and Ions, Plenum,New York, 1988, pp. 227.
36. C. Ravikumar, I. Hubert Joe, V.S. Jayakumar, Chem. Phys. Lett. 460 (2008)552–558.
37. Nour T. Abdel Ghani, Ahmed M. Mansour,Molecular structure of 2-chloromethyl-1H-benzimidazole hydrochloride: Single crystal, spectral, biological studies, and DFT calculations, Spectrochimica Acta Part A 86 (2012) 605– 613
38. F.J. Luque , J.M. Lopez , M. Orazco , Perspective on Electrostatic interactions of a solute with a continuum. A direct utilization of ab initio molecular potentials for the prevision of solvent effects, Theor. Chem. Acc. 103 (2000) 343–345
39. P.J. Black, M.L. Heffernan, Proton magnetic resonance spectra of A2B2 systems,Aust. J. Chem. 15 (1962) 862-863.
40. H.O. Kalinowski, S. Berger, S. Braun, Carbone13 NMR Spectroscopy, John Wiley and Sons, Chichester, 1988.
41. K. Pihlaja, E. Kleinpeter (Eds.), Carbone13 Chemical Shifts in Structural and Sterochemical Analysis, VCH Publishers, Deerfield Beach, 1994.
42. N.M.O.Boyle,A.L.Tenderholt and K.M.langner, Gausssum 3.0 J.Comp.chem.29 (2008),839- 845.
43. N.T. Abdel-Ghani, A.M. Mansour, J. Mol. Struct. 991 (2011) 108–126;
44. N.T. Abdel-Ghani, A.M. Mansour, Inorg. Chim. Acta 373 (2011) 249–258.
45. M. Krishnamurthy, P. Phaniraj, S.K. Dogra, J. Chem. Soc. Perkin Trans. II (1986) 1917–1925 (and the references therein);
46. A.K. Mishra, S.K. Dogra, J. Photochem. 31 (1985) 333–344; Indian J. Phys. Sect. B 54 (1984) 480;Spectrochim. Acta Part A 39 (1983) 609–615.
47. Fleming, I. Frontier Orbitals and Organic Chemical Reactions;John Wiley: London, 1976
48. H. Tandon , A. Shalini , T. Chakraborty , Molecular electrophilicity index-a promising descriptor for predicting toxological property, J. Bioeqiv. Availab. 9 (6) (2017) 518–527
.
49. A.O. Aptula , G. Patlewicz , D.W. Roberts , T.W. Schultz , Non-enzymatic glutathione reactivity and in vitriol toxicity; a non animal approach to skin sensitization, Toxicol. Vitro 20 (2006) 239–247.
49. Scrocco, E.; Tomasi, J. Adv Quantum Chem 1978, 11, 115.
50. Luque, F. J.; Lo´pez, J. M.; Orozco, M. Theor Chem Acc2000, 103, 343.
51. Okulik, N.; Jubert, A. H. Internet Electron. JMol Des 2005, 4, 17.

52. A.R. McCutcheon, S.M. Ellis, R.E.W. Hancock, G.H.N. Towers, J. Ethnopharmacol.37 (1992) 213–223.

53. N.T. Abdel-Ghani, A.M. Mansour, Spectrochim. Acta A 81 (2011) 529–543

54. Vaghasiya, Y. K., Nair, R., Soni, M., Baluja, S., & Shanda, S Synthesis, structural determination and antibacterial activity of compounds derived from vanillin and 4-aminoantipyrine. Journal of the Serbian Chemical Society, 69(12),(2004). 991-998.

55. M.K.Singh, R.Tilak, G.Nath, S.K. Awasthi and A.Agrawal, Eur.J.Med.Chem,63 (2013) 635-644.

CHEPTER VI

Synthesis, Spectroscopic studies and anti-microbial studies of 6-chloro-2-(4-aminophenyl)-1H-benzimidazole Using *Ab-intio* and DFT

Abstract

The synthesis of 6 -chloro-2-(4-aminophenyl)-1H-benzimidazole has been reported and characterized by FT-IR spectra in the region of 4000-400 cm^{-1}.UV-visible spectroscopy, ^{1}H NMR experimental techniques. The theoretical studies such as molecular structure parameter, vibrational frequencies, electronic absorption spectra has been investigated using gas and solvent phase, HOMO-LUMO, molecular electrostatic potential (MEP) and natural bond orbital (NBO), of the title compound has been computed using the HF and DFT (B3LYP, B3PW91) methods with 6-31+G (d, p) and 6-31++G (d, p) basis sets.^{1}H –NMR Gauge Including Atomic Orbital (GIAO) chemical were calculated using 6-311++ G (d, p) basis set. The vibrational wave number and the chemical shifts values were compared with the obtained experimental data of the title compound. The electronic properties were evaluated by TD-DFT methodology in different solutions and in gas-phase method using integral equation formalism of the polarisable continuum model (IEF-PCM) at B3LYP/6-311++G (d,p) basis set. HOMO-LUMO energy band gap has been determined. The intermolecular electronic interaction and the stabilization energy was determined using NBO analysis. In addition to this the antimicrobial evaluation of 6 -chloro-2-(4-aminophenyl)-1H-benzimidazole was also performed against some bacteria and fungi using Disc – diffusion method .The inhibition zone of growth was also determined for bacterial and fungal strain.

6.1 Introduction:

Benzimidazole is a heterocyclic compound. It is a cyclic compound where the rings of two different element fused together [1-2]. Benzimidazole has a wide range of application in nucleic acids, dyes and pharmacophore industry. The derivatives of the compound is easily interacts with DNA and it inhibits the growth of the bacterial and fungal infection, hence it has good antimicrobial and anti tumor activity [3-5].based on the literature studies we confirmed that the benzimidazole derivatives have good antimicrobial activity. The functions of the compounds depend on the structure, functional group and other parameter. To perceive the knowledge of the compound we consider quantum chemical theory, DFT and spectroscopy are plays a major role. In order to understand the structure and functions of 6-chloro-2-(4-aminophenyl)-1H-benzimidazole in quantum level, the quantum theory HF and DFT(B3LYP/B3PW91) methods with 6-311 G(d, p) and 6-311++ G (d, p) basis sets is considered for optimizing the structure, FT-IR, are compared with each other. NBO is analyzed the stability of the title compound. UV-Vis and NMR is calculated using Time dependent density function theory (TD-DFT) with integral equation formalism of the polarizable continuum model is used to analyze the various solvent effects on the compound and molecular electrostatic potential is obtained to understand the chemical reactive sites.

6.2 MATERIALS AND METHODS:

6.2.1 GENERAL

The compound 4-chloro-o-phenylenediamine and 4 amino benzoic acid was purchase from Sigma Aldrich Company with a state of 97% purity. 4- chloro -o-

phenylenediamine 1.425 gm (0.01 mol), 4 amino benzoic acid 1.374 gm (0.01 mol) and poly phosphoric acid 9.790 gm was taken in a beaker and mixed thoroughly with a glass rod and immersed in a silica gel bath beaker and irradiated in the microwave oven for about 10 min at maximum microwave power level of 600 watts with a break in two 5 min durations of intermittent cooling. After irradiation was over the silica gel was gently stirred with the thermometer, the reaction mixture was cooled. The completion of reaction was monitored by Thin-layer chromatography (TLC). The cooled mixture was poured into ice cold water and NaoH was added slowly to neutralize the mixture to 8 pH. The precipitation was collected by filtration, dried and later recrystallized from methanol [6].

6.2.2 COMPUTATIONAL METHODS

The theoretical calculation was carried out with Gaussian 16 W [7] and Gauss view 6.0[8]. In the present work we calculated the bond length, bond order and vibrational assignments of the title compound with HF and DFT methods with 6-311 G(d, p) and 6-311++ G (d, p) basis sets and the values are compared with each other. The optimized structure of the 6-chloro-2-(4-aminophenyl)-1H-benzimidazole is obtained. (TD-DFT) with integral equation formalism of the polarizable continuum model (IEF-PCM) is used to analyze the gas, DMSO, chloroform and water effect in the electronic spectra and the chemical shifts of the compound. The other properties HOMO-LUMO is used to analyze the band gap, chemical stability and reactivity of the compound. The electrophilicity and nucleophilicity index are analyzed using MEP.

6.3 Results and discussion

6.3.1 Geometry optimization

The optimized structure of the title compound is shown in Figure 1. It belongs to C1 symmetry. The bond length and bond angle parameters are shown in Table 6.1 All the data are very close to each other in all the basis sets. Generally the C-C bond length in the benzimidazole ring posses 1.40 Å. Here we also observed the C-C bond length around 1.401-1.461 Å this is due to like atoms repel each other. The longest bond observed here is in between the Cl1-C12 is 1.764 Å due to the strongest repulsion between the carbon and chlorine atom the benzimidazole ring. The shortest length is observed at N2-H17 is 1.006 Å this is due to strong interaction between the atoms. Drugs with amino group are bio active.

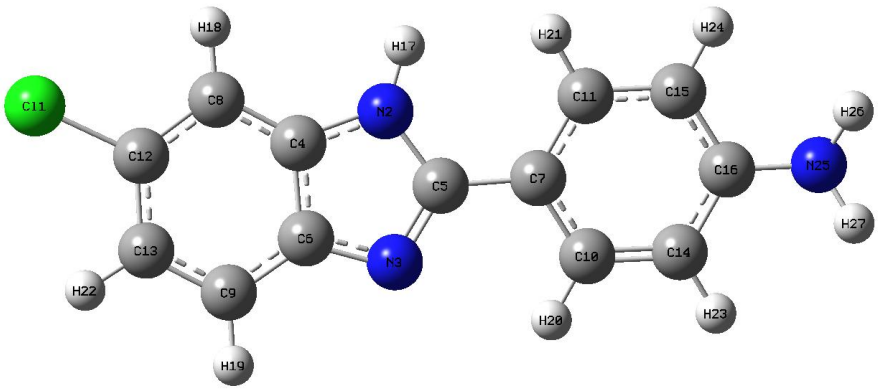

Figure 6.1 Optimized geometry of 6-chloro-2-(4-aminophenyl)-1H-benzimidazole .

Table 6.1Optimized geometrical parameters of 6-chloro-2-(4-aminophenyl)-1H-benzimidazole

Parameters	**B3LYP**	**B3PW91**	**HF**	**B3LYP**	**B3PW91**	**HF**
	6-311++ G(d,p)	**6-311++ G(d,p)**	**6-311++ G(d,p)**	**6-311 G(d,p)**	**6-311 G(d,p)**	**6-311 G(d,p)**
Bond length (Å)						
Cl1-C12	1.764	1.76	1.755	1.763	1.761	1.743
N2-C4	1.381	1.375	1.363	1.380	1.372	1.354
N2-C5	1.387	1.386	1.367	1.386	1.384	1.352
N2-H17	1.006	1.001	0.996	1.005	1.003	0.991
N3-C5	1.316	1.311	1.301	1.315	1.309	1.287
N3-C6	1.381	1.375	1.359	1.381	1.372	1.346
C4-C6	1.414	1.409	1.402	1.411	1.407	1.398
C4-C8	1.393	1.391	1.383	1.391	1.390	1.369
C5-C7	1.461	1.463	1.456	1.459	1.460	1.445
C6-C9	1.398	1.387	1.367	1.390	1.384	1.354
C7-C10	1.405	1.402	1.392	1.401	1.401	1.385
C7-C11	1.402	1.398	1.388	1.402	1.394	1.383
C8-C12	1.390	1.385	1.379	1.385	1.382	1.365
C8-H18	1.082	1.076	1.056	1.081	1.073	1.051
C9-C13	1.390	1.385	1.356	1.389	1.386	1.345
C9-H19	1.083	1.080	1.076	1.081	1.081	1.045
C10-C14	1.384	1.383	1.382	1.382	1.382	1.376
C10-H20	1.083	1.076	1.072	1.080	1.073	1.076
C11-C15	1.388	1.383	1.363	1.386	1.382	1.356
C11-H21	1.085	1.082	1.074	1.087	1.079	1.077
C12-C13	1.404	1.397	1.385	1.402	1.394	1.382
C13-H22	1.082	1.076	1.071	1.087	1.075	1.065
C14-C16	1.406	1.408	1.382	1.401	1.407	1.380
C14-H23	1.085	1.086	1.068	1.084	1.085	1.053
C15-C16	1.403	1.405	1.389	1.401	1.403	1.368
C15-H24	1.085	1.091	1.067	1.086	1.090	1.062
C16-N25	1.389	1.382	1.380	1.390	1.383	1.367
N25-H26	1.009	1.003	0.992	1.004	1.001	0.987
N25-H27	1.009	1.003	0.995	1.005	1.003	0.979
Bond angle (°)						
C4-N2-C5	107.48	107.43	106.340	107.45	107.38	106.340
C4-N2-H17	126.06	126.01	125.060	126.03	126.03	125.060
C5-N2-H17	126.38	126.36	126.560	126.35	126.28	125.560
C5-N3-C6	105.91	105.91	104.430	105.92	105.91	104.430
N2-C4-C6	104.53	104.50	103.890	104.51	104.33	103.890
N2-C4-C8	132.58	132.58	132.980	132.53	132.38	132.990
C6-C4-C8	122.89	122.78	121.900	122.86	122.69	121.900
N2-C5-N3	111.83	111.78	110.990	111.80	111.73	110.890

N2-C5-C7	123.09	123.05	122.090	123.09	123.09	122.090
N3-C5-C7	125.08	125.03	125.980	125.06	125.18	125.980
N3-C6-C4	110.24	110.21	110.980	110.22	110.20	110.980
N3-C6-C9	130.25	130.20	130.650	130.22	130.25	130.560
C4-C6-C9	119.51	119.48	119.430	119.52	119.51	117.430
C5-C7-C10	119.26	119.25	118.740	119.24	119.16	118.740
C5-C7-C11	122.94	122.87	121.450	122.90	122.94	122.450
C10-C7-C11	117.81	117.76	117.640	117.76	117.81	115.640
C4-C8-C12	115.86	115.81	115.720	115.81	115.66	114.720
C4-C8-H18	122.99	122.92	122.830	122.92	122.79	121.830
C12-C8-H18	121.15	121.09	121.520	121.11	121.15	121.520
C6-C9-C13	118.56	118.58	117.870	118.52	118.56	118.650
C6-C9-H19	120.47	120.46	120.760	120.43	120.37	118.760
C13-C9-H19	120.97	120.96	119.530	120.95	120.77	119.530
C7-C10-C14	121.17	121.10	120.320	121.15	121.17	120.320
C7-C10-H20	118.48	118.48	118.760	118.45	118.28	116.760
C14-C10-H20	120.35	120.38	120.940	120.35	120.15	118.940
C7-C11-C15	121.36	121.36	120.650	121.34	121.36	120.650
C7-C11-H21	120.82	120.81	119.870	120.82	120.62	119.870
Torsional Angle (°)						
C15-C11-H21	117.82	117.79	117.950	117.82	117.82	115.950
Cl1-C12-C8	118.54	118.45	117.720	118.54	118.44	117.720
Cl1-C12-C13	118.63	118.57	118.980	118.67	118.53	116.980
C8-C12-C13	122.83	122.80	120.750	122.83	122.83	121.750
C9-C13-C12	120.37	120.29	120.540	120.34	120.37	120.320
C9-C13-H22	120.49	120.45	121.040	120.47	120.49	120.240
C12-C13-H22	119.15	119.12	117.550	119.15	119.44	117.550
C10-C14-C16	120.83	120.77	118.430	120.83	120.63	118.430
C10-C14-H23	119.70	119.64	118.79	119.70	119.50	118.79
C16-C14-H23	119.48	119.46	119.760	119.48	119.48	119.760
C11-C15-C16	120.58	120.51	119.420	120.58	120.58	119.420
C11-C15-H24	119.75	119.75	119.430	119.75	119.35	118.430
C16-C15-H24	119.67	119.61	119.980	119.60	119.47	1179.760
C14-C16-C15	118.26	118.24	117.320	118.27	118.26	117.320
C14-C16-N25	120.79	120.79	119.650	120.77	120.79	120.650
C15-C16-N25	120.90	120.90	119.520	120.91	120.78	119.520
C16-N25-H26	116.80	116.76	116.71	116.80	116.50	116.17
C16-N25-H27	116.66	116.56	116.870	116.60	116.46	116.650
H26-N25-H27	113.21	113.22	113.740	113.21	113.11	113.470

6.3.2 Vibrational Assignments

The vibrational assignments were performed on the theoretically predicted wave numbers by HF and DFT (B3LYP/B3PW91) methods with 6-311 G (d, p) and 6-311 ++ G (d, p) basis sets are presented on the Table 6.2 The discrepancies are corrected by the proper scaling factor [8]. The assignments were performed using VEDA 4 program [9] and animation view of Gauss View 6.0. All the data are in good agreement with each other.

The characteristic regions of N-H stretching vibrations are 3500-3400 cm^{-1} [10]. In FT-IR of the title compound shows a peak of N-H stretching at 3441-3530 cm^{-1} in DFT (B3LYP/B3PW91) method whereas in the HF method the vibration peak observed at 3394-3496 cm^{-1}. The aromatic C-H vibrations are available in the region of 3100- 3000 cm^{-1} [11].we observed this stretching of C-H vibration in the 3025-3040 cm^{-1} for all the DFT basis sets methods whereas for HF it is the region of 2960-2980 cm^{-1}.apart from this stretching of C-H mixed mode of vibration with bending of HCC and also HCCC is observed in and around the region of 1600-1650 cm^{-1} in all the HF and the DFT methods.

The characteristic region of the benzimidazole derivate is 1500-1650 cm^{-1} which associates to υ (C-N) and υ (C=C) and this may differ based on their substituent. We observed υ (C=N) in the title compound at 1480 cm^{-1} , υ (C=C) is observed at 1430 cm^{-1} [1] in all the ab-intio and DFT basis sets . differentiating the υ (C=N) and υ (C-N) is difficult task with the animation option of Gauss view and VEDA 4 we differentiated that υ (C-N) stretching observed at 1320-1350 cm^{-1}. The stretching of υ

(C-Cl) is observed at 550 cm $^{-1}$ in all the basis sets another vibration of out of bending of υ (C-Cl) is observed with the mixed vibration of bending of CNC in around region of 430-450 cm^{-1}.

Table 6.2: Theoretical calculated vibrational frequency of 6-chloro-2-(4-aminophenyl)-1H-benzimidazole

Assignments	**B3LYP**	**B3LYP**	**B3PW91**	**B3PW91**	**HF**	**HF**
	6-311++G (d, p)	**6-311 G (d, p)**	**6-311++G (d, p)**	**6-311 G (d, p)**	**6-311++G (d, p)**	**6-311 G (d, p)**
ν(N-H) sym	3525	3518	3533	3530	3490	3496.00
ν(N-H) sym	3443	3432	3445	3441	3394	3380
ν(C-H)	3040	3031	3027	3025	2980	2960
ν(C-H)+ β (HCC) + τ (HCCC)	1600	1599	1601	1604.3	1624	1616
ν(C=N)	1483	1480	1491	1486	1488	1480
ν(C=C) +β (HCC)	1435	1432	1419	1410	1432	1430
β(C-N)	1358	1345	1328	1320	1378	1367
ν(N-C) +β(C-H)	1273	1261	1254	1245	1248	1240
ν(C-C)	1043	1035	1039	1036	1032	1027
o(N-H)	815	796	823	812	832	824
ν(C-Cl) +β (HCC)	528	512	531	524	568	560
β(CCC)	483	471	468	456	521	515
o (C-Cl)+β (CNC)	437	426	439	434	368	384

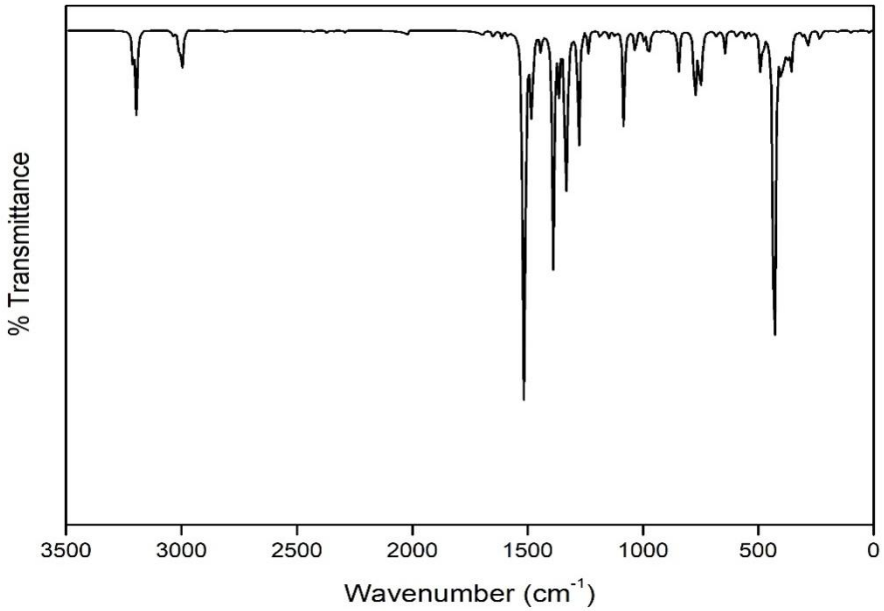

Fig 6.2: Experimental vibrational frequency of 6-chloro-2-(4-aminophenyl)-1H-benzimidazole compound.

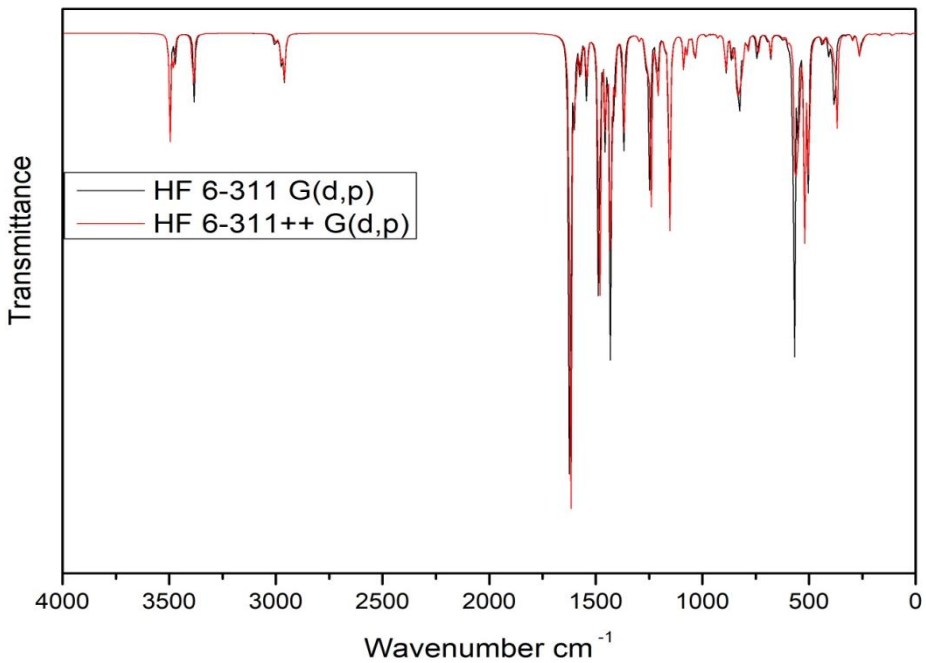

Fig. 6.3 Calculated FT-IR spectra of 6-chloro-2-(4-aminophenyl)-1H-benzimidazole For Basis set HF 6-311 G(d,p) & HF 6-311++ G(d,p)

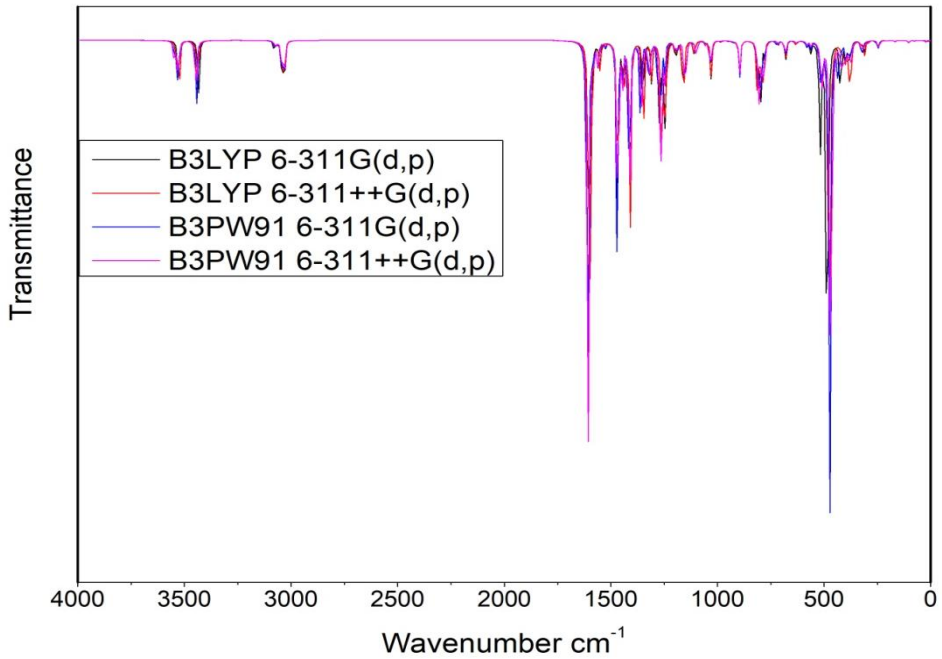

Fig. 6.4 Calculated FT-IR spectra of 6-chloro-2-(4-aminophenyl)-1H-benzimidazole For Basis set B3LYP 6-311G(d,p), B3LYP6-311++G(d,p),B3PW916-311G(d,p), & B3PW916-311++G(d,p),

6.3.4 NBO analysis

The electronic structure, stability, donor and acceptor, intra and intermolecular interaction are analyzed using NBO. The NBO analysis of the 6-chloro-2-(4-aminophenyl)-1H-benzimidazole compound was performed using DFT/B3LYP method with 6-311 ++ G (d, p) basis set provided by Gaussian 16 W. Large E(2) values gives us the strong interaction between electron donor and acceptor of the compound. The important interaction are given in Table 6.3 The highest stabilization of the energy is from π*(N3-C5) to π*(C7-C11) with a value of 262.01 Kcal/mol. The other important interaction for stabilization of the 6-chloro-2-(4-aminophenyl)-1H-benzimidazole compound was σ (C14-C16) to σ* (C4-C6) with a value of 118.8 Kcal/mol.

Table 6.3 Significant donor acceptor interaction of 6-chloro-2-(4-aminophenyl)-1H-benzimidazole and their second order perturbation energies calculated at B3PW91/6-311++G (d, p) basis set.

Cl1-C12	σ	1.9881	C4-C8	σ*	0.02176	2.1	1.27	0.046
N2-C4	σ	1.9845	C5-C7	σ*	0.03519	3.05	1.29	0.056
N2-C5	σ	1.9858	C4-C8	σ*	0.02176	4.55	1.38	0.071
N3-C5	σ	1.9804	C6-C9	σ*	0.0224	4.85	1.46	0.075
N3-C5	π	1.8441	C4-C6	π*	0.47779	19.39	0.34	0.079
N3-C6	σ	1.97759	C5-C7	σ*	0.0352	6.03	1.24	0.078
C4-C6	σ	1.57406	C8-C12	σ*	0.4072	20.59	0.27	0.067
C8-C12	σ	1.9761	N2-C4	σ*	0.0229	5.89	1.16	0.074
C8-C12	π	1.7408	C4-C6	π*	0.4778	18.63	0.3	0.071
C9-C13	σ	1.9692	C6-C9	σ*	0.0224	2.73	1.32	0.054
C10-C14	σ	1.975	C4-C6	σ*	0.0381	31.9	0.76	0.139
C11-C15	σ	1.9737	C4-C6	σ*	0.0381	8.15	0.75	0.07
C14-C16	σ	1.9727	C4-C6	σ*	0.03806	118.8	0.75	0.267
C14-H23	σ	1.9791	N3-C6	σ*	0.01911	8.26	0.93	0.078
C15-C16	σ	1.9724	C14-C16	σ*	0.02385	3.94	1.27	0.063
C16-N25	σ	1.9920	N25-H27	σ*	0.00756	2.94	2.91	0.083
N25-H26	σ	1.9882	N3-C6	σ*	0.0191	15.71	1.07	0.116
Cl1	e	1.9728	C15-C16	σ*	0.02337	24.42	0.06	0.037
N3-C5	π*	0.3722	C7-C11	π*	0.41778	262.01	0.01	0.073
N25 - H26	σ	1.9882	C8-H18	σ*	0.0144	15.33	1.25	0.124
C4-C6	π*	0.4778	N25-H26	σ*	0.00756	8.15	3.21	0.293

6.3.5 NMR SPECTRAL ANALYSIS

The theoretical chemical shifts are simulated using Gaussian 16 W with DFT – B3LYP/6-311 ++ G (d, p) basis set using Gauge independent atomic orbital method [12] with IEF-PCM model to discuss the effect of solvent on the title compound. The readings are tabulated in the Table 6.4

The NMR chemical shift of ^{13}C the benzimidazole compound gives signal in the range of 112-153 as per literature value. The title compound shows the chemical shift values from 113-157 ppm in various solvents. The highest chemical shift was observed in C5 and C16 atom was 154 and 157 ppm due to low shielding. The experimental proton shift of the title compound was also taken into consideration the proton of benzimidazole gave signal in the range of 7.17- 7.71 ppm in DMSO solution

from the literature value . the title compound shows the proton signal in the range of 7.5-9 ppm in gas phase, 7.1 -8.2 ppm in DMSO, 7.07-8.59 ppm in chloroform and 7.17-8.65 ppm in water. The chemical shifts in all the compound are almost equal.

Table 6.5: Experimental and calculated (GIAO)^{1}H and ^{13}C NMR chemical shifts for of 6-chloro-2-(4-aminophenyl)-1H-benzimidazole

Atom	B3LYP/6-311++G(d,p)			
	Gas	DMSO	Chloroform	Water
C4	137.61	138.48	138.19	138.50
C5	154.64	157.12	156.45	157.16
C6	148.65	148.25	148.45	148.23
C7	126.05	124.23	124.73	124.20
C8	113.13	115.37	114.52	115.42
C9	127.99	126.25	126.90	126.21
C10	135.89	134.26	134.90	134.23
C11	130.14	132.46	131.66	132.50
C12	137.95	136.38	136.67	136.37
C13	128.40	127.64	127.86	127.63
C14	123.00	122.88	122.97	122.88
C15	119.62	121.03	120.52	121.06
C16	154.82	156.49	156.05	156.51
H18	8.03	7.64	7.53	7.65
H19	8.49	7.81	7.81	7.81
H20	9.07	8.24	8.29	8.24
H21	8.19	7.86	7.73	7.86
H22	8.04	7.40	7.38	7.40
H23	7.73	7.22	7.16	7.22
H24	7.57	7.17	7.07	7.17

6.3.5 Electronic Properties

HOMO-LUMO energy gap is used to determine the chemical reactivity, stability of the compound and other important parameters. The highest occupied molecular orbital energy level is -5.681 eV and the lowest unoccupied molecular energy level is -2.9589 eV and the energy gap between them is 4.2472 eV. The other parameters such as

electron affinity, electronegativity, global hardness and softness, and electrophilicity index can be determined using the HOMO-LUMO values. This shows the compound is stable and charge transfer take place within a molecule. The UV-Vis spectral analysis of the title compound is shown in Figure 6.5

TD-DFT and B3LYP with 6-311 ++ G(d, p) basis set was used by IEF-PCM model with various solvents such as gas, DMSO, chloroform and water to determine the electronic spectra. The maximum wavelength, oscillator strength and band gap is tabulated in Table 6.5. The maximum absorption wavelength is observed as 288 nm with a band gap of 4.30 eV experimentally with DMSO. The maximum absorption wavelength is absorbed as 305 nm with a band gap of 4.07 eV with oscillator strength of 0.826 .this transition corresponds to 97 % contribution from HOMO→LUMO in gas phase, for DMSO the maximum absorption wavelength is 315 nm with an oscillator strength of 0.985 where the transition corresponds to 98% from HOMO→LUMO. Similarly, for the solvents chloroform and water it is observed to be 315 and 314 nm with the transition corresponds to 98% from HOMO→LUMO. All the values are nearly same hence we conclude the solvent effect is negligible to the title compound.

Table 6.6 Calculated electronic transition states of title compound for 6-chloro-2-(4-aminophenyl)-1H-benzimidazole with TD-DFT/IEF-PCM method.

DFT/B3LYP with 6-311 ++ G(d,p)					
	λ (nm)	Band gap (eV)	Osc. Strength	Major contributions	Minor contributions
Gas	305	4.07	0.8259	HOMO->LUMO (97%)	
	289	4.29	0.0188	HOMO->LUMO+1 (90%)	HOMO-3->LUMO (6%)
	270	4.59	0.0123	HOMO-1->LUMO (71%), HOMO->LUMO+3 (12%)	HOMO-2->LUMO (7%), HOMO->LUMO+5 (3%)
DMSO	315	3.94	0.985	HOMO->LUMO (98%)	
	285	4.35	0.0216	HOMO->LUMO+1 (89%)	HOMO-3->LUMO (7%)
	268	4.63	0.032	HOMO-1->LUMO (70%), HOMO->LUMO+2 (11%)	HOMO->LUMO+4 (5%)
CHLOROFORM	315	3.94	1.0072	HOMO->LUMO (98%)	
	286	4.34	0.0224	HOMO->LUMO+1 (89%)	HOMO-3->LUMO (7%)
	268	4.63	0.0283	HOMO-1->LUMO (71%), HOMO->LUMO+2 (11%)	HOMO->LUMO+5 (4%)
WATER	314	3.94	0.9567	HOMO->LUMO (98%)	
	285	4.34	0.0203	HOMO->LUMO+1 (89%)	HOMO-3->LUMO (7%)
	267	4.63	0.0311	HOMO-1->LUMO (70%), HOMO->LUMO+2 (11%)	HOMO->LUMO+4 (5%)

Table 6.7 Global chemical reactivity description of 6-chloro-2-(4 aminophenyl)- 1H-benzimidazole

Properties	B3LYP/6-311++G(d,p)
EHUMO(eV)	-5.6817
ELUMO(eV)	-2.9589
Ionisation potential (I)	5.6817
Electron affinity(A)	2.9589
Chemical potential (μ)	-4.3203
Electronegativity (χ)	4.3203
Global hardness(η)	1.3614
Global softness (*S*)	0.3673
Electrophilicity index (ω)	6.8551

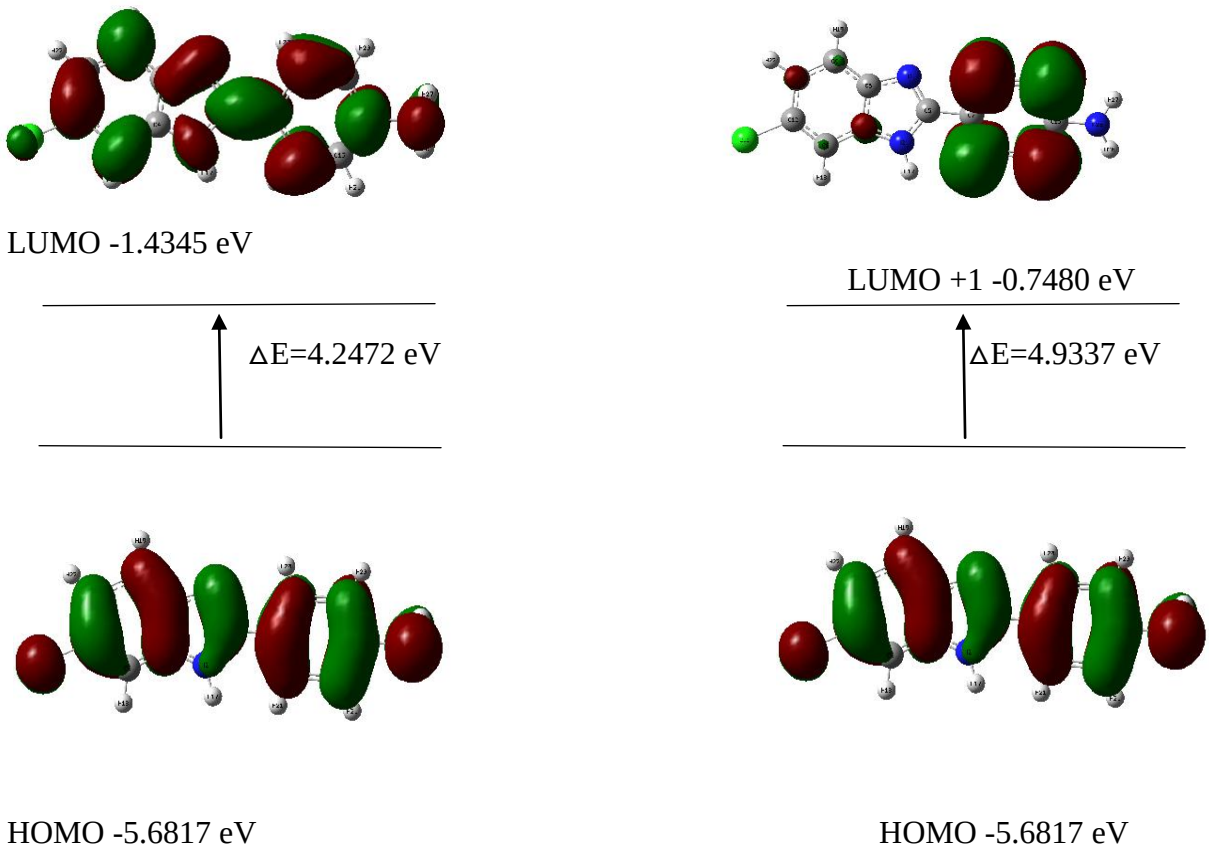

Figure 6.5 The molecular orbital of 6-chloro-2-(4-aminophenyl)-1H-benzimidazole using DFT/B3LYP with 6-311++G (d, p) and the selected electronic transition

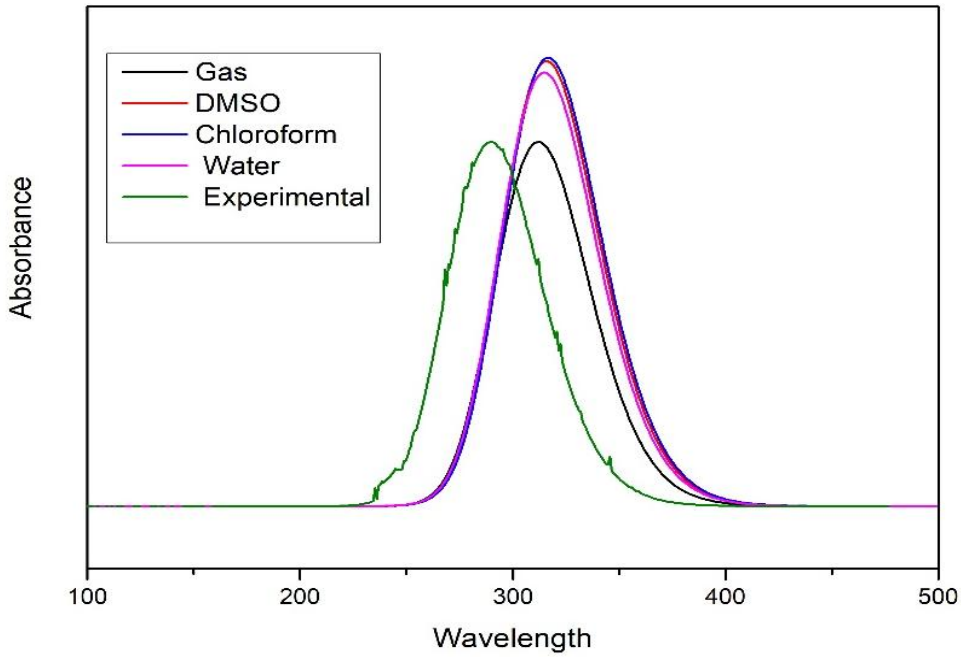

Figure 6.6 UV-Vis theoretical and experimental spectral analysis.

6.3.6 Molecular electrostatic potential

Molecular electrostatic potential is useful descriptor to determine the electrophilicity and nucleophilicity reactions as well as hydrogen bonding interactions in the title compound, the 3 D visual representation provides all the interactions which is discussed by means of colour grading. The MEP diagram of the optimized structure is shown in Figure 5. The Electrophilic site is represented in red colour which is most negative region is present in the Cl1 and N3 atom the title compound. The nucleophilic site is represent in the blue colour which is most positive region is present around the N2-H15 and N4 atom of the title compound. Thus the reactive sides are easily determined.

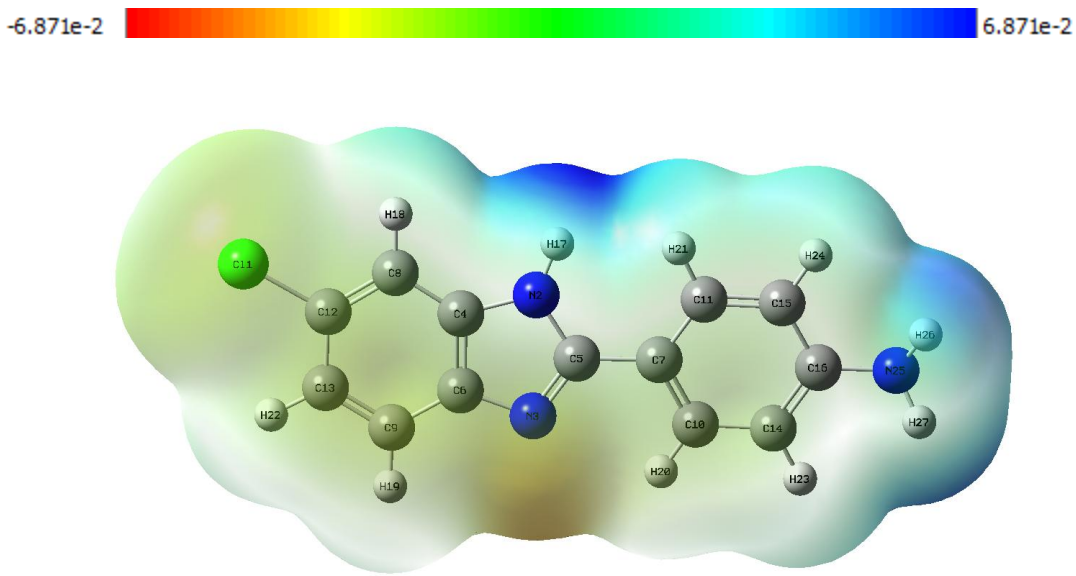

Figure 6.7 The molecular electrostatic potential of 6-chloro-2-(4 aminophenyl)- 1H-benzimidazole using DFT/B3LYPwith 6-311++G (d, p).

6.3.7. Anti-microbial activity

The anti-microbial activity of the 6-chloro-2-(4 aminophenyl)- 1H-benzimidazole compound was tested by Disc-diffusion method. We chose *Staphylococcus aureus* (MTCC-3160) causes serious infection in lungs. *Enterococcus faecalis* (MTCC-3159) causes gastrointestinal and UTI infection, *Pseudomonas aeruginosa*(MTCC-4030) is a human pathogen causes nosocomial infection, *Escherichia coli*(MTCC-1667) is responsible for food poisoning are gram-positive and gram-negative bacterias. *Aspergillus niger*(MTCC-282) causes allergy and lungs infections and *Candida albicans*(MTCC-227) are more often responsible for urinary tract infection are two fungal strains selected for the test. They were all obtained from

Institute of microbial technology, Chandigarh. Each bacteria and fungi were inoculated on to the Mueller-Hinton agar medium.

The anti-bacterial activity was determined by agar disc diffusion assay and the anti-fungal activity was obtained from potato dextrose agar. All the standards are followed as per NCCLS. A bacterial culture to be tested was spread on Muller Hinton agar plate with a sterile cotton swab each agar plate has five 6mm disc, three for impregnating the 6-chloro-2-(4 aminophenyl)- 1H-benzimidazolecompound of different concentration (25, 50,100µg/ml). The positive control reference drug ciprofloxacin of 25 µg/mlis used whereas ethanol is used for negative control. For anti-bacterial study the plates are kept for 2 hours at room temperature for diffusion after that it is incubated at 37 °C for 24 h similarly simultaneously for anti-fungal activity the plates are kept for incubation at 28°C for 48 h. the plates are examined, diameter of the inhibition zone is measured (in mm). Three replicates were carried out for any recorded activity.

The result of the zone of inhibition of the 6-chloro-2-(4 aminophenyl)- 1H-benzimidazolecompound is tabulated in the table 7. The antimicrobial activity of this benzimidazole derivative is mainly due to benzimidazole moiety and the functional group in the structure. It was found that the antibacterial activity of the derivative of benzimidazole compound shows moderate activity against all the gram-positive and gram-negative bacteria. The inhibition zone area around 11±0.6 to 26±0.4 mm in gram-positive bacteria whereas in gram-negative it is around 9±0.7 to 22±0.4 mm in all different concentrations of the tested compound. The title compound shows an good anti-fungal against the Aspergillus *niger* the zone of inhibition is 18±0.6 to

31±0.4 for different concentrations. As the results are compared with reference compound Ciprofloxacin, the benzimidazole derivative shows an better activity than the reference drug this activity is due to presence of the chloro group in the benzimidazole moiety, which is the electron withdrawing groups at para position of benzoyl group may have the positive effect on the fungal activity [2]. It was evident that the present study results were confirmed the modification of the structure, the ortho and para position of the halogen compound in the benzimidazole moiety will improve the antimicrobial inhibition activity against all the tested organism.

Table 6.8 : Antimicrobial activity of the synthesized compounds by disc diffusion method

Microbial Compound	**Diameter of the Inhibition Zone (mm)**			
Gram positive	25 µg/ml	50 µg/ml	100 µg/ml	Ciprofloxacin 25 µg/ml
*Staphylococcus aureus (*MTCC-3160)	12±0.6	18±0.5	26±0.4	14±0.7
Enterococcus faecalis (MTCC-3159)	11±0.6	14±0.5	17±0.5	20±0.5
Gram -Negative				
Pseudomonas aeruginosa (MTCC-4030)	9±0.7	14±0.6	18±0.5	37±0.4
Escherichia coli (MTCC-1667)	15±0.6	19±0.5	22±0.4	29±0.5
Fungal Compound				
Aspergillus niger (MTCC 282),	18±0.6	24±0.5	31±0.4	15±0.6
Candida albicans (MTCC 227)	26±0.4	32±0.4	37±0.4	27±0.5

6.3.7 Molecular docking

Molecular docking has become an increasingly important tool for drug discovery. The molecular docking approach can be used to model the interaction between a small molecule and a protein at the atomic level, which allow us to

characterize the behavior of small molecules in the binding site of target proteins as well as to elucidate fundamental biochemical processes. The docking process involves two basic steps: prediction of the ligand conformation as well as its position and orientation within these sites (usually referred to as *pose*) and assessment of the binding affinity. Knowing the location of the binding site before docking processes significantly increases the docking efficiency. In many cases, the binding site is indeed known before docking ligands into it. Also, one can obtain information about the sites by comparison of the target protein with a family of proteins sharing a similar function or with proteins co-crystallized with other ligands. In the absence of knowledge about the binding sites, cavity detection programs can be utilized to identify putative active sites within proteins. Docking without any assumption about the binding site is called blind docking.

The title compound of the study 6-chloro-2-(4 aminophenyl)-1H-benzimidazole called ligand interacts with suitable protein selected using online drug target prediction swiss ADME-Target prediction. By using Auto dock software, 6-chloro-2-(4 aminophenyl)-1H-benzimidazole molecules are docked with 3EQA protein. The ligand of 6-amino-2-(4-nitrophenyl)-1H-benzimidazole molecules binds at the active site of the substrate is shown in Fig 6.7. The molecular docking binding energy (kcal/mol) was also obtained to be -6.50 kcal/mol. The bonded residues corresponding to 3EQA protein is GLY 254 and ASP 369 and observed bond length is enlisted in Table 6.7. This low value of binding energy shows the title compound is bio-active nature of the molecule

.

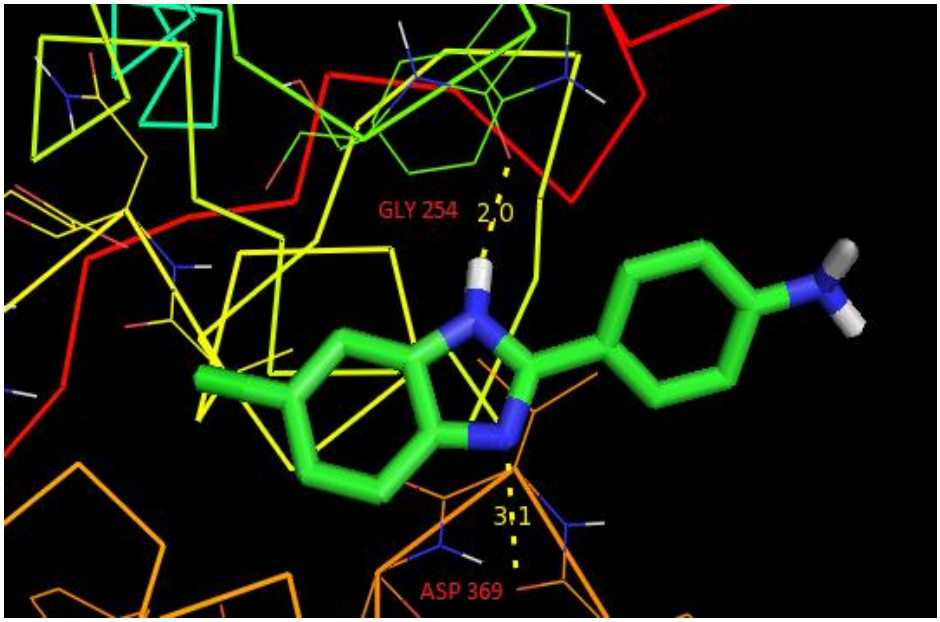

Fig-6.8 Ligand 6-chloro-2-(4 aminophenyl)-1H-benzimidazole embedded in the active site of 3EQA protein

Table 6.9 Hydrogen bonding and molecular docking for protein target-3EQA

Protein ID	Bonded residue	No of bonds	Bond distance	Binding energy (Kcal/mol)	Ref RMSD (Å)
3EQA	GLY 254	1	2.0	-6.50	24.74
	ASP 369	1	3.1		

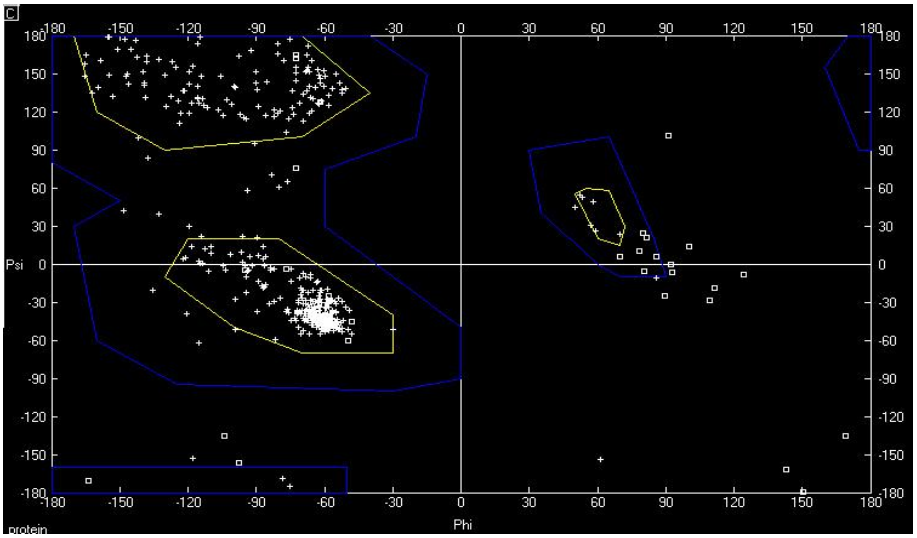

Fig. 6.9 Ramachandran Plot of the protein 3EQA with binding residues GLY 254 & ASP 369

A Ramachandran plot is a way to visualize backbone dihedral angles ψ against φ of amino acid residues in protein structure. A Ramachandran plot can be used in two somewhat different ways. One is to show in theory which values, or conformations, of the ψ and φ angles are possible for an amino-acid residue in a protein. On the basis of phi and psi angles, we decide that either this kind of rotation and torsion is possible theoretically in the periphery of structure biology. A second is to show the empirical distribution of data points observed in a single structure. On observing the Ramachandran Plot, the energetically allowed regions of the binding residue GLY 254 has the torsion angle psi (ψ) against phi (ϕ) lying in the most allowed blue region as shown in Fig. 8. From the plot, it is concluded that the selected protein has majority of the residues in allowed region thus indicating the 3EQA protein to be a stable protein.

Conclusion:

Theoretical investigation of the 6-chloro-2-(4 aminophenyl)- 1H-benzimidazole has been studied in detail . The structure is optimized and the parameter like bond length, bond angle and vibrational spectrum analysis has been done using HF and DFT(B3LYP/B3PW91) methods 6-311 G(d, p) and 6-311 ++ G (d, p) basis set and compared.NBO analysis has been done to know the stabilization energy of the title molecule. NMR chemical shifts for different solvents have been analyzed to know the solvent effect on the compound. Electronic state transition has been performed with different solvents and the adsorption wavelength, oscillator strength and energy gap is determined. HOMO-LUMO energies and the energy gap of the title molecule are determined to know the stability of the molecule and chemical reactivity. MEP identified the chemical reactive sites for the ligand bonding of the compound.

References:

1. Adrien Albert and the rationalization of heterocyclic chemistry, J. Chem. Educ.63 (1986) 860.
2. L. Thomas, Gilchrist, Heterocyclic Chemistry, Addision Wesley, England, 1997.
3. Xue-Jie Fang, Ponmani Jeyakkumar, Srinivasa Rao Avula, Qian Zhou, Cheng-He-Zhour, Bio. Org. & Med. Chem. Letters 26 (2016) 2584-2588.
4. Goro Tsuakamoto, Koichiro Yoshino, Toshihiko Kohna, Hiroshi Ohtaka, Hajimi kagaya, Keizo eto, J. of med.chem. 23 (1980) 738-744.
5. J.P. Seiler, The mutagenicity of benzimidazole and benzimidazole derivatives,Mutat. Res. 15 (1972) 273-276.
6. M. J. Frisch, G. W. Trucks, H. B. Schlegel, G. E. Scuseria, M. A. Robb, J. R. Cheeseman,G.Scalmani, V. Barone, G. A. Petersson, H. Nakatsuji, X. Li, M. Caricato, A. V. Marenich,J. Bloino, B. G. Janesko, R. Gomperts, B. Mennucci, H. P. Hratchian, J. V. Ortiz, A.F. Izmaylov, J. L. Sonnenberg, D. Williams-Young, F. Ding, F. Lipparini, F. Egidi, J. Goings,B. Peng, A. Petrone, T. Henderson, D. Ranasinghe, V. G. Zakrzewski, J.

Gao,.J.W. Ochterski, R. L. Martin, K. Morokuma, O. Farkas, J. B. Foresman, and D. J. Fox, Gaussian 16, Revision B.01 Gaussian, Inc., Wallingford CT, 2016.

7. Roy Dennington, Todd A. Keith, and John M. Millam, Gauss view Version 6.Semichem Inc., Shawnee Mission, KS, 2016
8. J.P.Merrick, JD.Moran,L.Radom, J.Phy, ChemA111 (2007)11683-11700
9. M.H. Jamr´oz, Vibrational Energy Distribution Analysis VEDA-4, Warsaw, 2004.
10. S. Anand, R.S. Sundararajan, C. Ramachandraraja, S. Ramalingam, R. Durga, Spec. Chim. Acta 138 (2015) 203e215.
11. P. Manjusha, , Johanan Christian Prasana, S. Muthu, B. Fathima Rizwana, Chem.Data.Collections20(2019)100191.
12. F.J. Luque , J.M. Lopez , M. Orazco , Perspective on Electrostatic interactions of a solute with a continuum. A direct utilization of ab initio molecular potentials for the prevision of solvent effects, Theor. Chem. Acc. 103 (2000) 343–345

CHAPTER VII

Synthesis, spectroscopic characterization, theoretical studies and antimicrobial evaluation of 6 bromo-2-(4-chlorophenyl)-1H-benzimidazole

Abstract

The synthesis of 6 bromo-2-(4-chlorophenyl)-1H-benzimidazole has been reported and characterized by FT-IR spectra in the region of 4000-400 cm^{-1}.UV-visible spectroscopy, ^{1}H NMR experimental techniques. The theoretical studies such as molecular structure parameter, vibrational frequencies, electronic absorption spectra has been investigated using gas and solvent phase, HOMO-LUMO, molecular electrostatic potential (MEP) and natural bond orbital (NBO), of the title compound has been computed using the HF and DFT (B3LYP, B3PW91) methods with 6-31+G (d, p) and 6-31++G (d, p) basis sets.^{1}H –NMR Gauge Including Atomic Orbital (GIAO) chemical were calculated using 6-311++ G (d, p) basis set. The vibrational wave number and the chemical shifts values were compared with the obtained experimental data of the title compound. The electronic properties were evaluated by TD-DFT methodology in different solutions and in gas-phase method using integral equation formalism of the polarisable continuum model (IEF-PCM) at B3LYP/6-311++G (d,p) basis set. HOMO-LUMO energy band gap has been determined. The intermolecular electronic interaction and the stabilization energy was determined using NBO analysis. In addition to this the antimicrobial evaluation of 6 bromo-2-(4-chlorophenyl)-1H-benzimidazole was also performed against some bacteria and fungi using Disc – diffusion method .The inhibition zone of growth was also determined for bacterial and fungal strain.

7.1 Introduction:

Benzimidazole is bicyclic and considered as a most significant class of bio-active heterocyclic aromatic organic compound where N-containing organic compound fused with benzene and imidazole that exhibit a wide range of biological and pharmaceutical activities [1-2], based on their importance several drugs have been developed such as omeparazole, bendazol, mebendazole and astemizole and marketed by various pharmaceutical companies [3-4].Benzimidazole derivatives have distinctive properties such as antihelminitic [5], antitumor[6-7], antihismantic and antimicrobial activities[8].

Ghani et al.,[9] reported the molecular structure, spectral, biological and DFT studies of 2-chloromethyl-1H-benzimidazole hydrochloride single crystal where the compared the experimental and theoretical data of vibrational and NMR spectra which shows good agreement with each other along with this the investigation of biological activity shows the capacity of inhibiting the metabolic growth of bacteria to different extent. Ozdemir et al.,[10] carried out an Quantum-Chemical, IR, NMR and X-ray Diffraction Studies on 2-(4-Chlorophenyl)-1-methyl-1H-benzo[d]imidazole and concluded that the title compound possess NLO properties and it is a second order nonlinear optical material. Molecular structure and spectroscopic analysis of 1,4-Bis (1-methyl-2-benzimidazolyl)benzene; XRD, FT-IR, dispersive-Raman, NMR and DFT studies was carried out by Bilge et al., [11] the BMBB compound was synthesized and the stable conformer was analyzed and the frontier molecular orbital and NBO analysis showed that the BMBB is potential candidate for biological activity.

The substituted benzimidazole molecules shows unique chemical fictionalization and important selective binding abilities with the biological targets this plays a vital role for drug discovery [12] owing to these above facts and uniqueness of the benzimidazole moiety, the goal of this study is to perform an experimental and theoretical work on 6 bromo-2-(4-chlorophenyl)-1H-benzimidazole to examine the structural and spectroscopic properties. We

synthesis title compound and characterized it using FT-IR, UV-vis, NMR. In addition to this geometrical optimization and vibrational analysis of the title molecule was done using HF and DFT (B3LYP/B3PW91) methods with basis sets 6-311 G (d, p) and 6-311++G (d, p) and the results were compared. The UV and NMR spectral studies at different solutions has been investigated using TD-DFT methodology using IEF-PCM at B3LYP/6-311++ G (d, p) basis set apart from this NBO and MEP was performed to elucidate the charge transformation information of the compound.

7.2. MATERIALS AND METHODS

7.2.1 GENERAL

The compound 4-bromo-o-phenylenediamine and 4 Chloro benzoic acid was purchase from Sigma Aldrich Company with a state of 97% purity. 4-bromo -o-phenylenediamine 1.873 gm (0.01 mol), 4 chloro benzoic acid 1.564 gm (0.01 mol) and20 ml of triethylamine was taken in a beaker and mixed thoroughly with a glass rod and heated at 120° C for 12 h [13]. The completion of reaction was monitored by Thin-layer chromatography (TLC).The solvent was removed and the obtained product is drained and washed with hot ethanol of 150 ml and the product is recrystallized from the solution of ethanol and tetrahydrofuran(THF) of 1:1 ratio[14-15].FT-IR spectrum of the title compound in the solid state have been recorded in the region of 4000-200 cm^{-1} and the spectral data have been collected from VIT- Vellore. The UV-absorption of the compound is examined in the region 250-600 nm using UV -1700 series recording spectrometer. Bruker advance 500 NMR spectrometer was used to record NMR spectra.

7.2.2 Computational method

The molecular structure of the 6 bromo-2-(4-chlorophenyl)-1H-benzimidazole compound has been optimized by HF and DFT (B3LYP/B3PW91) with basis sets 6-311 G (d, p) and 6-311 ++G (d, p) which are taken to calculate the molecular structure, vibrational

frequencies. The calculations of geometrical parameters have been performed in the ground state by using the GAUSSIAN 16 W software [16] through GAUSS VIEW 6 visualized program [17] all the theoretical and the experimental values are compared, DFT(B3LYP/6-311 ++ G(d, p)) standard basis set is considered for calculating the electronic transitions, HOMO-LUMO energies, oscillator strength , UV- Visible spectra in gas and different solvent phase such as DMSO, water and chloroform using IEF-PCM provided by Gaussian 16 W, similarly by using gauge-independent atomic orbital (GIAO) ^{1}H and ^{13} C NMR chemical shift are obtained using the same level of theory. To identify the reactive sites molecular electrostatic potential was also performed.

7.3. RESULTS AND DISCUSSION

7.3.1 Geometry optimization

The optimized molecular structure of 6 bromo-2-(4-chlorophenyl)-1H-benzimidazole has been obtained from Gaussian 16 W and a Gauss View 6.0 program is shown in Figure 7.1 The geometrical parameters such as bond length, bond angle and dihedral angle are important parameter for structural conformations through the bond mechanism this are calculated using HF and DFT(B3LYP/B3PW91) methods with 6-311 G (d, p) and 6-311 G ++ (d, p) and the values are listed in Table 7.1 To the best of our knowledge no investigation has been carried out in the title compound. Saral et al and Arslan et al reported geometrical parameters of structural similar compound of 1-Methyl-2-(2'-hydroxy-4'-chlorophenyl) benzimidazole[18] and 2-(4-methoxyphenyl)-1 H benzimidazole[19]. The calculated N1-C3, N2-C5, C5-C8, C15-Cl25 bond length of the related compound is reported as 1.377, 1.387, 1.399, 1.741Å. The calculated N1-C3, N2-C5, C5-C8, C15-Cl25 bond length of the 6 bromo-2-(4-chlorophenyl)-1H-benzimidazole compound is reported as 1.375-1.381 Å, 1.375-1.386 Å, 1.390-1.399 Å, 1.742-1.755 Å, in all the basis sets there was a very good agreement between the theoretical and experimental values. The imine N2-C4 and amine N1-C4 bond distance in

the benzimidazole group is 1.330 and 1.372 Ǻ they are not equal, imine length is always shorter than the amine length as expected [20].Halogen substitutions in the title compound shows higher bond length C9-Br24,C15-Cl25 at exp/theo:1.867/(1.903-1.925) Ǻ,1.741/(1.742-1.756) Ǻ respectively. The highest bond angle observed N2-C5-C8 at exp/theo: 130.84°/(130.14-130.19°),whereas the crossed torsion angles at the junction is N1-C3-C5-C8 is -179.84° and N2-C5-C3-C7 is 179.97° respectively.

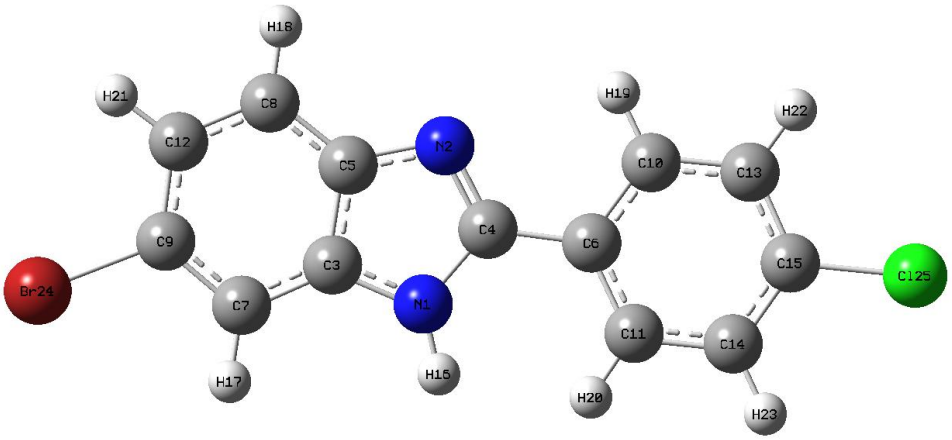

Figure 7.1 Optimized molecular structure of 6 bromo-2-(4-chlorophenyl)-1H-benzimidazole

Table 7.1: Optimized geometrical parameters of 6 bromo-2-(4-chlorophenyl)-1H-benzimidazole bond length (Å), bond angle (°) and dihedral angle (_).

Parameters	**Exp.**	**B3LYP**	**B3LYP**	**B3PW91**	**B3PW91**	**HF**	**HF**
Bond length(Å)		**6-311++G (d, p)**	**6-311 G (d, p)**	**6-311++G (d, p)**	**6-311 G (d, p)**	**6-311++G (d, p)**	**6-311 G (d, p)**
N1-C3	1.377	1.381	1.376	1.377	1.380	1.375	1.376
N1-C4	1.372	1.385	1.380	1.368	1.385	1.379	1.368
N2-C4	1.330	1.315	1.313	1.285	1.314	1.313	1.285
N2-C5	1.386	1.380	1.375	1.386	1.379	1.374	1.379
C3-C5	1.387	1.414	1.412	1.391	1.415	1.412	1.392
C3-C7	1.387	1.394	1.392	1.387	1.394	1.392	1.387
C4-C6	1.468	1.465	1.461	1.475	1.464	1.461	1.475
C5-C8	1.399	1.399	1.397	1.390	1.398	1.397	1.390
C6-C10	1.394	1.403	1.401	1.391	1.403	1.400	1.391
C6-C11	1.414	1.401	1.399	1.388	1.401	1.398	1.388
C7-C9	1.372	1.389	1.387	1.377	1.388	1.386	1.376
C9-C12	1.404	1.405	1.404	1.398	1.405	1.404	1.398
C9-Br24	1.867	1.920	1.905	1.903	1.921	1.905	1.903
C15-Cl25	1.741	1.755	1.742	1.742	1.756	1.742	1.742
bond angle (°)							
C3-N1-C4	106.50	107.35	107.36	106.77	107.34	107.37	106.75
C4-N2-C5	104.46	105.85	105.65	105.71	105.76	105.60	105.67
N1-C3-C5	105.29	104.59	104.54	104.72	104.55	104.49	104.70
C5-C3-C7	122.56	122.87	122.95	122.86	122.87	122.95	122.85
N1-C4-N2	111.16	112.01	112.16	112.88	112.09	112.21	112.92
N1-C4-C6	121.61	123.27	123.28	122.57	123.36	123.41	122.61
N2-C4-C6	125.02	124.72	124.56	124.55	124.56	124.38	124.47
N2-C5-C3	109.75	110.20	110.29	109.92	110.26	110.34	109.95
N2-C5-C8	130.84	130.19	130.15	130.19	130.18	130.14	130.19
C3-C5-C8	120.07	119.61	119.56	119.89	119.56	119.52	119.86
C4-C6-C10	120.55	118.87	118.71	119.02	118.71	118.54	118.94
C4-C6-C11	120.54	122.55	122.64	121.96	122.67	122.80	122.03
C10-C6-C11	118.88	118.58	118.64	119.02	118.62	118.66	119.03
C3-C7-C9	116.91	115.78	115.72	115.91	115.77	115.72	115.91
C5-C8-C12	118.18	118.47	118.45	118.34	118.53	118.50	118.39
C7-C9-Br24	117.99	118.55	118.57	118.71	118.54	118.57	118.71
C12-C9-Br24	120.13	118.55	118.56	118.64	118.53	118.53	118.62
C13-C15-Cl25	120.10	119.57	119.60	119.49	119.54	119.60	119.48
C14-C15-Cl25	119.89	119.47	119.50	119.47	119.44	119.49	119.46
Dihedral angle (_).							
C4-N1-C3-C7	-	179.74	179.71	179.42	179.77	179.82	179.49
H16-N1-C3-C5	-	-177.25	-177.02	-171.66	-176.56	-177.41	-171.44
H16-N1-C3-C7	-	2.730	2.920	8.540	3.520	2.640	8.880
C3-N1-C4-N2		0.230	0.240	0.860	0.310	0.210	0.880
C3-N1-C4-C6	-	-179.80	-179.78	-179.12	-179.66	-179.73	-179.07

Parameters	Exp.	B3LYP	B3LYP	B3PW91	B3PW91	HF	HF
Dihedral angle (_).		**6-311++G (d, p)**	**6-311 G (d, p)**	**6-311++ G (d, p)**	**6-311 G (d, p)**	**6-311++G (d, p)**	**6-311 G (d, p)**
H16-N1-C4-N2	-	177.22	177.00	171.76	176.53	177.37	171.49
N1-C3-C5-C8	-	-179.84	-179.83	-179.43	-179.76	-179.82	-179.38
C7-C3-C5-N2	-	-179.81	-179.77	-179.67	-179.84	-179.86	-179.72
N2-C5-C3-C7	-	179.97	179.97	179.92	179.94	179.95	179.88
C5-C3-C7-H17	-	179.95	179.93	179.93	179.96	179.96	179.93
N1-C4-C6-C10	-	173.49	172.75	160.67	172.86	174.26	161.75
N1-C4-C6-C11		-6.710	-7.480	-19.870	-7.420	-5.960	-18.860
N2-C4-C6-C10	-	-6.550	-7.270	-19.310	-7.110	-5.680	-18.180
BR24-C9-C12-C8	-	-179.96	-179.95	-179.91	-179.96	-179.97	-179.91
BR24-C9-C12-H21		0.010	0.020	0.0700	0.030	0.020	0.070
C6-C10-C13-C15	-	-0.030	-0.040	-0.1800	-0.030	-0.020	-0.160
C6-C10-C13-H22		179.90	179.88	179.74	179.89	179.91	179.75
H19-C10-C13-C15	-	180.00	180.00	179.85	179.95	179.97	179.82
H19-C10-C13-H22	-	-0.070	-0.080	-0.220	-0.140	-0.110	-0.260
C6-C11-C14-C15	--	0.150	0.170	0.110	0.160	0.130	0.170
C6-C11-C14-H23	-	179.88	179.86	179.64	179.86	179.88	179.69
H20-C11-C14-C15		-179.10	-178.98	-178.39	-178.90	-179.12	-178.34

7.3.2 Vibrational assignments

The functional groups conformational analysis in organic molecule can be evaluated by vibrational spectroscopy. The title compound 6 bromo-2-(4-chlorophenyl)-1H-benzimidazole has 69 normal modes of vibration. The selected theoretical and vibrational assignments of the title compound and their assignments have been attempted through Gauss view 6.0 molecular visualization program graphical interfaced with Gaussian 16 W [17] and VEDA 4 program [21]. We have calculated the theoretical vibrational spectra of title compound by using HF, B3LYP and B3PW91 with 6-311 G (d, p) and 6-311 ++ G (d, p) basis sets. Theoretical, experimental results and they assignments are tabulated in Table 2. All the calculated and the experimental spectral result are in good agreement with each other. The systematic errors of theoretical wave numbers were reduced for the 6 bromo-2-(4-chlorophenyl)-1H-benzimidazole compound were reduced using scaling factor 0.892 for HF, 0.961 for B3LYP and 0.957 for B3PW91 [22]. The comparative recorded and computed FT-IR spectra of the title compound are shown in Figure 2-3.

Benzimidazole derivatives have complex vibrational spectrum and they are strongly associated with intermolecular hydrogen bonding. The heterocyclic compound shows free

stretching υ (N-H) vibrations at 3400 cm^{-1} [23]. The spectrum of the title compound shows υ (N-H) strong bond in the region of 3511 cm^{-1} experimentally while the theoretical υ (N-H) bond for HF/DFT is observed in the region of 3490-3528 cm^{-1} this shows polymeric association of intermolecular hydrogen bonding. The υ (N-H) and υ (C-H) ring vibrations occurs in this region however it is difficult to distinguish. The heteroaromatic structure shows υ (C-H) stretching in the frequency region 3000-3150 cm^{-1} [24]. The band observed at 3097 cm^{-1} is ascribed to υ (C-H) stretching vibration of the title compound, which has been calculated with HF /DFT (B3LYP/B3PW91) at the frequency region of 3012-3086 cm^{-1}.

The benzimidazole derivatives has characteristic spectrum in the 1500-1650 cm^{-1} region which is assigned to stretching vibrations of υ (C=N) and υ (C=C). The title compound shows a strong band at 1470 cm^{-1} experimentally which is assigned to υ (C=N) vibration stretching. These bands have been computed theoretically around the region of 1571-1599 cm^{-1} for HF /DFT (B3LYP/B3PW91) respectively. The frequency band observed at 1424 cm^{-1} is attributed to stretching vibration of υ (C=C),it has been calculated at the region of 1534 -1556 cm^{-1} for HF /DFT (B3LYP/B3PW91) theoretically. The observed vibrational frequencies in this range are very intense due to the conjugation of benzene and imidazole rings and also the variation of the vibrational band may varied due to presence of the substituent and its electronegativity. All these data agree with those reported in the literature [25-26].

The bands observed at 1365 cm^{-1} experimentally were assigned to (C-N) and for HF/DFT (B3LYP/B3PW91) observed at the band region of 1425 -1502 cm^{-1}. These values supports the result reported [27-28]. The other band observed at 1254 cm^{-1} observed is assigned to stretching of ν(N-C) along with the bending of β(C-H) and theoretically this band in the region of 1280-1408 cm^{-1} however differentiating (C-N) is difficult task .The C-Br stretching vibration gives strong band in the region of 650-485 cm^{-1} [29-30].The title

compound shows vibrational spectra around the region of 659 and 591 cm^{-1} experimentally whereas for HF/DFT (B3LYP/B3PW91) observed at the band region of 570 -620 cm^{-1} this bands are raised due to bending of the (C-Br) along with out of plane and stretching of (C-Cl). The strong intense bands are observed due to influence of the Br the smaller the halide atom, the greater the influence of the neighbor. Bands of weak to medium intense also observed in this region.

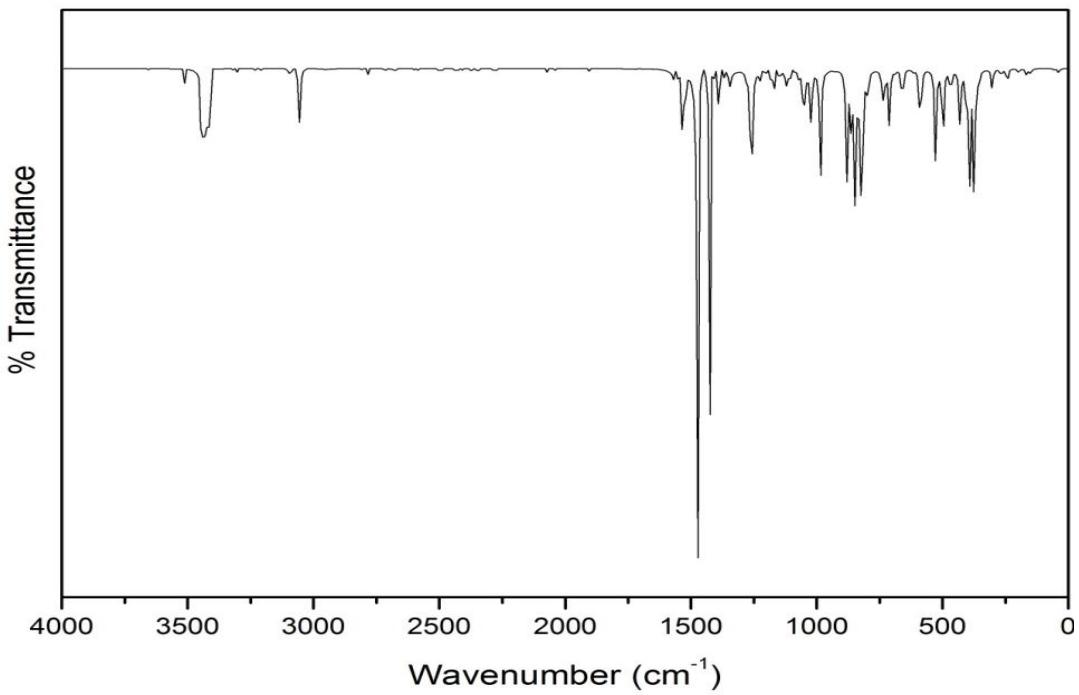

Figure 7.2 Experimental FT-IR spectra of
6 bromo-2-(4-chlorophenyl)-1H-benzimidazole for

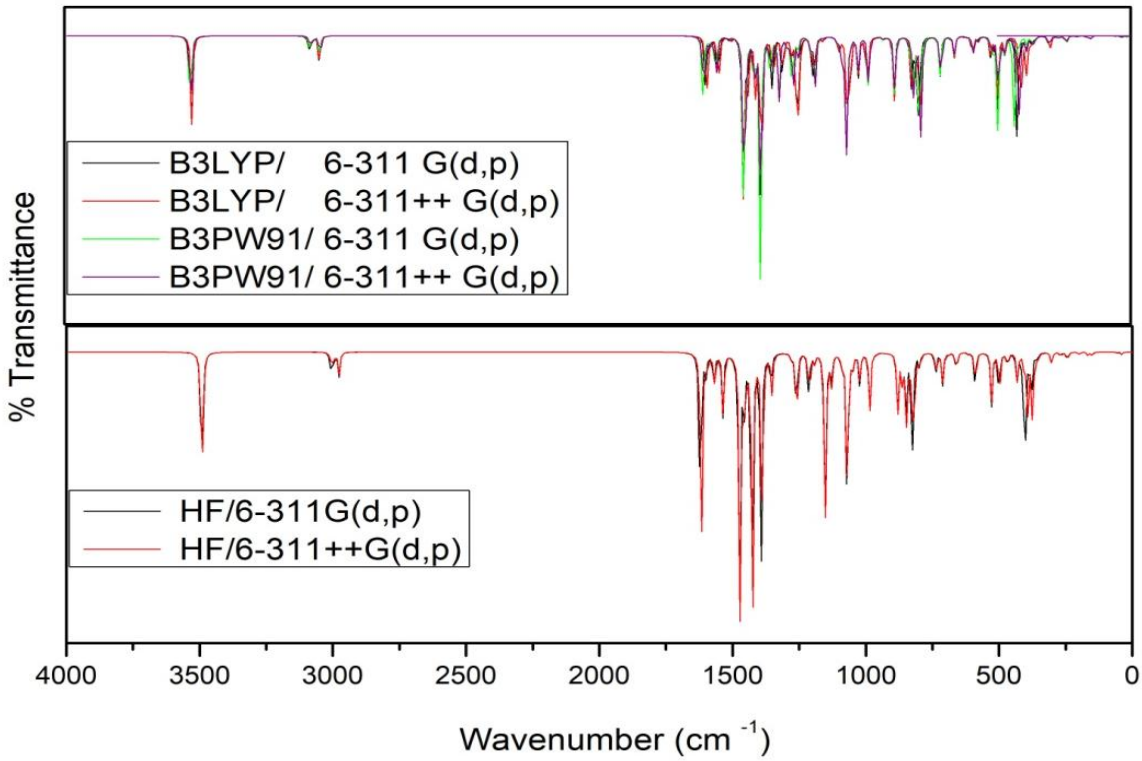

Figure 7.3 Calculated FT-IR spectra of
6 bromo-2-(4-chlorophenyl)-1H-benzimidazole for

Table 7.2 Exp. and calculated frequencies of 6 bromo-2-(4-chlorophenyl)-1H-benzimidazole

Assignments	B3LYP	B3LYP	B3PW91	B3PW91	HF	HF	Exp.
	6-311++G (d, p)	6-311 G (d, p)	6-311++G (d, p)	6-311 G (d, p)	6-311++G (d, p)	6-311 G (d, p)	
ν(N-H) sym	3522.49	3523.54	3526.4	3528.07	3490.93	3491.64	3511
ν(C-H)	3084.68	3086.46	3079.87	3082.3	3012.39	3015	3097
ν(C-H) +β (HCC)	3081.73	3083.02	3078.51	3080.74	3005.07	3006	3062
β (HCC)+τ(HCCC)	3066.43	3067	3063.88	3066.16	2988.72	2998	2980
ν(C-H)+ β (HCC) + τ (HCCC)	1591	1594.45	1601.28	1604.27	1617.21	1621	1533
ν(C=N)	1571.59	1574.34	1580.41	1582.08	1596.07	1599	1470
ν(C=C) +β (HCC)	1547.05	1548.45	1555.52	1556.88	1534.52	1536.92	1424
β(C-N)	1501.32	1502.98	1449.47	1451.05	1425.52	1427.37	1365
ν(N-C) +β(C-H)	1407.03	1408.65	1319.3	1320.25	1280.09	1281.01	1254
ν(C-C) +β (NCN)	1304.97	1306.02	1266.84	1269.48	1259.06	1260	1023
o(C-N)	1271.72	1272.3	1085.11	1085.64	984.67	985.59	982
ν(C-N) +β (CCC)	1091.74	1091.36	705.93	711.48	711.32	711,32	879
β(CCC)	708.6	712.36	660.8	614.14	615.58	616.96	736
β (C-Br) + o (C-Cl)	619.54	620.32	590.84	591.26	589.22	592.03	659
β (C-Br)+ ν (C-Cl)	570.97	576.39	569.24	574.77	586.17	589.21	591
o(ClCCC)+τ(CCCC)	389.22	393.54	389.79	390.56	406.36	404.63	371

ν, stretching; δ, twisting; β, bending; τ, torsion; θ, breathing; s, symmetric; as, asymmetric;

7.3.3 Natural bond orbital (NBO) analysis

The natural bond orbital (NBO) calculation [31] of the title compound was performed using Gaussian 16 W package at DFT/B3LYP/6-311 ++ G (d, p) basis set. The ideal Lewis structure picture is constructed from Lewis σ-type (donor) and the non- Lewis σ-type (acceptor) NBOs. The σ- σ* interactions between donor and acceptor orbital is associated with non-covalent delocalization effect, it can also be described as donor-acceptor and charge transfer. Weak occupancies of the valence anti-bonds signals delocalization effects. Hence, NBO analysis provides an effective method for understanding intra and intermolecular bonding, charge transfer or conjugative interaction in a system.

Hyperconjugation may be considered as stabilizing effect which arises on overlapping of the filled and electron deficient orbital when they are properly oriented this energy can be deduced using the second order perturbation approach of Fock Matrix in NBO basis between the donor-acceptor orbitals [32]. The important interactions are shown in Table 3. The intensive interaction between the electron donor and electron acceptor leads to larger E (2) values [33]. The highest stabilization energy is from π*(N2-C4) to π*(C3-C5) with a value of 143.72 kcal/mol. Where E(j) – E(i) is inversely proportional to stabilization energy. The lone pair electron of N1 donate to π*((N2-C4) with stabilization energy of 46.63 kcal/mol. From the Table-3, it is clear that the nitrogen atoms are donating the electrons to the other bonds. The hyperconjugative interaction of the electron occurs from π (C3-C5) to π* (C8-C12), π* (C7-C9) with the stabilization energy of 18.69 and 19.86 kcal/mol leads to stabilization of benzimidazole moiety [34]. The interaction between the donor π (C7-C9) distributes energy to anti-bonding acceptor π* (C3-C5) with stabilization energy of 17.91 kcal/mol.

The hyperconjugative interaction was observed between the donor σ (C15-Cl25) to the acceptor σ* (C14-H23) with stabilization energy 13.42 kcal/mol. The interaction between the donor π (C10-C13) distributes the energy to anti bonding acceptor π* (C6-C11) with stabilization energy 19.43 kcal/mol. These are the some important transition for the stability of the title compound molecules, from the above analysis it is clear that we can identify the stabilization energy, Lewis donor and acceptor interactions.

Table 7.3: Significant donor acceptor interaction of 6 bromo-2-(4-chlorophenyl)-1H-benzimidazole and their second order perturbation energies calculated at B3LYP/6-311 ++ G(d, p)

Donor Orbital(i)	Type	ED/e	Acceptor orbital (j)	Type	ED/e	E (2) (kcal/mol) [a]	E(j)-E(i) (a.u.) [b]	F (i, j) (a.u.) [c]
N1-C3	σ	1.98437	N1-C4	σ*	0.04365	1.78	1.23	0.042
N1-C3	σ	1.98437	C4-C6	σ*	0.03561	3.19	1.27	0.057
N1-C4	σ	1.98592	N1-C3	σ*	0.0230	1.81	1.25	0.043
N1-C4	σ	1.98592	C3-C7	σ*	0.02265	4.51	1.38	0.071
N1-H16	σ	1.98867	N2-C4	σ*	0.0129	1.99	1.27	0.045
N2-C4	σ	1.98057	N1-H16	σ*	0.0185	2.3	1.22	0.047
N2-C4	σ	1.98057	C5-C8	σ*	0.0224	5.25	1.41	0.077
C3-C5	σ	1.96427	N1-H16	σ*	0.0185	4.68	1.06	0.063
C3-C5	σ	1.96427	C3-C7	σ*	0.0227	4.56	1.24	0.067
C3-C5	σ	1.96427	C5-C8	σ*	0.0224	3.49	1.25	0.059
C3-C5	π	1.5755	N2-C4	π*	0.3675	14.22	0.26	0.055
C3-C5	π	1.5755	C7-C9	π*	0.39426	19.86	0.28	0.067
C3-C5	π	1.5755	C8-C12	π*	0.3010	18.69	0.29	0.068
C3-C7	σ	1.9671	N1-C3	σ*	0.0230	2.39	1.15	0.047
C3-C7	σ	1.9671	C9-Br24	σ*	0.03203	5.45	0.82	0.059
C4-C6	σ	1.9729	N2-C4	σ*	0.01288	2.72	1.24	0.052
C4-C6	σ	1.9729	C6-C11	σ*	0.02377	3.01	1.22	0.054
C5-C8	σ	1.9766	C3-C5	σ*	0.03778	3.39	1.23	0.058
C5-C8	σ	1.9766	C8-C12	σ*	0.01425	2.59	1.29	0.052
C6-C11	σ	1.96907	C6-C10	σ*	0.02308	4.13	1.24	0.064
C7-C9	π	1.74289	C3-C5	π*	0.47598	17.91	0.29	0.069
C7-H17	σ	1.97778	C3-C5	σ*	0.03778	3.81	1.07	0.057
C8-C12	π	1.71426	C3-C5	π*	0.47598	17.9	0.28	0.066
C9-C12	σ	1.98007	C7-C9	σ*	0.02359	3.04	1.29	0.056
C10-C13	π	1.66156	C6-C11	π*	0.39072	19.43	0.28	0.067
C12-H21	σ	1.97821	C7-C9	σ*	0.02359	4.66	1.09	0.064
C13-C15	σ	1.9801	C10-H19	σ*	0.01304	2.04	1.19	0.044
C14-C15	π	1.67048	C6-C11	π*	0.39072	18.86	0.3	0.068
C15-Cl25	σ	1.98869	C14-H23	σ*	0.01321	13.42	2.18	0.153
N1	e	1.62816	N2-C4	π*	0.3675	46.63	0.29	0.104
Br 24	e	1.9407	C7-C9	π*	0.39426	9.69	0.31	0.054
C7-C9	π*	0.39426	C14-H23	σ*	0.01321	1.84	1.45	0.102
C14-C15	π*	0.39024	C14-C15	σ*	0.02798	1.55	0.54	0.056

[a] $E^{(2)}$, energy of hyperconjugative interactions.

[b] Energy difference between donor and acceptor i and j NBO orbitals

[c] F_{ij} is the Fock matrix element between i and j NBO orbitals

7.3.4 NMR spectra analysis

In order to analyze ^{1}H and ^{13}C NMR spectra, theoretical computation on chemical shifts were carried out by Integral equation formalism polarized continuum model (IEF-PCM) using Gauge independent atomic orbital(GIAO) method at B3LYP/6-311 ++ G(d, p) basis set with DMSO, water, chloroform as solvents, the obtained result is tabulated in Table 7.4

The experimental and computed ^{1}H chemical shift values show no significant difference in the benzimidazole and substituted chlorophenyl ring in the studied structure. In DMSO solution the benzimidazole protons gave signal in between the 7.71-7.17 ppm [35]. The hydrogen atom H16-H23 present in the benzimidazole and chlorophenyl rings shows NMR peaks in the range of 7.20 -7.66 ppm, respectively except the proton attached to nitrogen atom which shows 5.39 ppm experimentally, In different solvents the NMR peaks of the aromatic hydrogen atom is in the range of 6.73-8.67 ppm for gas phase, 7.42-8.65 ppm for DMSO, 7.21-8.67 ppm for chloroform and 7.41-8.65 ppm for water [Fig.-4] All the values agree to the reported literature value [18].

The chemical shift values are in the range of 100-200 ppm in aromatic carbon atoms [36]. Ozdemir et al reported the ^{13}C NMR chemical shift of structural similar compound of 2-(4-chlorophenyl)-1-methyl-1H-benzo[d]imidazole [10] the benzimidazole the title compound shows the signal in the range of 129.21-152.32 ppm. This chemical shifts were calculated 130.62-150.02 ppm in gas phase,132.94-151.16 ppm in DMSO, 132.13-150.75 in chloroform and 132.99- 151.19 ppm in water. All these values agree to the reported literature values. The chemical shift values don’t show significant shift in different solvents hence there is no effect of solvents on the title compound.

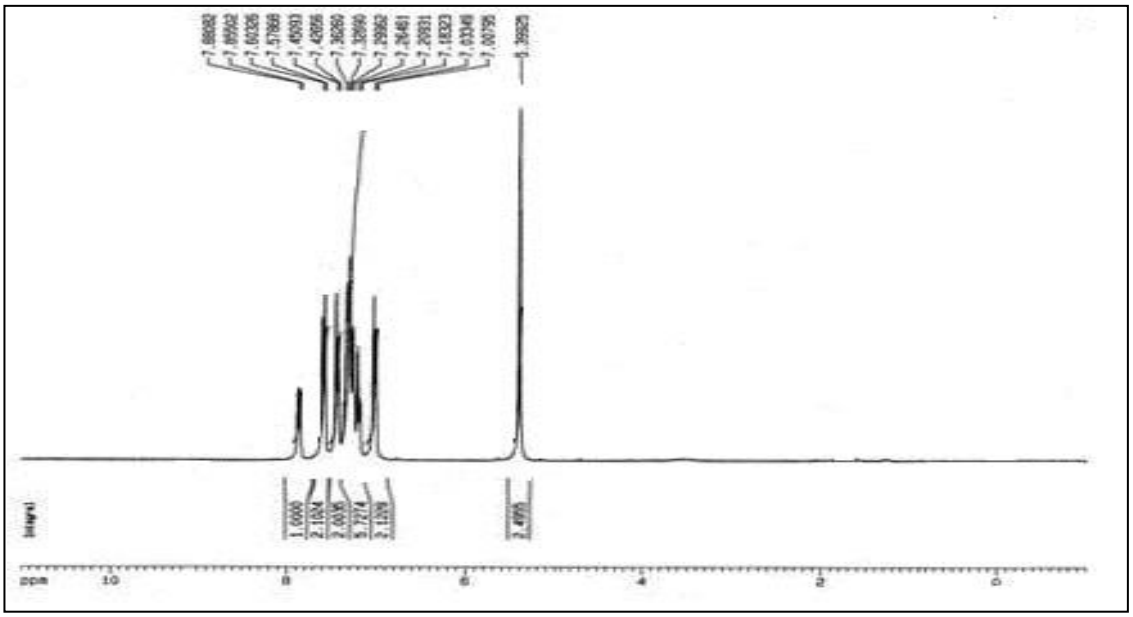

Figure 7.4 ^{1}H –NMR spectra of 6 bromo-2-(4-chlorophenyl)-1H-benzimidazole

Table 7.4 Experimental and calculated (GIAO) ^{1}H and ^{13}C NMR chemical shift of 6 bromo-2-(4-chlorophenyl)-1H-benzimidazole

Atom	Exp.	B3LYP/6-311++G(d,p)			
1H		Gas	DMSO	Chloroform	Water
H16	5.39	6.7336	7.4503	7.218	7.4631
H17	7.42	7.4167	7.7061	7.6084	7.7116
H18	7.60	7.7309	7.8424	7.8210	7.8432
H19	7.66	8.6774	8.6584	8.6749	8.6572
H20	7.45	7.5415	7.9001	7.7841	7.9065
H21	7.32	7.2852	7.4244	7.3839	7.4265
H22	7.36	7.5326	7.6772	7.6399	7.67900
H23	7.20	7.3624	7.5555	7.4965	7.5587
^{13}C	Exp [a]				
C-3	152.32	150.0241	151.1685	150.7547	151.1923
C-6	137.07	143.5615	143.7079	143.6456	143.7118
C-7	129.44	130.6218	132.9455	132.1363	132.9917
C-8	135.01	136.7019	136.0900	136.4027	136.0698
C-10	131.52	138.8095	138.3194	138.5846	138.3021
C-11	129.21	136.6468	138.5064	137.8746	138.5417
C-12	142.83	145.702	145.8231	145.7673	145.8265
C-13	131.52	139.2639	139.3756	139.4169	139.3713
C-14	137.07	144.3873	144.7744	144.6365	144.7824

Reference taken from [10]

7.3.5 Electronic properties

The electronic transition of the 6 bromo-2-(4-chlorophenyl)-1H-benzimidazole compound has been investigated using time dependent density functional theory (TD-DFT) and B3LYP 6-311++ G(d,p) basis set have been used by Including IEF-PCM with various solvents such as Gas, DMSO, chloroform and water the electronic spectra is stimulated . The experimental and theoretical computed spectra of different solvents are as shown in figure 4.4. HOMO-LUMO band gap is used to determine the stable nature and chemical reactivity of the compound [37]. HOMO energy value is -6.2241 eV, LUMO energy value is -2.0035 eV, LUMO +1 energy value is -1.17444 eV and the energy value between the HOMO-LUMO is 4.2405 eV using DFT/B3LYP method from Figure 7.5 The maximum absorption wavelength , oscillator strength and band gap is shown in Table 7.5. The UV absorption spectra wavelength is available at 312,279,273 nm in the theoretical spectra of the title compound in gas phase. The more intense peak is at 312 nm with an oscillator strength 0.7183 and band gap of 3.98 eV . this transition corresponds to 98 % from HOMO→ LUMO, in DMSO solvent the more intense peak is available at 316 nm with an oscillator strength of 0.8784 and band gap is 3.92 eV this transition corresponds to 98 % from HOMO→ LUMO similarly for the chloroform and water the more intense peak is available at 317 and 315 nm with an oscillator strength of 0.8851 and 0.8560 whereas the band gap are found to be 3.91 and 3.94 eV both of this transition corresponds to 98 % from HOMO→ LUMO. From the above table we conclude that the concentration of the solvents doesn't has any impact on the adsorption wavelength of the compound, so we conclude there is no change in bonding, position and intensities of the compound in different solvents.

The other parameters such as ionization potential, electron affinity, chemical potential, global hardness, global softness, electronegativity and electrophilicity index are calculated using HOMO-LUMO values and tabulated the readings in the Table 7.6.the global

hardness is 2.1203 which shows that the compound is stable and has good chemical stability .all the above parameters confirms that the title compound is stable and charge transfer take place within the molecule [38].

Table 7.5 Ionization potential, electron affinity, chemical potential, global hardness, global softness, electronegativity and electrophilicity index are calculated using HOMO-LUMO

DFT/B3LYP with 6-311 ++ G(d,p)					
Medium	λ (nm)	Band gap (eV)	Osc. Strength	Major contributions	Minor contributions
Gas	312	3.98	0.7183	HOMO->LUMO (98%)	
	279	4.44	0.0025	HOMO-3->LUMO (13%), HOMO-1->LUMO (10%), HOMO->LUMO+1 (71%)	
	273	4.54	0.003	HOMO-1->LUMO (55%), HOMO->LUMO+2 (26%)	HOMO-3->LUMO (13%)
DMSO	316	3.92	0.8784	HOMO->LUMO (98%)	
	275	4.51	0.002	HOMO-3->LUMO (12%), HOMO-1->LUMO (40%), HOMO->LUMO+1 (39%)	HOMO->LUMO+2 (4%)
	272	4.55	0.0038	HOMO-1->LUMO (33%), HOMO->LUMO+1 (22%), HOMO->LUMO+2 (18%)	HOMO-2->LUMO (8%)
CHLOROFORM	317	3.91	0.8851	HOMO->LUMO (98%)	
	276	4.49	0.0025	HOMO-3->LUMO (13%), HOMO-1->LUMO (28%), HOMO->LUMO+1 (50%)	HOMO->LUMO+2 (3%)
	272	4.55	0.0033	HOMO-1->LUMO (42%), HOMO->LUMO+1 (17%), HOMO->LUMO+2 (20%)	HOMO-3->LUMO (8%), HOMO-2->LUMO (6%), HOMO->LUMO+4 (2%)
WATER	315	3.94	0.856	HOMO->LUMO (98%)	
	275	4.51	0.0019	HOMO-3->LUMO (12%), HOMO-1->LUMO (40%), HOMO->LUMO+1 (38%)	HOMO->LUMO+2 (4%)
	272	4.55	0.0037	HOMO-1->LUMO (32%), HOMO->LUMO+1 (23%), HOMO->LUMO+2 (18%)	HOMO-2->LUMO (8%)

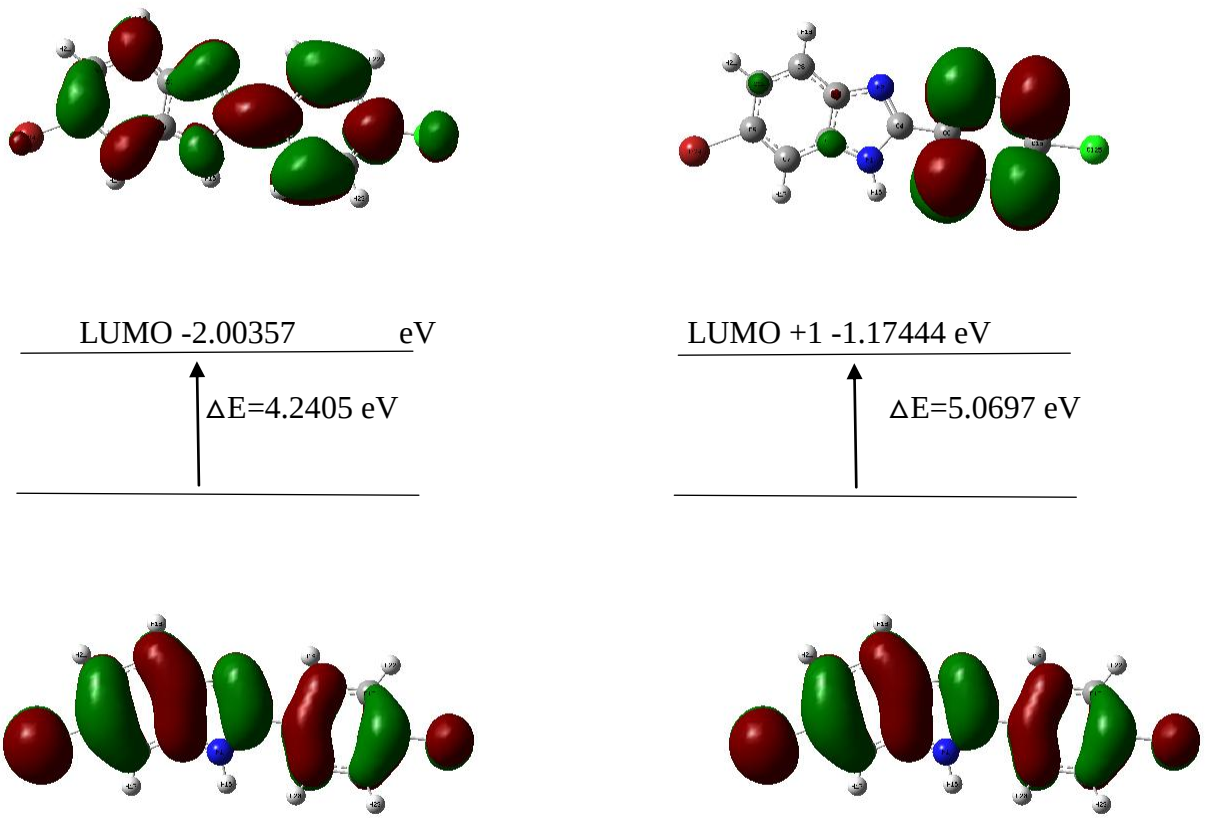

Figure 7.5 The molecular orbital of 6-bromo-2-(4-Chlorophenyl)-1H-benzimidazole using DFT/B3LYP with 6-311++G (d, p) and the selected electronic transition

Table 7. 6 Global chemical reactivity description of 6 bromo -2-(4 chlorophenyl)-1 H benzimidazole.

Properties	B3LYP/6-311++G(d,p)
E_{HUMO}(eV)	-6.2441
E_{LUMO}(eV)	-2.0035
Ionisation potential (I)	6.2441
Electron affinity(A)	2.0035
Chemical potential (μ)	-4.1238
Electronegativity (χ)	4.1238
Global hardness(η)	2.1203
Global softness (*S*)	0.2358
Electrophilicity index (ω)	4.0102

7.3.6 Molecular electrostatic potential (MEP)

The 3D visual pictorial representation of the title molecule in terms of color grading can be obtained from MEP [40]. The MEP diagram of optimized structure 6 bromo-2-(4chlorophenyl)-1 benzimidazole was visualized using Gauss view 6.0 is shown in figure 7.6 we can determine the electrostatic potential, Electrophilic and nucleophilic site from molecular electrostatic potential. The Electrophilic site (negative region) is -7.523e-2 represented by red colour. The nucleophilic site (positive region) is +7.253 e-2 represented by blue color around the Br 24 and N2, it is more negative represent by red color this region can bond with proteins. The blue color (Electrophilic site) is around N1 –H16 bond. Thus we found the most reactive site of the title compound.

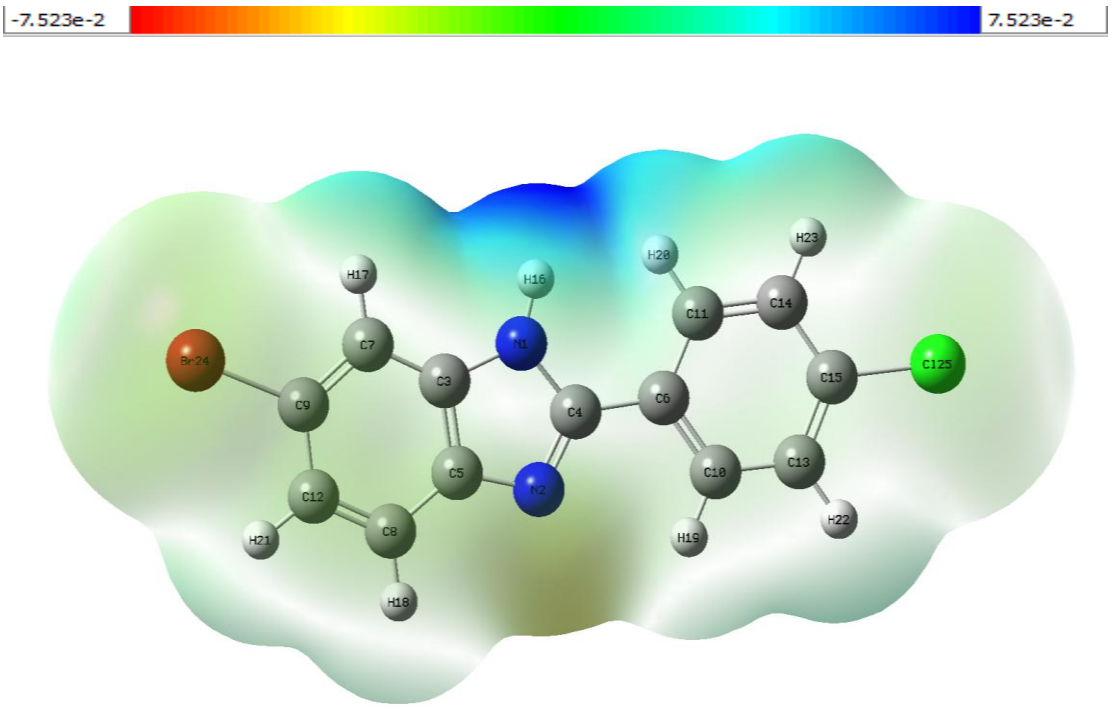

Figure 7.6 The molecular electrostatic potential of 6-bromo-2-(4-Chlorophenyl)-1H-benzimidazole using DFT/B3LYP with 6-311++G (d, p).

7.4 Molecular docking

Molecular docking is the process that involves placing molecules in appropriate configurations to interact with a receptor. Molecular docking is a natural process which occurs within seconds in a cell when bound to each other to form a stable complex. The purpose of ligand-protein docking is to predict the predominant binding mode(s) of a ligand with a protein of known three-dimensional structure. Docking can be used to perform virtual screening on large libraries of compounds, rank the results, and propose structural hypotheses of how the ligands inhibit the target, which is invaluable in lead optimization.

The title compound of the study 6-bromo-2-(4-Chlorophenyl)-1H-benzimidazole called ligand interacts with suitable protein selected using online drug target prediction swiss ADME-Target prediction. By using Auto dock software, 6-bromo-2-(4-Chlorophenyl)-1H-benzimidazole molecules are docked with 3EQA protein. The ligand of 6-amino-2-(4-nitrophenyl)-1H-benzimidazole molecules binds at the active site of the substrate is shown in Fig 7. The molecular docking binding energy (kcal/mol) was also obtained to be -6.73 kcal/mol. The bonded residues corresponding to 3EQA protein is ASP 354 and observed bond length is enlisted in Table 7. This low value of binding energy shows the title compound is bio-active nature of the molecule.

Table 7.7 Hydrogen bonding and molecular docking for protein target-3EQA

Protein ID	Bonded residue	No of bonds	Bond distance	Binding energy (Kcal/mol)	Ref RMSD (Å)
3EQA	ASP 354	1	2.1	-6.73	26.96

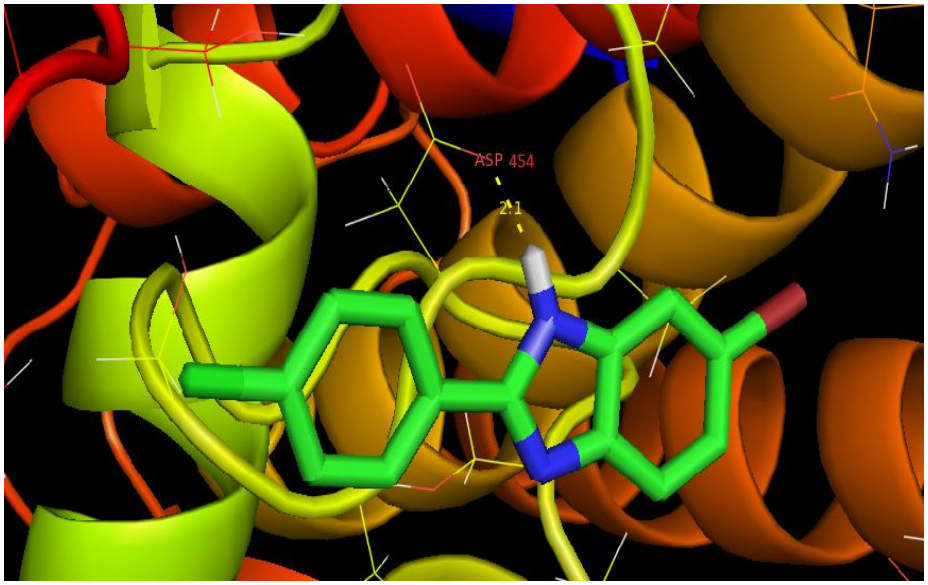

Fig-7.7 Ligand 6-chloro-2-(4 aminophenyl)-1H-benzimidazole embedded in the active site of 3EQA protein

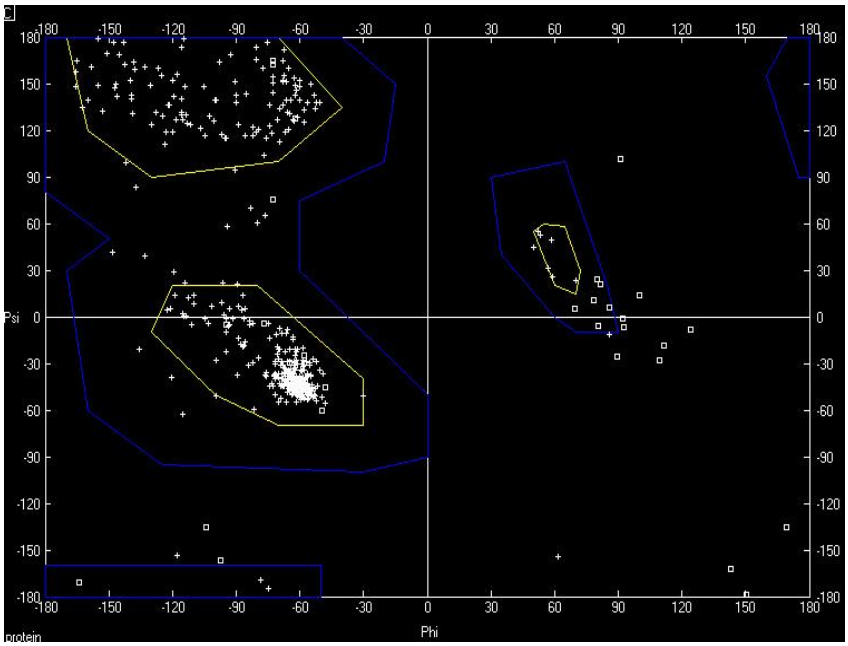

Fig. 7.8 Ramachandran Plot of the protein 3EQA with binding residues ASP 354

A Ramachandran plot is a way to visualize backbone dihedral angles ψ against φ of amino acid residues in protein structure. On the basis of phi and psi angles, we decide that either this kind of rotation and torsion is possible theoretically in the periphery of structure biology. A second is to show the empirical distribution of data points observed in a single structure. On observing the Ramachandran Plot, the energetically allowed regions of the binding residue ASP 354 has the torsion angle psi (ψ) against phi (ϕ) lying in the most allowed blue region as shown in Fig. 8. From the plot, it is concluded that the selected protein has majority of the residues in allowed region thus indicating the 3EQA protein to be a stable protein.

4. Anti-microbial activity

The synthesized title compound was screened for anti microbial activity. We chose four bacteria and two fungi using Disc-diffusion method. *Staphylococcus aureus* (MTCC-3160) causes serious infection in lungs. *Enterococcus faecalis* (MTCC-3159) causes gastrointestinal and UTI infection, *Pseudomonas aeruginosa* (MTCC-4030) is a human pathogen causes nosocomial infection, *Escherichia coli* (MTCC-1667) is responsible for food poisoning and the two fungal are Aspergillus *niger* (MTCC-282) causes allergy and lungs infections and Candida *albicans* (MTCC-227) are more often responsible for urinary tract infection .They were all obtained from Institute of microbial technology, Chandigarh. Each bacteria and fungi were inoculated on to the Mueller-Hinton agar medium.

The anti bacterial activity was determined by agar disc diffusion assay and the anti fungal activity was obtained from potato dextrose agar. All the standards are followed as per National Committee for clinical Laboratory Standards (NCCLS)

A bacterial culture to be tested was spread on Muller Hinton agar plate with a sterile cotton swab Each agar plate has five 6mm disc, three for impregnating the title compound (25, 50,100 µg/ml) one positive control reference drug (ciprofloxacin 25 µg/ml) and one negative

control ethanol . the plates are kept for 2 hour at room temperature for diffusion after that it is incubated at 37 °C for 24 h similarly for anti fungal activity he plates are keptfor incubation at 28°C for 48 h. the plates are examined , diameter of the inhibition zone is measured (in mm). Three replicates were carried out for any recorded activity.

The zone of inhibition of the title compound is tabulated in the Table 7. It is clearly seen from the result that the 6 bromo-2-(4chlorophenyl)-1 benzimidazole compound shows notable effects against the entire tested organism. It shows more antimicrobial activity against gram positive rather than gram negative bacteria .it shows strong inhibiting property against the *Staphylococcus aurous* which is better than the reference compound. Similarly the anti-fungal activity against the *A.nigerria is* notable one. This compound shows good anti microbial property against all the tested organism, this is due to presence of chloro, bromo in the benzimidazole moiety. These halogens are electron with drawing compounds which causes effective anti microbial activity.

Table 7.8 : Antimicrobial activity of the synthesized compounds by disc diffusion method

Microbial Compound	**Diameter of the Inhibition Zone (mm)**			
Gram positive	25 µg/ml	50 µg/ml	100 µg/ml	Ciprofloxacin 25 µg/ml
*Staphylococcus aureus (*MTCC-3160)	18±0.6	24±0.5	36±0.4	14±0.7
Enterococcus faecalis (MTCC-3159)	17±0.6	22±0.5	27±0.5	20±0.5
Gram -Negative				
Pseudomonas aeruginosa (MTCC-4030)	14±0.7	22±0.6	28±0.5	37±0.4
Escherichia coli (MTCC-1667)	25±0.4	34±0.3	42±0.2	29±0.5
Fungal Compound				
Aspergillus niger (MTCC 282),	19±0.6	26±0.5	33±0.4	15±0.6
Candida albicans (MTCC 227)	25±0.5	31±0.4	38±0.4	27±0.5

Conclusion:

In this study we synthesized the compound 6 bromo-2-(4chlorophenyl)-1 benzimidazole and characterized by FT-IR, UV-Vis, NMR .The optimized structure obtained from B3LYP/6-311++ G(d, p) basis sets. The parameters bond length, bond angle, torsion angle and vibrational analysis are computed using HF and DFT (B3LYP/B3PW91) methods with 6-311 G (d, p) and 6-311++ G(d.p) and compared with the experimental data . all the data satisfactorily agree.NBO analysis reveals the stabilization energy of the molecule and it is maximum for π*(N2-C4) to π*(C3-C5) with a a value of 143.72 kcal/mol. HOMO-LUMO calculation reveals the energy gap is 4.2405 eV which shows the molecule is stable and bio active. TD-DFT/IEF-PCM salvation method is used to obtain electronic transition in UV –Vis and chemical shifts in NMR with different solvents and they are compared with the experimental data .all the data agree with each other. Molecular electrostatic potential represents the active site for Electrophilic and nucleophilic reaction visually the N2 and Br 24 atoms of the benzimidazole moiety shows Electrophilic sites for interaction of proteins. The synthesized compound shows symbolic antimicrobial activity. It is more active against the gram positive bacteria than gram negative, anti fungal activity is remarkable, this is due to presence of bromo and chlorophenyl in the benzimidazole moiety. These halogens at ortho, para position enhanced the activity of the compound. This is one of the most promising compounds for pharmacophore industry; hence toxicology of the compound has to be studied.

Reference:

[1] M. Tuncbilek, T. Kiper, N. Altanlar, Synthesis and in vitro antimicrobial activity of some novel substituted benzimidazole derivatives having potent activity against MRSA, Eur. J. Med. Chem. 44 (2009) 1024-1033.

[2] M.L. Richards, S.C. Lio, A. Sinha, H. Banie, R.J. Thomas, M. Major, M. Tanji, J.C. Sircar, Substituted 2-phenyl-benzimidazole derivatives: novel compounds that suppress key markers of allergy, Eur. J. Med. Chem. 41 (2006) 950-969.

[3] M. Pfeffer, K. Swedberg, C. Granger, P. Held, J. McMurray, E. Michelson,B. Olofssan, J. Ostergren, S. Yusuf, S. Pocock, Effects of candesartan on mortality and morbidity in patients with chronic heart failure: the CHARM-Overallprogramme, Lancet 362 (2003) 759-766.

[4] S.J. Konturek, M. Cieszkowski, N. Kwiecien, J. Konturek, J. Taslar, J. Bilski, Effects of omeprazole, a substituted benzimidazole, on gastrointestinal secretions,serum gastrin, and gastric mucosal blood flow in dogs, Gastroenterology86 (1984) 71-77.

[5] P.N. Preston, Chem. Rev. 74 (1974) 279 – 314.

[6] V. Rajendiran, M. Murali, E. Suresh, S. Sinha, K. Somasundaram, M. Palaniandavar, Dalton Trans. (2008) 2157 – 2170;

[7] J. Mann, A. Baron, Y. Opoku-Boahen, E. Johansson, G. Parkinson, L.R. Kelland, S. Neidle, J. Med. Chem. 44 (2001) 138 – 144.

[8] N.M. Goudgaon, V. Dhondiba, A. Vijayalaxmi, Indian J. Heterocycl. Chem. 13 (2004) 271 – 272.

[9] Nour T. Abdel Ghani, Ahmed M. Mansour Molecular structure of 2-chloromethyl-1H-benzimidazole hydrochloride: Single crystal, spectral, biological studies, and DFT calculations, Spectrochimica Acta Part A 86 (2012) 605– 613

[10] Namik ozdemir, Bilge eren, Muharremdincer, Yunusbekdemir. Quantum-Chemical, IR, NMR and X-ray Diffraction Studies on 2-(4-Chlorophenyl)-1-methyl-1H-benzo[d]imidazole, International Journal of Quantum Chemistry, Vol 111, 3112–3124 (2011)

[11] Bilge Eren a, Arslan Unal Molecular structure and spectroscopic analysis of 1,4-Bis (1-methyl-2-benzimidazolyl)benzene; XRD, FT-IR, dispersive-Raman, NMR and DFT studies, Spectrochimica Acta Part A: Molecular and Biomolecular Spectroscopy 103 (2013) 222–231

[12] S. Dhole, M. Selvaraju, B. Maiti, K. Chanda, C.M. Sun, Microwave controlled reductive cyclization: a selective synthesis of novel benzimidazole-alkyloxypyrrolo[1,2-a]quinoxalinones, ACS Comb. Sci. 17 (2015) 310-316

[13] Mohamed Al Messmary., Mohamed Gebriel Elarfi., Rahim Mohamed. Synthesis and spectral studies of mannich bases derived from 2-substituted benzimidazoles. International Journal of Chem. Research, 2010, 2 (3), 1714-1716

[14] Mohammad A., Mohammad G., Rahim M. Synthesis and spectral studies of mannich bases derived from 2-subsituted benzimidazoles. International Archive of Applied Sciences and Technology. 2010, 1(1), 84-86.

[15] Na Zhao., Yu-Lu Wang., Jin-Ye Wang. A rapid and convenient synthesis of derivatives of imidazoles under microwave irradiation, Journal of the Chinese Chemical Society. 2005, 52, 535-538.

[16]M. J. Frisch, G. W. Trucks, H. B. Schlegel, G. E. Scuseria, M. A. Robb, J. R. Cheeseman, Scalmani, V. Barone, G. A. Petersson, H. Nakatsuji, X. Li, M. Caricato, A. V. Marenich, Bloino, B. G. Janesko, R. Gomperts, B. Mennucci, H. P. Hratchian, J. V. Ortiz, A. F. Izmaylov, J. L. Sonnenberg, D. Williams-Young, F. Ding, F. Lipparini, F. Egidi, J. Goings, B. Peng, A. Petrone, T. Henderson, D. Ranasinghe, V. G. Zakrzewski, J. Gao, N. Rega,G. Zheng, W. Liang, M. Hada, M. Ehara, K. Toyota, R. Fukuda, J. Hasegawa, M. Ishida, Nakajima, Y. Honda, O. Kitao, H. Nakai, T. Vreven, K. Throssell, J. A. Montgomery.

[17] Roy Dennington, Todd A. Keith, and John M. Millam, Gauss view Version 6.Semichem Inc., Shawnee Mission, KS, 2016.

[18] Hasan Saral, Ozgürozdamar, Ibrahim uçar synthesis, structural and spectroscopic studies of two new benzimidazole derivatives: A comparative study Journal of Molecular Structure 1130 (2017) 46-54

[19] Hakan Arslan, Oztekin Algul Vibrational spectrum and assignments of 2-(4-methoxyphenyl)-1H-benzo[d]imidazole by ab initio Hartree–Fockanddensity functional methods Spectrochimica Acta Part A 70 (2008) 109–116.

[20] Stibrany, R. T.; Schugar, H. J.; Potenza, J. A. Acta Cryst 2005, C61, -354.

[21] M.H. Jamr´oz, Vibrational Energy Distribution Analysis VEDA-4, Warsaw, 2004.

[22] J.P.Merrick, JD.Moran,L.Radom, J.Phy, ChemA111 (2007)11683-11700

[23] D.J. Rabiger, M.M. Joullie, J. Org. Chem. 29 (1964) 476.

[24] N.P.G. Roeges, A Guide to the Complete Interpretation of Infrared Spectra of Organic Structures, John Wiley and Sons Inc., New York, 1994.

[25] Infante-Castillo, R.; Rivera-Montalvo, L. A.; Herna´ndez- Rivera S. P. J Mol Struct 2008, 877, 10

[26] B. Smith, Infrared Spectral Interpretation: A Systematic Approach, CRC, Washington, DC, 1999

[27] N.P.G. Roeges, A Guide to the Complete Interpretation of Infrared Spectra of Organic Structures, John Wiley and Sons Inc., New York, 1994.

[28] Y.S. Mary, P.J. Jojo, C.Y. Panicker, C.V. Alsenoy, S. Atael, I. Yildiz, Quantum mechanical and spectroscopic (FT-IR, FT-Raman, 1H NMR and UV) investigations of 2-(phenoxymethyl)benzimidazole, Spectrochim. Acta A 125 (2014) 12-24.

[29] D.H. Wiffen, Spectrochimica Acta 7 (1955) 253 – 256.

[30] V. Sortur, J. Jayashree Yenagi, V.B. Tonannavar, M.V. Jadhav, Kulkarni, Spectrochimica Acta Part A 71 (2008) 688 – 694.

[31] F. Weinhold, J.E. Carpenter, The Structure of Small Molecules and Ions, Plenum,New York, 1988, pp. 227.

[32] C. Ravikumar, I. Hubert Joe, V.S. Jayakumar, Chem. Phys. Lett. 460 (2008) 552 – 558.

[33] P. Ramesh, S. Gunasekaran, G. R. Ramkumar, Int.J.CurrentReaseach Aca.Rev.2015; 3{11}: 117-138

[34] Nour T. Abdel Ghani, Ahmed M. Mansour,Molecular structure of 2-chloromethyl-1H-benzimidazole hydrochloride: Single crystal, spectral, biological studies, and DFT calculations, Spectrochimica Acta Part A 86 (2012) 605– 613

[35] P.J. Black, M.L. Heffernan, Proton magnetic resonance spectra of A2B2 systems,Aust. J. Chem. 15 (1962) 862-863

[36] K. Pihlaja, E. Kleinpeter (Eds.), Carbone13 Chemical Shifts in Structural and Sterochemical Analysis, VCH Publishers, Deerfield Beach, 1994

[37] A.S. Ben Geoffrey, Johanan Christian Prasana, S. Muthu, Christina susan abraham, host antony david, Spectr. Chim. Acta 218 (2019) 374-387.

[38] Suvidha Shinde, Nagaiyan Sekar, Dyes Pigments 168 (2019) 12-27.

[39] Habibe Tezcan, Hulya Senoz, Nesrin Tokay, J. Mol. Struct. 1190 (2019) 171-183

[40] T. Shanmugavadivu, M. Dhandapani, G. Vinitha, T. Joselin Beula, J. Phys. Chem. Solids 130 (2019) 69-83.

[41] M.k. Singh, R.Tilak, G.Nath S.K.Awasthi and A.Agrawal, Eur, J.Med.Chem.63 (2013) 635- 644.

SUMMARY AND CONCLUSION

In resent year the main focus of medicinal chemistry has increases towards the synthesis and characterizing of benzimidazole derivatives are due to the remarkable medicinal and pharmacological properties of its derivatives. Benzimidazole occupies a central place in the class of heterocyclic compound used in pharmaceutical and medicinal chemistry. This compound is bicyclic in nature, which consists of the fusion of benzene and imidazole.

Nowadays infectious microbial diseases are causing many problems in world-wide, because of resistances to many numbers of antimicrobial agents, despite of the availability of a huge numbers of antimicrobial compounds, the main matter of concern in the treatment of antimicrobial infections is the limited number of efficacious antimicrobial drug. Many of the currently available medicines are toxic, which enable recurrence because they are bacteriostic or fungistic and not bactericidal or fungicidal or lead to the development of resistance due to prolonged periods of administrations.

Apart from its applications in medicinal field, its application has been further expanded in the area of Nano material chemistry as optical sensors, NLO materials, with special application in environmental science, chemical technology and has obvious applications over other sensing devices such as easy of operations and low cost materials. Benzimidazole also proved to be an essential core for organic light emitting devices (OLEDs) with superior phosphorescence, thermal properties and morphological stabilities.

In order to expand the group of benzimidazole derivatives, we synthesized several new benzimidazole ring containing compounds. The O-phenylene diamine reacted with appropriate carboxylic acid under harsh dehydrating reaction condition to give the corresponding benzimidazole in good yield by Phillips reaction.

The synthesis, characterize and study of antimicrobial activity of some novel halogenoderivatives of benzimidazole compounds remain a main focus of our project. Since this compound exhibit a large number of biological activities towards antioxidant, Antimicrobial activity, antiflammatory – analgestic, anticancer, CNS depressant, androgen receptor antagonist, antitubercular, antihelmintic, diabetic drugs, anti-ulcer, anticonvulsant, antiviral-antifungal and antiprotozoal were used in treatment of cardiovascular disease, neurology, and endocrinology. In addition the benzimidazole have played a very important role in the development of theory in heterocyclic chemistry and also extensively in organic synthesis. Benzimidazole nucleus is present in vitamin-B12.

In this present study halogenoderivatives of benzimidazole compounds were known to possess anti-microbial some novel halogenoderivatives of benzimidazole compounds have been synthesized and characterized by spectral studies such as FT-IR in the region of 4000-400 cm^{-1}, UV-Visible and ^{1}H NMR experimental techniques and computational theoretical studies such as molecular structure parameter, vibrational frequencies, electronic absorption spectra has been investigated using gas and solvent phase. HOMO-LUMO, molecular electrostatic potential (MEP) and natural bond orbital (NBO), of all halogenoderivatives of benzimidazole compound has been computed using the HF and DFT (B3LYP, B3PW91) methods with 6-31+G (d, p) and

6-31++G (d, p) basis sets. Since our all activity, the synthesized compounds were screened for their anti-bacterial and anti-fungal activity using Disc – diffusion method.

The theoretical vibrational spectra of 6-nitro-2-(4-nitrophenyl)-1H-benzimidazole were calculated at the HF and DFT (B3LYP/B3PW91) methods with the 6-31+G(d,p) and 6-311++G(d,p) basis sets. FT-IR spectrum was recorded for both the experimental and theoretical methods. From FTIR spectra The C-H Symmetric stretching vibration of the title compound observed in and around the region of 3100 cm^{-1} for all the DFT and HF basic sets and 3114 cm^{-1}experimentally. The asymmetric C-H was observed at 3061cm^{-1} experimentally whereas for DFT /B3LYP [6-311++G(d,p)/6-31+G(d,p)]we observed 3098cm^{-1} /3117cm^{-1} for DFT /B3PW91 [6-311++G(d,p)/6-31+G(d,p)] 3092 cm^{-1}/3112cm^{-1} and for HF [6-311++G(d,p)/6-31+G(d,p)] 3031cm^{-1}/3052cm^{-1}. The HOMO-LUMO energy gap is very important parameter for the stability of the structure [37] and also it reflect the biological activity of the compound. The energy value of the band gap is 3.4155 eV for HOMO to LUMO and 3.7232 for HOMO to LUMO +1.This ensure that the compound is stable.

The global hardness is another good indicator of chemical stability. The global hardness of 6-nitro-2-(4-nitrophenyl)-1H-benzimidazole compound is 1.7075, which indicates the good chemical stability and the compound is stable, electronegativity (χ) is calculated as 5.5157, which measure the attraction of an atom to electron. The extremely low global softness of 0.2928 observed theoretical shows that the

compound is nontoxic. The Electrophilicity index (ω) was found to be 8.9086 this ensures that there is strong energy transformation between HOMO and LUMO

The molecular docking binding energy (kcal/mol) was also obtained to be -5.36 kcal/mo. for title compound 6-nitro-2-(4-nitrophenyl)-1H-benzimidazole. The bonded residues corresponding to 3EQA protein is SER 483, ARG 184 and THR 486. This low value of binding energy shows the bio-active nature of the title compound. From Ramachandra plot, it is concluded that the selected protein has majority of the residues in allowed region thus indicating the 3EQA protein to be a stable protein.

The antimicrobial activities were carried for 6-nitro-2-(4-nitrophenyl)-1H-benzimidazole for four bacterial strains viz. *Staphylococcus aureus (*MTCC-3160), *Enterococcus faecalis* (MTCC-3159) as Gram –positive bacteria and *Pseudomonas aeruginosa* (MTCC-4030), *Escherichia coli* (MTCC-1667) as Gram-negative bacteria and two fungal strains viz. *Aspergillusniger* (MTCC 282),*Candida albicans* (MTCC 227). This compound has shown moderate activity against the entire gram positive and gram negative bacteria and fungi except *Staphylococcus aureus.*

The spectral studies such as FT-IR, UV-visible and NMR for 6 amino-2-(4 nitrophenyl)-1H-benzimidazole was carried out. The υ(C-H) vibration of the 6 amino-2-(4 nitrophenyl)-1H-benzimidazole compound was observed at 3091-3097 cm^{-1} for DFT (B3LYP/B3PW91) calculations and 3062 cm^{-1} from experimental spectra and for HF the bands are observed in the region of 3030 cm^{-1}. This shows the strongly association of intermolecular hydrogen bonding of the benzimidazole compounds. NBO analysis shows that the σ (N5-C13) participates as donor and the σ* (N4-C8) as

acceptor and the intermolecular hyper conjugative interaction was observed with the stabilization energy of 173.23 Kcal/mol which reflect charge transfer takes place within the molecule.

^{1}H NMR result for 6 amino-2-(4 nitrophenyl)-1H-benzimidazole shows 1,2-disubstituted benzene system at the ring of benzimidazole nucleus and 1,4 disubstituted benzene system because of the 4-nitrophenyl group at 2 –position. From HOMO and LUMO studies the value of the energy separation between HOMO and LUMO is 2.8036 eV and 4.3793 eV for HOMO and LUMO+1. This low value shows that the title molecule is more reactive. The electrophilicity index (ω) is 6.7826, this high value shows that there is maximum flow between the donor and acceptor of the title compound. This ensures that, there is strong energy transformation between HOMO and LUMO. From the MEP studies, the negative region is localized on the oxygen atom of the nitrophenol ring N6, this is one of the possible sites for the electrophilic attack similarly the positive region is localized around the H atoms of the benzimidazole ring indicates the possible site for nucleophilic attack.

The molecular docking binding energy (kcal/mol) was also obtained to be -5.40 kcal/mol. The bonded residues corresponding to 3EQA protein is VAL 485, SER 484, ALA 110 and SER 107. This low value of binding energy shows the bio-active nature of the molecule. From Ramachandra Plot, the energetically allowed regions of the binding residue VAL 485,SER 484, ALA 110 and SER 107 has the torsion angle psi (ψ) against phi (ϕ) lying in the most allowed blue region as shown in Fig. 8. From the plot, it is concluded that the selected protein has majority of the residues in allowed region thus indicating the 3EQA protein to be a stable protein. The synthesized 6

amino-2-(4 nitrophenyl)-1H-benzimidazole compound exhibits antibacterial and antifungal activity. It is more active towards the Gram-positive bacteria than Gram-negative bacteria this is due to presence of NH_2 (electron donor) in benzimidazole ring.

The vibrational assignments for 6-chloro-2-(4-aminophenyl)-1H-benzimidazole were performed on the theoretically and predicted wave numbers by HF and DFT (B3LYP/B3PW91) methods with 6-311 G (d, p) and 6-311 ++ G (d, p) basis sets. The aromatic C-H vibrations are available in the region of 3100- 3000 cm^{-1}[11]. We observed this stretching of C-H vibration in the 3025-3040 cm^{-1} for all the DFT basis sets methods whereas for HF it is the region of 2960-2980 cm^{-1}.apart from this stretching of C-H mixed mode of vibration with bending of HCC and also HCCC is observed in and around the region of 1600-1650 cm^{-1} in all the HF and the DFT methods. From NBO analysis, the highest stabilization of the energy is from π*(N3-C5) to π*(C7-C11) with a value of 262.01 Kcal/mol. The other important interaction for stabilization of the 6-chloro-2-(4-aminophenyl)-1H-benzimidazole compound was σ (C14-C16) to σ* (C4-C6) with a value of 118.8 Kcal/mol.

From HOMO LUMO studies, the highest occupied molecular orbital energy level is -5.681 eV and the lowest unoccupied molecular energy level is -2.9589 eV and the energy gap between them is 4.2472 eV. The other parameters such as electron affinity, electronegativity, global hardness and softness, and electrophilicity index can be determined using the HOMO-LUMO values. This shows the compound is stable and charge transfer take place within a molecule.

The antimicrobial activity of title compound 6-chloro-2-(4-aminophenyl)-1H-benzimidazole shows an good anti-fungal against the *Aspergillus niger* the zone of inhibition is 18±0.6 to 31±0.4 for different concentrations . As the results are compared with reference compound Ciprofloxacin, the benzimidazole derivative shows a better activity than the reference drug this activity is due to presence of the Chloro group in the benzimidazole moiety and the ortho and para position of the halogen compound in the benzimidazole moiety will improve the antimicrobial inhibition activity against all tested organism.

From Molecular docking studies, the binding energy (kcal/mol) was also obtained to be -6.50 kcal/mol. The bonded residues corresponding to 3EQA protein is GLY 254 and ASP 369. This low value of binding energy shows the title compound is bio-active nature of the molecule. From Ramachandra Plot it is also concluded that the selected protein has majority of the residues in allowed region thus indicating the 3EQA protein to be a stable protein.

The optimized molecular structure, vibrational frequencies, corresponding vibrational assignment of 6 bromo-2-(4-chlorophenyl)-1H-benzimidazole have been investigated. The spectrum of the title compound shows υ (N-H) strong bond in the region of 3511 cm^{-1} experimentally while the theoretical υ (N-H) bond for HF/DFT is observed in the region of 3490-3528 cm^{-1} this shows polymeric association of intermolecular hydrogen bonding.

From NBO analysis, the hyperconjugative interaction was observed between the donor σ (C15-Cl25) to the acceptor σ* (C14-H23) with stabilization energy 13.42 kcal/mol. The interaction between the donor π (C10-C13) distributes the energy to anti

bonding acceptor π* (C6-C11) with stabilization energy 19.43 kcal/mol. These are the some important transition for the stability of the title compound 6 bromo-2-(4-chlorophenyl)-1H-benzimidazole. From the studies of HOMO & LUMO the HOMO energy value is -6.2241 eV, LUMO energy value is -2.0035 eV, LUMO +1 energy value is -1.17444 eV and the energy value between the HOMO-LUMO is 4.2405 eV using DFT/B3LYP method.

By using Auto dock software, 6-bromo-2-(4-Chlorophenyl)-1H-benzimidazole molecules are docked with 3EQA protein. The ligand of 6-amino-2-(4-nitrophenyl)-1H-benzimidazole molecules binds at the active site of the substrate. The molecular docking binding energy (kcal/mol) was also obtained to be -6.73 kcal/mol. The bonded residues corresponding to 3EQA protein is ASP 354. This low value of binding energy shows the title compound is bio-active nature of the molecule.

In this study HF and DFT methods are adopted for the computational harmonic vibrational analysis using GAUSSAIN 16W program package. The calculated results were visualized by means of Gass view 6.0. On comparing with HF, DFT (B3LYP) method is more reliable and correlates well with the experimental results, due to the inclusion of electron correlation. Simulation of FT-IR and UV-Visible spectra utilizing the results of these calculations led to good overall agreement with the observed spectral patterns, especially with the higher level basis set. By using Auto dock software, the synthesized compounds are docked with 3EQA protein for various residues such as SER 483, ARG 184, THR 486 and corresponding binding energies of all the synthesized compounds were calculated. This low value of binding energy shows the bio-active nature of the molecule. All the synthesized halogenoderivatives

of benzimidazole compounds were known to possess anti-microbial activity, were screened for their anti-bacterial and anti-fungal activity using Disc – diffusion method.

SOCIAL RELEVANCE OF THE MINOR RESEARCH PROJECT

Today's medicinal chemist is part of a team that handles essentially all the components of the drug discovery process. They need excellent communication and interpersonal skills in order to be able to function effectively as a part of a multi-functional and multi-dimensional project team that consists of biologists, computational chemists, structural biologists, high throughput screeners, , information management technologists, toxicologists, etc.

Nowadays infectious microbial diseases are causing many problems in world-wide, because of resistances to many numbers of antimicrobial agents, despite of the availability of a huge numbers of antimicrobial compounds, the main matter of concern in the treatment of antimicrobial infections is the limited number of efficacious antimicrobial drug. Many of the currently available medicines are toxic, which enable recurrence because they are bacteriostic or fungistic and not bactericidal or fungicidal or lead to the development of resistance due to prolonged periods of administrations.

The study of Minor Research Project on "Molecular Structure and Vibrational Spectroscopic Analysis of some Antimicrobial Activity Compounds – A Combined Experimental and Quantum Chemical Approach" focus on the role & response synthesized novel halogenoderivatives of benzimidazole compounds towards the Antimicrobial activity against Gram-negative bacteria *Pseudomonas aeruginosa (MTCC-4030), Escherichia coli (MTCC-1667) and Gram-positive bacteria Staphylococcus aureus (MTCC-3160), Enterococcus faecalis(MTCC-3159) and fungal compounds Aspergillusniger(MTCC 282) & Candida albicans(MTCC 227).*

The study highlights the activity of synthesized pharmaceutical compound towards antioxidant, antimicrobial activity, antiflammatory – analgestic, anticancer, CNS depressant, androgen receptor antagonist, antitubercular, antihelmintic, diabetic drugs, anti-ulcer, anticonvulsant, antiviral-antifungal and treatment of cardiovascular disease, neurology, and endocrinology. The study also highlight introduction of halogen derivatives at 6th position of benzimidazole compound enhance bioactive stimulation to higher levels. The computational & molecular docking studies for all the synthesized compounds to a great extent will help the chemist for new drug design uses computational approaches to discover, develop, and analyze drugs and similar biologically active molecules.

****